Thesis

On

MECHANICAL BEHAVIOUR OF ALUMINIUM BASED METAL MATRIX COMPOSITES REINFORCED WITH ALUMINIUM OXIDE

Submitted in partial fulfillment of the requirement for the award of the degree of

Master of Engineering

IN

PRODUCTION & INDUSTRIAL ENGINEERING

Submitted By

KAMALJIT SINGH

ROLL No. 801082015

Under the Guidance of

Mr. Gagandeep Bhardwaj

Lecturer

Thapar University, Patiala

Mr. Lalit Kumar

Lecturer

Thapar University, Patiala

DEPARTMENT OF MECHANICAL ENGINEERING

THAPAR UNIVERSITY

PATIALA-147004, INDIA

DECLARATION

I hereby declare that the thesis entitled "**MECHANICAL BEHAVIOUR OF ALUMINIUM BASED METAL MATRIX COMPOSITES REINFORCED WITH ALUMINIUM OXIDE**" is an authentic record of my study carried out as requirements for the award of degree of **Master of Engineering** in **Production and Industrial Engineering** at **Thapar University, Patiala,** under the guidance of Mr.Gagandeep bhardwaj, Lecturer and Mr. Lalit Kumar, Lecturer of Department of Mechanical Engineering, Thapar University, Patiala during July 2011 to July 2012. The matter embodied in this thesis has not been submitted in part or full to any other university or institute for the award of any degree.

Kamaljit Singh

Kamaljit Singh

This is to certify that above declaration made by the student concerned is correct to the best of my knowledge & belief.

Gagan

(Mr. Gagandeep Bhardwaj)

Lecturer

Thapar University,

Patiala, 147004

(Mr. Lalit Kumar)

Lecturer

Thapar University,

Patiala, 147004

Countersigned by:

(Dr. AJAY BATISH)

Professor& Head

Department of Mechanical Engineering

Thapar University,

Patiala, 147004

(Dr S.K. MOHAPATRA)

Dean of Academic Affairs,

Thapar University,

Patiala, 147004

ACKNOWLEDGEMENTS

With deep sense of gratitude I express my sincere thanks to my guides, ***Mr.. Gagandeep Bhardwaj*** and ***Mr. Lalit Kumar,*** for their valuable guidance, proper advice and constant encouragement during the thesis work from the initial level to final level. I am thankful to ***Dr. Rahul Chhibber*** for their encouragement and support during my work. I am also very grateful to ***Dr. V.P. Agrawal*** for their help during my thesis. I also feel very much obliged to ***Dr. Ajay Batish***, Associate Professor& Head of Mechanical Engineering Department.

I am thankful to Mr. Sukbir Singh, A.S. Cheema& Rajinder Kumar for helping me to give guidance about the equipments used during my thesis work.

I am grateful to the Mr. Gurpreet Singh & Gurmail Singh for helping to run smoothly and for assisting me in many different ways.

I offer my regards to all of those who supported me in any respect during the completion of the work.

Lastly, and most importantly, I wish to thank my parents. They supported me and loved me. To them I dedicate this thesis.

KAMALJIT SINGH

Registration No. 801082015

ABSTRACT

Aluminium metal matrix composites are one of the new materials used for various applications due to their less cost and light weight. The present study has been done to study the effect of different input parameters namely composition of Al_2O_3, type of cooling and stirring speed on the micro hardness, and wear rate with conditions i.e. time, sliding distance and load. The effect of various input parameters on output responses have been analyzed using Analysis of Variance (ANOVA). Optical microstructure and SEM was done to see the distribution and presence of Al2O3 particles in aluminium alloy. EDS and XRD was completed to analyze the various elements present in different composites. Main effect plot and interaction plot has been used to determine the optimal design for each output response.

ABBREVATIONS

ANOVA	Analysis of Variance
MMC	Metal Matrix Composite
Dof	Degree of Freedom
SD	Sliding distance
SEM	Scanning Electron Microscope
EDS	Energy Dispersive Spectroscopy
X-RD	X-Ray diffraction
S/N	Signal to Noise Ratio
MIN	Minutes

NOTATIONS

OA	Orthogonal Array
A	Composition
B	Cooling
C	Stirring Speed
CI	Confidence Interval
SS	Sum of Squares

CONTENTS

LIST OF FIGURES

LIST OF TABLES

CHAPTER 1

INTRODUCTION

1.1 INTRODUCTION

Conventional monolithic materials have limitations in achieving good combination of strength, stiffness, toughness and density etc. To overcome these shortcomings and to meet the ever increasing demand of modern day technology, composites are most promising materials of recent interest. Metal matrix composites (MMCs) possess significantly improved properties including high specific strength; specific modulus, damping capacity and good wear resistance compared to unreinforced alloys. There has been an increasing interest in composites containing low density and low cost reinforcements. Among various discontinuous dispersoids used, fly ash is one of the most inexpensive and low density reinforcement available in large quantities as solid waste by-product during combustion of coal in thermal power plants. Hence, composites with fly ash as reinforcement are likely to overcome the cost barrier for wide spread applications in automotive and small engine applications. It is therefore expected that the incorporation of fly ash particles in aluminium alloy will promote yet another use of this low-cost waste by-product and, at the same time, has the potential for conserving energy intensive aluminium and thereby, reducing the cost of aluminium products [1-3].

Now a days the particulate reinforced aluminium matrix composite are gaining importance because of their low cost with advantages like isotropic properties and the possibility of secondary processing facilitating fabrication of secondary components. Cast aluminium matrix particle reinforced composites have higher specific strength, specific modulus and good wear resistance as compared to unreinforced alloys [4-6].While investigating the opportunity of using fly-ash as reinforcing element in the aluminium melt, R.Q.Guo and P.K.Rohatagi [7-8] observed that the high electrical resistivity, low thermal conductivity and low density of fly-ash may be helpful for making a light weight insulating composites. The particulate composite can be prepared by injecting the reinforcing particles into liquid matrix through liquid metallurgy route by casting [9-10]. Casting route is preferred as it is less expensive and amenable to mass production. Among the entire liquid state production routes, stir casting is the simplest and

cheapest one. The only problem associated with this process is the non uniform distribution of the particulate due to poor wet ability and gravity regulated segregation. Mechanical properties of composites are affected by the size, shape and volume fraction of the reinforcement, matrix material and reaction at the interface.

1.2 COMPOSITE MATERIALS

A typical composite material is a system of materials composing of two or more materials (mixed and bonded) on a macroscopic scale. Generally, a composite material is composed of reinforcement (fibers, particles, flakes, and/or fillers) embedded in a matrix (polymers, metals, or ceramics). The matrix holds the reinforcement to form the desired shape while the reinforcement improves the overall mechanical properties of the matrix. When designed properly, the new combined material exhibits better strength than would each individual material. Many of common materials (metals, alloys, doped ceramics and polymers mixed with additives) also have a small amount of dispersed phases in their structures, however they are not considered as composite materials since their properties are similar to those of their base constituents. Favorable properties of composites materials are high stiffness and high strength, low density, high temperature stability, high electrical and thermal conductivity, adjustable coefficient of thermal expansion, corrosion resistance, improved wear resistance etc. Composites are multifunctional material systems that provide characteristics not obtainable from any discrete material. They are cohesive structures made by physically combining two or more compatible materials, different in composition and characteristics and sometimes in form. [11]

1.3 CHARACTERISTICS OF COMPOSITES

Properties of composites are strongly dependent on the properties of their constituent materials, their distribution and the interaction among them. The composite properties may be the volume fraction sum of the properties of the constituents or the constituents may interact in a synergistic way resulting in improved or better properties. Apart from the nature of the constituent materials, the geometry of the reinforcement (shape, size and size distribution) influences the properties of the composite to a great extent. The concentration distribution and orientation of the reinforcement also affect the properties. The shape of the discontinuous phase

(which may by spherical, cylindrical, or rectangular cross-sanctioned prisms or platelets), the size and size distribution (which controls the texture of the material) and volume fraction determine the interfacial area, which plays an important role in determining the extent of the interaction between the reinforcement and the matrix. Composites as engineering materials normally refer to the material with the following characteristics:

1. These are artificially made (thus, excluding natural material such as wood).
2. These consist of at least two different species with a well defined interface.
3.Their properties are influenced by the volume percentage of ingredients.
4. These have at least one property not possessed by the individual constituents

Generally, a composite material is composed of reinforcement and matrix. The matrix holds the reinforcement to form the desired shape while the reinforcement improves the overall mechanical properties of the matrix. When designed properly, the new combined material exhibits better strength than would each individual material.

1.3.1 Matrix phase

The primary phase, having a continuous character, is called matrix. Matrix is usually more ductile and less hard phase. It holds the dispersed phase and shares a load with it. Functions of matrix to take the load and transfers it to the reinforcement and it binds or holds the reinforcement and protects the same from mechanical or chemical damage that might occur by abrasion of their surface. Matrix also separates the individual fibres and prevents brittle cracks from completely across the section of the composite

1.3.2 Dispersed (reinforcing) phase

The second phase is imbedded in the matrix in a discontinuous form. This secondary phase is called dispersed phase. Dispersed phase is usually stronger than the matrix, therefore it is sometimes called reinforcing phase.

1.4 CLASSIFICATION OF COMPOSITES

Composite materials can be classified in the two different ways:

1. On the basis of Matrix Material

2. On the basis of Material Structure

1.4.2 On the basis of Matrix Material

1.4.1.1 Metal matrix composites (MMC)

Metal matrix composites (MMCs), like all composites consist of at least two chemically and physically distinct phases, suitably distributed to provide properties not obtainable with either of the individual phases. Generally, there are two phases, e.g. a fibrous or particulate phase in a metallic matrix. A metal matrix composite (MMC) combines into a single material a metallic base with a reinforcing constituent, which is usually non-metallic and is commonly a ceramic. By definition, MMC's are produced by means of processes other than conventional metal alloying. Like their polymer matrix counterparts, these composites are often produced by combining two pre-existing constituents (e.g. a metal and a ceramic fibre).

Common types of MMC are

- Aluminum Matrix Composites (AMC)
- Magnesium Matrix Composite
- Titanium Matrix Composite
- Copper Matrix Composites

Aluminum is the most popular matrix for the metal matrix composites (MMCs). The Al alloys are quite attractive due to their low density, their capability to be strengthened by precipitation, their good corrosion resistance, high thermal and electrical conductivity, and their high damping capacity. Aluminum matrix composites (AMCs) have been widely studied since the 1920s and are now used in sporting goods, electronic packaging, armours and automotive industries. They offer a large variety of mechanical properties depending on the chemical composition of the Al-matrix. They are usually reinforced by Al_2O_3, SiC, and carbon. As proposed by the American Aluminum Association the AMCs should be designated by their constituents: accepted designation of the matrix / abbreviation of the reinforcement's designation / arrangement and volume fraction in % with symbol of type (shape) of reinforcement. Aluminum Matrix Composites are manufactured by the following fabrication methods

- Powder metallurgy
- Stir casting
- Squeeze casting

1.4.1.2 Ceramic matrix composites (CMC)

Ceramic Matrix Composites are composed of a ceramic matrix and imbedded fibres of other ceramic material (dispersed phase). Ceramic Matrix Composites are designed to improve toughness of conventional ceramics, the main disadvantage of which is brittleness. Ceramic Matrix Composites are reinforced by either continuous (long) fibers or discontinuous (short) fibers. Short-fiber (discontinuous) composites are produced by conventional ceramic processes from an oxide (alumina) or non-oxide (silicon carbide) ceramic matrix reinforced by whiskers of silicon carbide (SiC), titanium boride (TiB2), aluminum nitride (AlN), zirconium oxide (ZrO2) and other ceramic fibers. Most of CMC are reinforced by silicon carbide fibers due to their high strength and stiffness. Whiskers incorporated in a short-fiber Ceramic Matrix Composite improve its toughness resisting to cracks propagation. However a character of failure of short-fiber reinforced materials is catastrophic.

Long-fiber composites are reinforced either by long monofilament of long multifilament fibers. The best strengthening effect is provided by dispersed phase in form of continuous monofilament fibers, which are fabricated by chemical vapor deposition (CVD) of silicon carbide on a substrate made of tungsten (W) or carbon (C) fibers. Monofilament fibers produce stronger interfacial bonding with the matrix material improving its toughness.

1.4.1.3 Polymer Matrix Composites (PMC)

Polymer Matrix Composite (PMC) is the material consisting of a polymer (resin) matrix combined with a fibrous reinforcing dispersed phase. Polymer Matrix Composites are very popular due to their low cost and simple fabrication methods. Use of non-reinforced polymers as structure materials is limited by low level of their mechanical properties such as tensile strength of one of the strongest polymers - epoxy resin is 20000 psi (140 MPa). In addition to relatively low strength, polymer materials possess low impact resistance.

1.4.2. On the basis of Material Structure

1.4.2.1 Particulate Composites

These are of two types

- Particulate Composites with random orientation of particles.
- Composites with preferred orientation of particles. Dispersed phase of these materials consists of two-dimensional flat platelets (flakes), laid parallel to each other.

Effect of the dispersed particles on the composite properties depends on the particles dimensions. Very small particles (less than 0.25 micron in diameter) finely distributed in the matrix impede the movement of dislocations and deformation of the material. Such strengthening effect is same

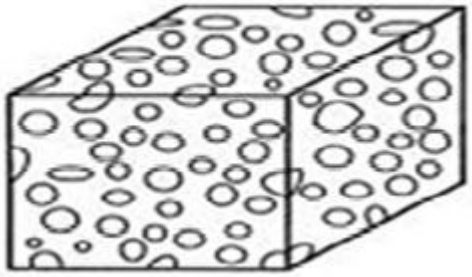

Figure 1.1: Particle reinforcement

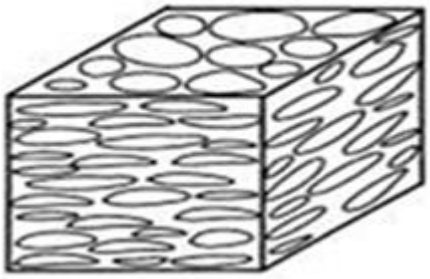

Figure 1.2: Flake reinforcement

to the precipitation hardening. In contrast to the precipitation hardening, which disappears at elevated temperatures when the precipitated particles dissolve in the matrix, dispersed phase of particulate composites is usually stable at high temperatures, so the strengthening effect is retained. Many of composite materials are designed to work in high temperature applications. Large dispersed phase particles have low strengthening effect but they are capable to share load applied to the material, resulting in increase of stiffness and decrease of ductility. Hard particles dispersed in a softer matrix increase wear and abrasion resistance. Soft dispersed particles in a harder matrix improve machinability (lead particles in steel or copper matrix) and reduce co efficient of friction.

1.5.2.2 Fibrous Composites

Short fibre reinforced composites. Short fibre reinforced composites consist of a matrix reinforced by a dispersed phase in form of discontinuous fibres.

- Composites with random orientation of fibers.
- Composite with preferred orientation of fibers.

Long-fibre reinforced composites. Long-fibre reinforced composites consist of a matrix reinforced by a dispersed phase in form of continuous fibres.

- Unidirectional orientation of fibres.
- Bidirectional orientation of fibres.

Figure 1.3: Fiber composite

Effect of the strength increase becomes much more significant when the fibers are arranged in a particular direction and a stress is applied along the same direction. The strengthening effect is higher in long-fiber reinforced composites than in short-fiber reinforced composites. Short-fiber reinforced composites, consisting of a matrix reinforced with a dispersed phase in form discontinuous fibers have a limited ability to share load. Load applied to a long-fiber reinforced composite, is carried mostly by the dispersed phase - fibers. Matrix in such materials serves only as a binder of the fibers keeping them in a desired shape and protecting them from mechanical or chemical damages.

1.5.2.3 Laminate Composites

When a fibre reinforced composite consists of several layers with different fibre orientations, it is called multilayer composite. Laminate composites provide increased mechanical strength in

two directions and only in one direction, perpendicular to the preferred orientations of the fibers or sheet, mechanical properties of the material are low. Laminar composite is composed of two-dimensional sheets or panels that have a preferred high strength direction such as found in wood and continuous and aligned fiber-reinforced plastics.

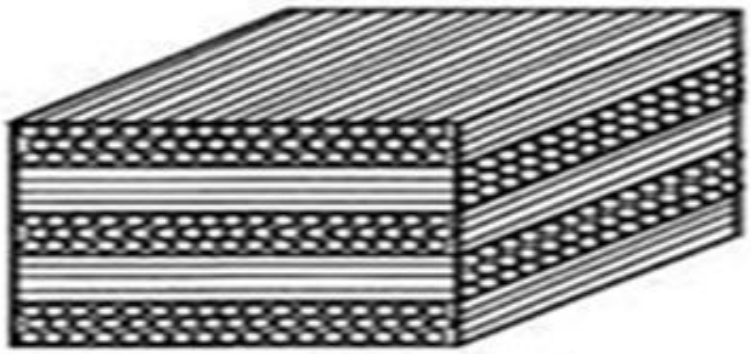

Figure 1.4: Laminated composite

The layers are stacked and subsequently cemented together such that the orientation of the high strength direction varies with each successive layer.

1.5 PROCESSING OF COMPOSITES

Metal matrix composite materials can be produced by many different techniques. The focus of the selection of suitable process engineering is the desired kind, quantity and distribution of the reinforcement components (particles and fibers), the matrix alloy and the application [12]. By altering the manufacturing method, the processing and the finishing, as well as by the form of the reinforcement components it is possible to obtain different characteristic profiles, although the same composition and amounts of the components are involved. Metal matrix composites can be made by liquid or solid state processes.

1.5.1 Liquid state fabrication of Metal Matrix Composites:

Liquid state fabrication of Metal Matrix Composites involves incorporation of dispersed phase into a molten matrix metal, followed by its Solidification. In order to provide high level of mechanical properties of the composite, good interfacial bonding (wetting) between the dispersed phase and the liquid matrix should be obtained. Wetting improvement may be

achieved by coating the dispersed phase particles (fibers). Proper coating not only reduces interfacial energy, but also prevents chemical interaction between the dispersed phase and the matrix.

The methods of liquid state fabrication of Metal Matrix Composites are:

a. Stir Casting
b. Infiltration
c. Gas Pressure Infiltration
d. Squeeze Casting Infiltration
e. Pressure Die Infiltration

1.8.1.1 Stir casting:

Stir Casting is a liquid state method of composite materials fabrication, in which a dispersed phase (ceramic particles, short fibers) is mixed with a molten matrix metal by means of mechanical stirring [fig. 1.5]. Stir Casting is the simplest and the most cost effective method of liquid state fabrication. The liquid composite material is then cast by conventional casting methods and may also be processed by conventional Metal forming technologies. In this process particles are often tend to form agglomerates, which can be only dissolved by intense stirring [12]. However, here gas access into the melt must be absolutely avoided, since this could lead to unwanted porosities or reactions. Careful attention must be paid to the dispersion of the reinforcement components, so that the reactivity of the components used is coordinated with the temperature of the melt and the duration of stirring, since reactions with the melt can lead to the dissolution of the reinforcement components. Because of the lower surface to volume ratio of spherical particles, reactivity is usually less critical with stirred particle reinforcement than with fibers.

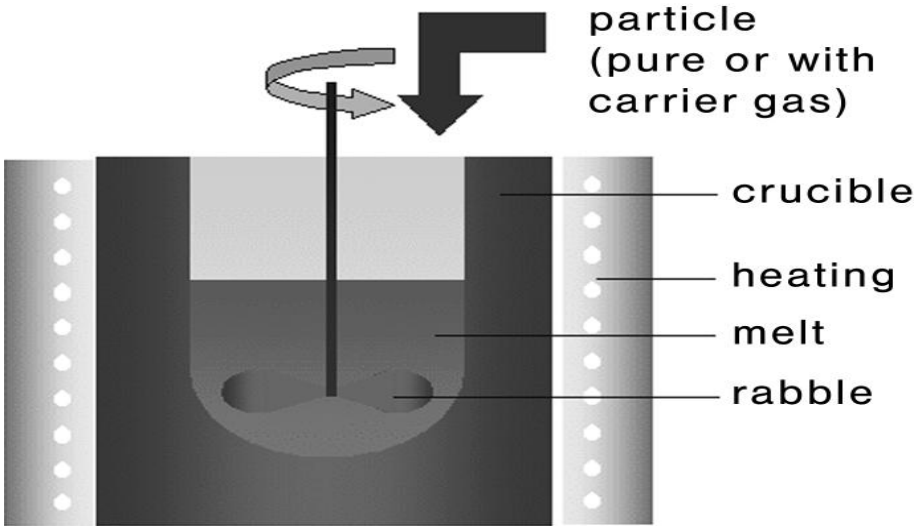

Figure 1.5: Stir casting [12]

Stir Casting is characterized by the following features:

i. Content of dispersed phase is limited (usually not more than 30% by volume).
ii. Distribution of dispersed phase throughout the matrix is not perfectly homogeneous:

    1. There are local clouds (clusters) of the dispersed particles (fibers)

    2. There may be gravity segregation of the dispersed phase due to a difference in the densities of the dispersed and matrix phase.

iii. The technology is relatively simple and low cost.

Distribution of dispersed phase may be improved if the matrix is in semi-solid condition. The method using stirring metal composite materials in semi-solid state is called Rheocasting. High viscosity of the semi-solid matrix material enables better mixing of the dispersed phase.

1.5.1.2 Infiltration:

Infiltration is a liquid state method of composite materials fabrication, in which a preformed dispersed phase (ceramic particles, fibers, woven) is soaked in a molten matrix metal, which fills the space between the dispersed phase inclusions. The motive force of an infiltration process0 may be either capillary force of the dispersed phase (spontaneous infiltration) or an

external pressure (gaseous, mechanical, electromagnetic, centrifugal or ultrasonic) applied to the liquid matrix phase (forced infiltration). Infiltration is one of the methods of preparation of tungsten-copper composites.

The principal steps of the technology are as follows:

i. Tungsten Powder preparation with average particle size of about 1-5microns.
ii. Optional step: Coating the powder with nickel. Total nickel content is about 0.04%.
iii. Mixing the tungsten powder with a polymer binder.
iv. Compacting the powder by a molding method (Metal injection molding, die pressing, isostatic pressing). Compaction should provide the predetermined porosity level (apparent density) of the tungsten structure.
v. Solvent debinding
vi. Sintering the green compact at 2200-2400F (1204-1315 ºC) in Hydrogen atmosphere for 2 hours. Placing the sintered part on a copper plate (powder) in the infiltration/sintering furnace.
vii. Infiltration of the sintered tungsten skeleton porous structure with copper at 2100-2300F (110-1260 ºC) in either hydrogen atmosphere or vacuum for 1 hour.

1.5.1.3 Gas Pressure Infiltration:

Gas Pressure Infiltration is a forced infiltration method of liquid phase fabrication of Metal Matrix Composites. It is using a pressurized gas for applying pressure on the molten metal and forcing it to penetrate into a preformed dispersed phase [fig. 1.6]. In gas pressure infiltration the melt infiltrates the preform with a gas applied from the outside [12]. A gas that is inert with respect to the matrix is used. The melting of the matrix and the infiltration take place in a suitable pressure vessel.

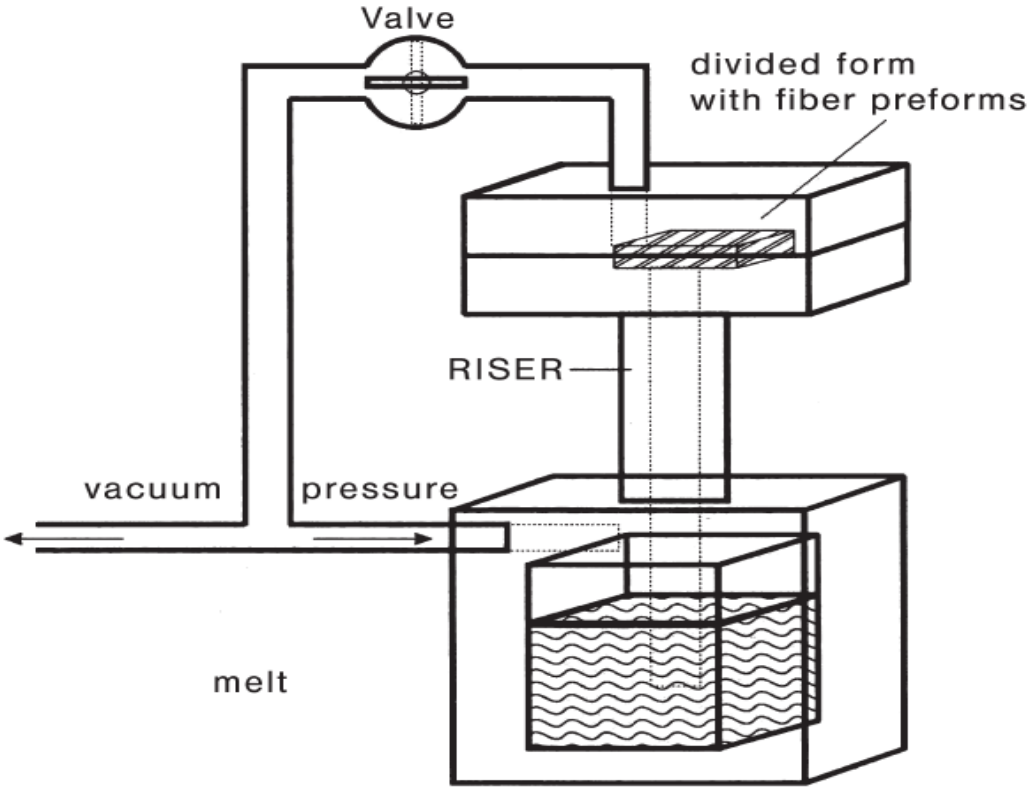

Figure 1.6: Gas pressure infiltration [12]

Gas Pressure Infiltration method is used for manufacturing large composite parts. The method allows using non-coated fibers due to short contact time of the fibers with the hot metal. In contrast to the methods using mechanical force, Gas Pressure Infiltration results in low damage of the fibers.

1.5.1.4 Squeeze Casting Infiltration:

Squeeze Casting Infiltration is a forced infiltration method of liquid phase fabrication of Metal Matrix Composites, using a movable mold part (ram) for applying pressure on the molten metal and forcing it to penetrate into a performed dispersed phase, placed into the lower fixed mold part [fig1.7]. Squeeze Casting Infiltration method is similar to the Squeeze casting technique used for metal alloys casting. Squeeze casting or pressure casting are the most common manufacturing variants for metal matrix composite [12]. After a slow mold filling the melt solidifies under very high pressure, which leads to a fine-grained structure. In comparison with

die-casted parts the squeeze-casted parts do not contain gas inclusions, which permit thermal treatment of the produced parts.

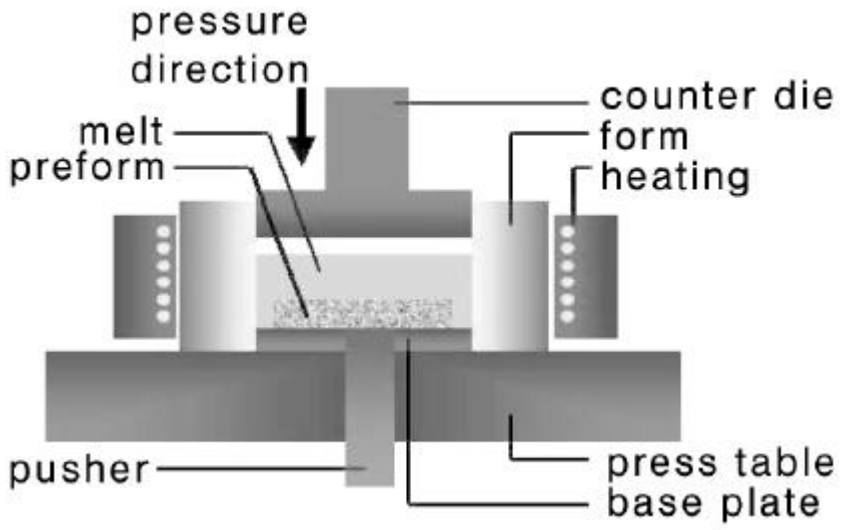

Figure 1.7: Squeeze casting infiltration [12]

Squeeze Casting Infiltration process has the following steps:

1. A preform of dispersed phase (particles, fibers) is placed into the lower fixed mold half.
2. A molten metal in a predetermined amount is poured into the lower mold half.
3. The upper movable mold half (ram) moves downwards and forces the liquid metal to infiltrate the preform.
4. The infiltrated material solidifies under the pressure.
5. The part is removed from the mold by means of the ejector pin.

The method is used for manufacturing simple small parts (automotive engine pistons from aluminium alloy reinforced by alumina short fibers).

1.5.1.5 Pressure Die Infiltration:

Pressure Die Infiltration is a forced infiltration method of liquid phase fabrication of Metal Matrix Composites, using a die casting technology, when a preformed dispersed phase (particles, fibers) is placed into a die (mold) which is then filled with a molten metal entering

the die through a sprue and penetrating into the preform under the pressure of a movable piston (plunger) [fig. 1.8].

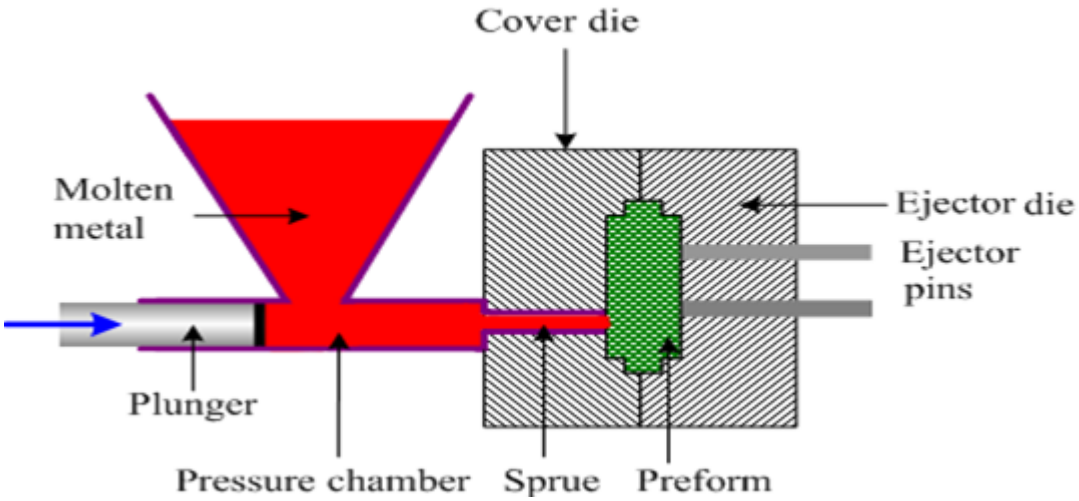

Figure 1.8: Pressure die infiltration [13]

1.5.2 Solid state fabrication of Metal Matrix Composites:

Solid state fabrication of Metal Matrix Composites is the process, in which Metal Matrix Composites are formed as a result of bonding matrix metal and dispersed phase due to mutual diffusion occurring between them in solid states at elevated temperature and under pressure. Low temperature of solid state fabrication process (as compared to Liquid state fabrication of Metal Matrix Composites) depresses undesirable reactions on the boundary between the matrix and dispersed (reinforcing) phases.

Metal Matrix Composites may be deformed also after sintering operation by rolling, Forging, pressing, Drawing or Extrusion. The deformation operation may be either cold (below the recrystallization temperature) or hot (above the recrystalization temperature). Deformation of sintered composite materials with dispersed phase in form of short fibers results in a preferred orientation of the fibers and anisotropy of the material properties (enhanced strength along the fibers orientation).

There are two principal groups of solid state fabrication of Metal Matrix Composites:

a. Diffusion bonding

b. Sintering

1.5.2.1 Diffusion Bonding

Diffusion Bonding is a solid state fabrication method, in which a matrix in form of foils and a dispersed phase in form of long fibers are stacked in a particular order and then pressed at elevated temperature [14].The finished laminate composite material has a multilayer structure. Diffusion Bonding is used for fabrication of simple shape parts (plates, tubes).

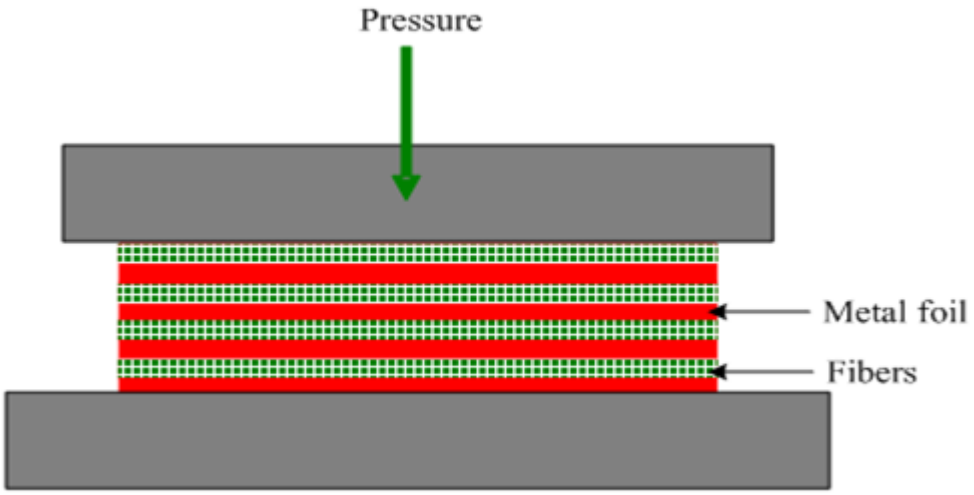

Figure 1.9: Diffusion bonding [13]

Variants of diffusion bonding are roll bonding and wire/fiber winding. Roll Bonding is a process of combined rolling (hot or cold) strips of two different metals (e.g. steel and aluminum alloy) resulted in formation of a laminated composite material with a metallurgical bonding between the two layers. Wire/fiber Winding is a process of combined winding continuous ceramic fibers and metallic wires followed by pressing at elevated temperature.

1.5.2.2 Sintering:

Sintering fabrication of metal matrix composites is a process, in which a powder of a matrix metal is mixed with a powder of dispersed phase in form of particles or short fibers for subsequent compacting and sintering in solid state (sometimes with some presence of liquid). Sintering is the method involving consolidation of powder grains by heating the "green" compact part to a high temperature below the melting point, when the material of the separate

particles diffuse to the neighbouring powder particles. In contrast to the liquid state fabrication of Metal Matrix Composites, sintering method allows obtaining materials containing up to 50% of dispersed phase [14]. When sintering is combined with a deformation operation, the fabrication methods are called:

i. Hot Pressing Fabrication of Metal Matrix Composites
ii. Hot Isostatic Pressing Fabrication of Metal Matrix Composites
iii. Hot Powder Extrusion Fabrication of Metal Matrix Composites

i. Hot Pressing Fabrication of Metal Matrix Composites:

In this fabrication process sintering under a unidirectional pressure applied by a hot press. The fabrication stages of hot pressing process is done in three stages.

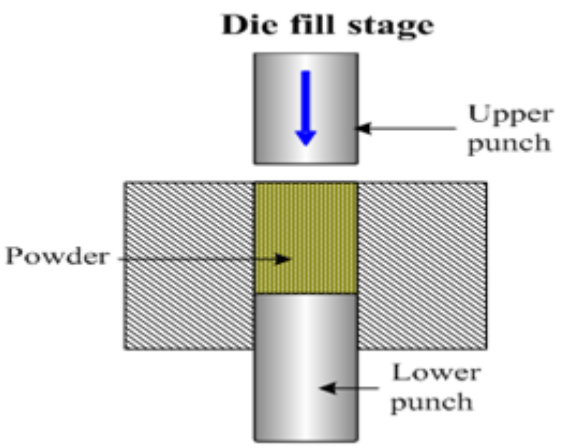

Figure 1.10: Die fill stage [13]

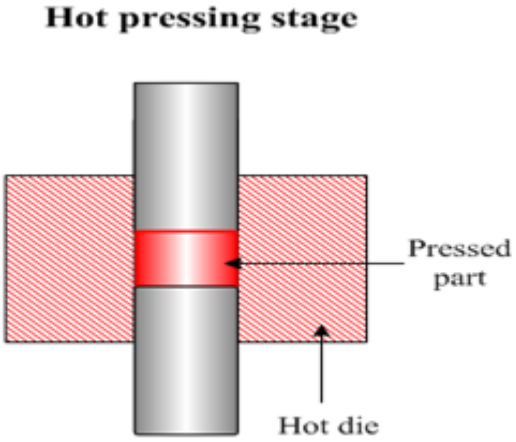

Figure 1.11: Hot pressing [13]

In the die fill stage [fig. 1.10], powder is put into the die and in second stage. There is hot pressing is to be done to pressed part in the die [fig. 1.11].

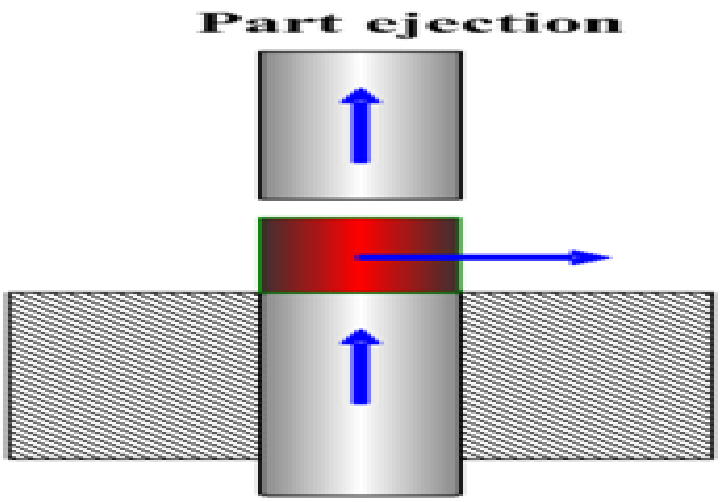

Figure 1.12: Part ejection [13]

In the last stage [fig 1.8], part is ejected, for this upper punch moves up to eject the part from the die.

ii. Hot Isostatic Pressing Fabrication of Metal Matrix Composites:

In this process of fabrication sintering under a pressure applied from multiple directions through a liquid or gaseous medium surrounding the compacted part and at elevated temperature [fig. 1.13].

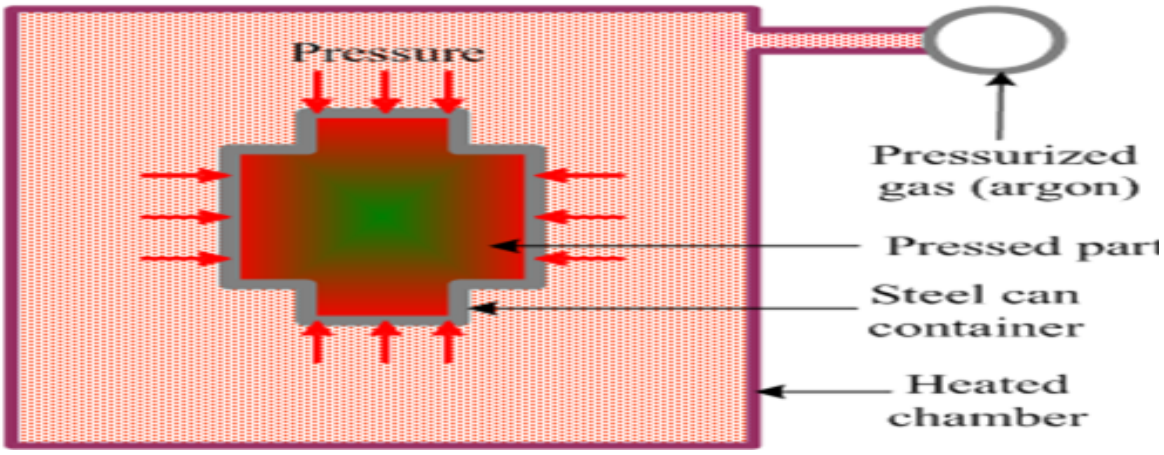

Figure 1.13: Hot isostatic pressing [13]

iii. Hot Powder Extrusion Fabrication of Metal Matrix Composites:

In this process sintering is under a pressure applied by an extruder at elevated temperature. It is of two type, forward extrusion and backward extrusion [fig. 1.14].

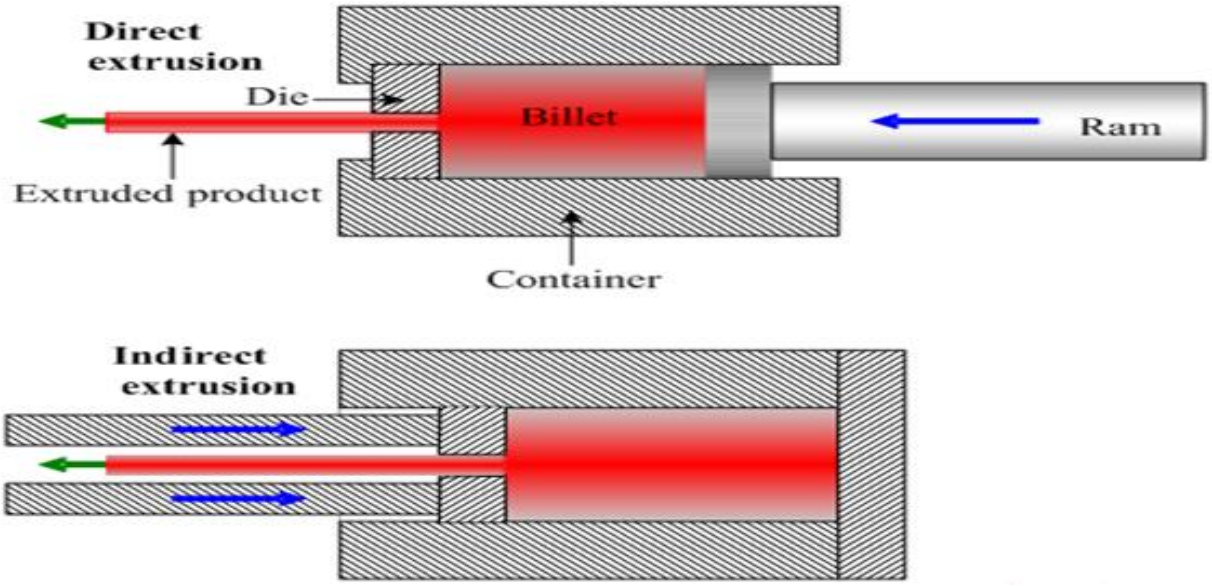

Figure 1.14: Extrusion [13]

1.6 APPLICATIONS:

Applications of metal matrix composites can be conveniently grouped by market area, since each area requires set of properties and cost that result in particular subsets of metal matrix composite materials being of primary interest [14]. The primary markets for MMCs are divided into aerospace, automotive, commercial and industrial products, and electronics packaging which represents the area of greater interest.

1. Aerospace applications are the original driving force for metal matrix composite development. This is due to the quest for weight reduction for improved performance and payload capabilities combined with high value placed on weight savings. Examples for aerospace application are aircraft structure, aero engine, space structure and other space applications.

2. In the automotive market, properties of interest to the automotive engineer include increased stiffness, wear resistance, and improved cycle fatigue resistance. Weight saving is also important in automotive applications for achieving performance

improvements with much lower cost. Examples for automotive applications are engines, brake system, driveshaft and other automotive applications

3. In commercial and industrial sector, improved performance is highly valued. As a result many of materials that gain favour in aerospace industry market are also applied in this sector also. Examples for commercial and industrial sector are recreational, computer hard disk drives and other industrial applications.

1.7 DEVELOPMENT OBJECTIVE:

The development objectives for metal composite materials are:

i. Increase in yield strength and tensile strength at room temperature and above while maintaining the minimum ductility or rather toughness
ii. Increase in creep resistance at higher temperatures compared to that of conventional alloy
iii. Increase in fatigue strength, especially at higher temperatures
iv. Improvement of thermal shock resistance
v. Improvement of corrosion resistance
vi. Increase in Young's modulus
vii. Reduction of thermal elongation

These are advantages metal matrix composites with respect to unreinforced metals and polymer matrix composites.

Advantage with respect to unreinforced metals:

i. Major weight savings due to strength-to weight ratio
ii. Exceptional dimensional stability
iii. Higher elevated temperature stability, i.e., creep resistance
iv. Significantly improved cyclic fatigue characteristics

With respect to Polymer matrix composite, MMCs offer these advantages:

i. Higher strength and stiffness
ii. Higher service temperatures

iii. Higher electrical conductivity (grounding, space charging)
iv. Higher thermal conductivity
v. Better transverse properties
vi. Improved joining characteristics
vii. Radiation survivability.
viii. Little or no contamination.[15-17]

1.8 THEORY OF WEAR

Wear occurs as a natural consequence when two surfaces with a relative motion interact with each other. Wear may be defined as the progressive loss of material from contacting surfaces in relative motion. Scientists have developed various wear theories in which the Physico-Mechanical characteristics of the materials and the physical conditions (e.g. the resistance of the rubbing body and the stress state at the contact area) are taken in to consideration. In 1940 Holm starting from the atomic mechanism of wear, calculated the volume of substance worn over unit sliding path.

Kragelski developed the fatigue theory of wear. Because of the Asperities in real bodies their interactions on sliding is discrete and contact occurs at individual locations, when taken together, form the real contact area. Under normal force the asperities penetrate into each other or are flattened out and in the region of real contact points corresponding stress and strain rise. In sliding, a fixed volume of material is subjected to the many times repeated action, which weakens the material and leads finally to rupture.

1.8.1Types of wear

In most basic wear studies where the problems of wear have been a primary concern, the so-called dry friction has been investigated to avoid the influences of fluid lubricants.

Dry friction' is defined as friction under not intentionally lubricated conditions but it is well known that it is friction under lubrication by atmospheric gases, especially by oxygen. Wear can be classified in 5 types.

(1) Abrasive (2) Adhesive (3) Erosive (4) Surface fatigue (5) Corrosive.

1.8.1.1 Abrasive wear

Abrasive wear can be defined as wear that occurs when a hard surface slides against and cuts groove from a softer surface. It can be account for most failures in practice. Hard particles or asperities that cut or groove one of the rubbing surfaces produce abrasive wear. This hard material may be originated from one of the two rubbing surfaces. In sliding mechanisms, abrasion can arise from the existing asperities on one surface (if it is harder than the other), from the generation of wear fragments which are repeatedly deformed and hence get work hardened for oxidized until they became harder than either or both of the sliding surfaces, or from the adventitious entry of hard particles, such as dirt from outside the system. Two body abrasive wear occurs when one surface (usually harder than the second) cuts material away from the second, although this mechanism very often changes to three body abrasion as the wear debris then acts as an abrasive between the two surfaces.

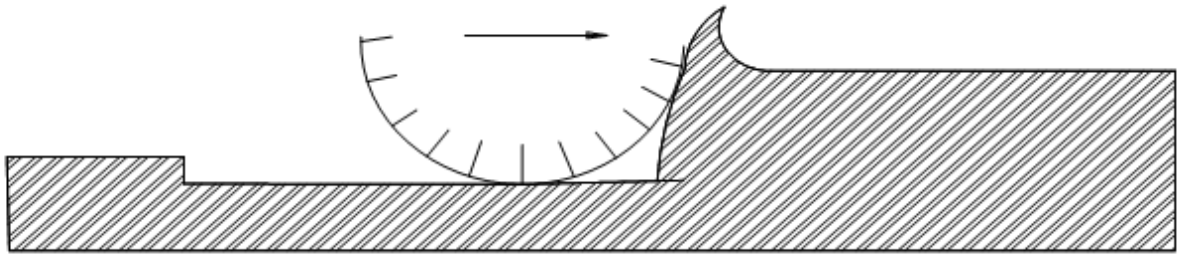

Figure 1.15: Abrasion wear mechanism

Abrasives can act as in grinding where the abrasive is fixed relative to one surface or as in lapping where the abrasive tumbles producing a series of indentations as opposed to a scratch. According to the recent tribological survey, abrasive wear is responsible for the largest amount of material loss in industrial practice.

1.8.1.2 Adhesive wear

Adhesive wear can be defined as wear due to localized bonding between contacting solid surfaces leading to material transfer between the two surfaces or the loss from either surface. For adhesive wear to occur it is necessary for the surfaces to be in intimate contact with each other. Surfaces, which are held apart by lubricating films, oxide films etc. reduce the tendency for adhesion to occur.

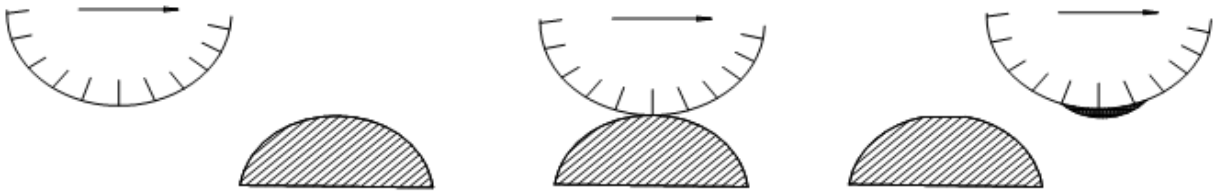

Figure 1.16: Adhesive wear mechanism

1.8.1.3 Erosive wear

Erosive wear can be defined as the process of metal removal due to impingement of solid particles on a surface. Erosion is caused by a gas or a liquid, which may or may not carry, entrained solid particles, impinging on a surface. When the angle of impingement is small, the wear produced is closely analogous to abrasion. When the angle of impingement is normal to the surface, material is displaced by plastic flow or is dislodged by brittle failure.

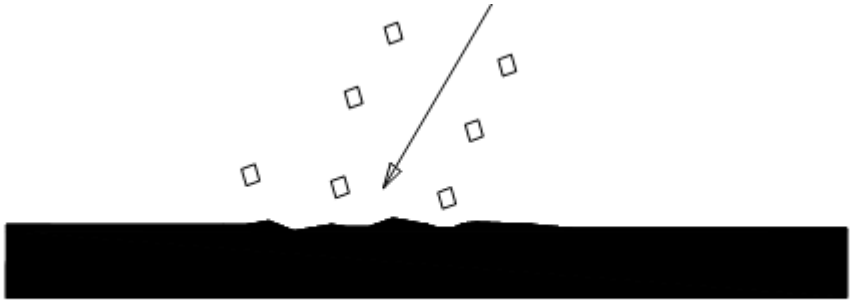

Figure 1.17: Erosive wear mechanism

1.8.1.4 Surface fatigue wear

Wear of a solid surface caused by fracture arising from material fatigue. The term ‘fatigue’ is broadly applied to the failure phenomenon where a solid is subjected to cyclic loading

involving tension and compression above a certain critical stress. Repeated loading causes the generation of micro cracks, usually below the surface, at the site of a pre-existing point of weakness. On subsequent loading and unloading, the micro crack propagates. Once the crack reaches the critical size, it changes its direction to emerge at the surface, and thus flat sheet like particles is detached during wearing. The number of stress cycles required to cause such failure decreases as the corresponding magnitude of stress increases. Vibration is a common cause of fatigue wear.

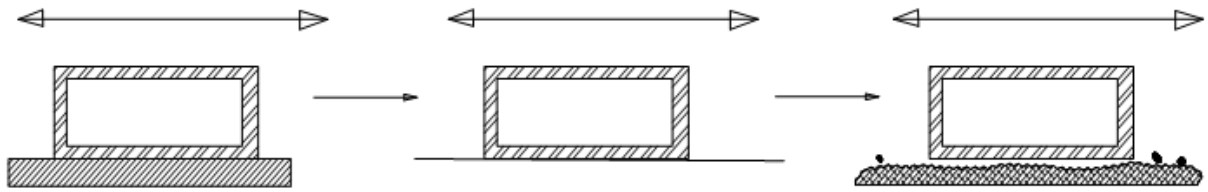

Figure 1.18: Surface fatigue wear mechanism

1.8.1.5 Corrosive wear

Most metals are thermodynamically unstable in air and react with oxygen to form an oxide, which usually develop layer or scales on the surface of metal or alloys when their interfacial bonds are poor. Corrosion wear is the gradual eating away or deterioration of unprotected metal surfaces by the effects of the atmosphere, acids, gases, alkalis, etc. This type of wear creates pits and perforations and may eventually dissolve metal parts.[18]

1.8 ORGANIZATION OF THESIS

The thesis has been organized in nine chapters. Brief description of the contents of each chapter is given below:

Chapter 1 highlights the introduction about the aluminum metal matrix composites. In this chapter types of composites and various processes to produce composites are discussed. This chapter gives brief knowledge about the wear and types of wear in case of materials.

Chapter 2 presents an available literature of aluminium composites. This chapter gives information about the research publications studied in case of composite to know about the different contribution by different researchers. Summary of the literature and gap in literature also discussed.

Chapter 3 presents the area of research work to be undertaken has been identified. Objective and work plan also discussed. Methodology to be adopted also described in brief.

Chapter 4 presents the analysis and results of the micro hardness. Results after the Analysis of Variance (ANOVA) and Taguchi Signal-to-Noise ratio are outlined in this chapter. Main effect plot for micro hardness are discussed in this chapter. Optimal design conditions have been discussed.

Chapter 5 presents the analysis and results of the wear rate with time and sliding distance. Results after the Analysis of Variance (ANOVA) and Taguchi Signal-to-Noise ratio are outlined in this chapter. Main effect plot for wear rate are discussed in this chapter. Optimal design conditions have been discussed.

Chapter 6 presents the analysis of microstructure of composites. Optical micrographs and SEM images at different magnifications are discussed in this chapter to see the presence and distribution of Al_2O_3 particles. Also at higher magnification particles and metal interface are studied in this chapter.

Chapter 7 presents the analysis of surface properties. XRD and EDS analysis has been completed to understand the different elemental phases present in the composites at different compositional level.

Chapter 8 presents the results, conclusions and recommendations from the experimental work.

CHAPTER 2

LITERATURE REVIEW

2.1 REVIEW OF LITERATURE

This chapter presents a review of the literature data available on the effect of various reinforcement types, their size and volume fraction, ageing behavior with Al based MMCs. Matrices can be selected from a number of Aluminium alloys and many reinforcement types SiC, B_4C, Al_2O_3 etc. are available in different sizes, morphologies and volume fractions. These reinforcements can be combined with the different matrices, resulting in large composite systems. Furthermore, several different processing routes, such as powder metallurgy, stir casting, squeeze casting, hot extrusion etc. Composite structures have shown universally a savings of at least 20% over metal counterparts and a lower operational and maintenance cost.

Rahimian et al.[19] studied the effect of production parameters on wear resistance of Al–Al_2O_3 composites. Alumina powder with a particle size of 12, 3 and 48 μ and pure aluminum powder with particle size of 30μ were used. The amount of added alumina powder was up to 20%. The range of sintering temperature and time were 500, 550 and 600°C and 30, 45, 60 and 90 minutes respectively. It was found that increasing sintering temperature results in increasing density, hardness and wear resistance and homogenization of the microstructure. However at certain sintering temperatures and time, considerable grain growth and reduction of hardness value occurred, leading to the degradation of wear resistance. The results showed that at high alumina content, relative density of the composite increases. After raising the particle size of alumina, relative density initially increases and then drops to lower values. Increasing weight percent of alumina powder leads to higher hardness and consequently improves the wear resistance of Al–Al_2O_3 composite. The use of fine alumina particles has a similar effect on hardness and the wear resistance. Finally, a finer grain size was observed, at high amount and low size of the reinforcement particle.

Rao and Das [20] studied the effect of SiC content and sliding speed on the wear behaviour of aluminium alloy and composite was studied using pin-on-disc apparatus against EN32 steel counterface. These tests were conducted at varying SiC particles in 10, 15 and 25 wt.% and

sliding speeds of 0.52, 1.72, 3.35, 4.18 and 5.23 m/s for a constant sliding distance of 5000 m. The results revealed that as the SiC content increases the wear rate and temperature decreases, but reverse trend can be observed for coefficient of friction.

Sajjadi et al. [21] performed the research on nano and micro-composites (A356/Al_2O_3) with different weight percent of particles were fabricated by two melt techniques such as stir-casting and compo-casting. Microstructural characterization was investigated by optical (OP) and scanning electron microscopy (SEM). Tensile, hardness and compression tests were carried out in order to identify mechanical properties of the composites. The results of micro structural study revealed uniform distribution, grain refinement and low porosity in micro and nano-composite specimens. The mechanical results showed that the addition of alumina (micro and nano) led to the improvement in yield strength, ultimate tensile strength, compression strength and hardness. It was indicated that type of fabrication process and particle size were the effective factors influencing on the mechanical properties. Decreasing alumina particle size and using compo-casting process obtained the best mechanical properties.

Swamy et al.[22] proposed that Addition of SiC as reinforcement in Al6061 alloy system improves its hardness, tensile strength and wear resistance. In the present investigation Al6061–SiC composites was fabricated by liquid metallurgy route with percentages of SiC varying from 4 wt% to 10 wt% in steps of 2 wt%. The cast matrix alloy and its composites have been subjected to solutionizing treatment at a temperature of 530°C for 1 h followed by quenching in different media such as air, water and ice. The quenched samples are then subjected to both natural and artificial ageing. Microstructural studies have been carried out to understand the nature of structure. Mechanical properties such as microhardness, tensile strength, and abrasive wear tests have been conducted both on matrix Al6061 and Al6061–SiCp composites before and after heat treatment. However, under identical heat treatment conditions, adopted Al6061–SiCp composites exhibited better microhardness and tensile strength reduced wear loss when compared with Al matrix alloy.

Prabu et al. [23] studied high silicon content aluminium alloy–silicon carbide metal matrix composite material, with 10%SiC were successfully synthesized, using different stirring speeds and stirring times. The microstructure of the produced composites was examined by optical

microscope and scanning electron microscope. The Brinell hardness test was performed on the composite specimens from base of the cast to top. The results revealed that stirring speed and stirring time influenced the microstructure and the hardness of composite. Microstructure analysis revealed that at lower stirring speed with lower stirring time, the particle clustering was more. Increase in stirring speed and stirring time resulted in better distribution of particles. The hardness test results also revealed that stirring speed and stirring time have their effect on the hardness of the composite. The uniform hardness values were achieved at 600 rpm with 10min stirring. But beyond certain stir speed the properties degraded again.

Wahab et al. [24] investigated the characterization of aluminum metal matrix composites reinforced with aluminum nitride. A graphite crucible and a stainless steel permanent mould was used to prepare the samples. Morphology of the composite and particle distribution were investigated by optical microscopy. The reinforcing particles were clearly shown present at the edges and around grains of silicon primary, silicon needles and inter-metallic compound of $FeMg_3Si_6Al_8$. The result of hardness test was 44 Hv for Al-Si matrix and increased to 89 Hv for an Al-Si composite reinforced with 5% wt.% AlN powder. The higher values in hardness indicated that the AlN particles contributed to the increase of hardness of the matrix.

Suresh et al. [25] researched on LM25 aluminum alloy metal matrix composites reinforced with weight fractions of micro and nano Al_2O_3 particles up to 10 wt. % were produced by stir casting. The composites thus produced were characterized for their mechanical properties such as hardness and tensile strength as well as for the dispersion of the micro and nano Al_2O_3 particles. The results reveal that stir casting could be an economical route for the production of nano composites. Nano particle reinforced MMCs exhibit better hardness and strength when compared to micro particles reinforced composites. Scanning electron microscopic observations of the microstructures revealed that the dispersion of the micron size particles where more uniform while nano particles led to agglomeration of the particles.

Wang et al. [26] was investigated, SiC particulate-reinforced Al composites were prepared by powder metallurgy (PM) method and conventional atmospheric sintering. Scanning electron microscope (SEM), X-ray diffraction (XRD) techniques were used to characterize the sintered composites. The effect of temperature on the density, hardness, strength, and microstructure of

composites& detailed failure behavior was analyzed. They had found that the segregation of SiC appeared at higher temperature. The highest micro-hardness of 80MPa occurred at 700° C. The strength tended to increase with the increasing temperature due to the formation of Al_2Cu. Both ductile and brittle fracture features were observed.

Hassan and Aigbodion [27] studied the microstructure and ageing behavior of Al–Si–Fe/Mg alloys produced through sand-casting route is presented. 4.0–6.0 wt% Mg was added to Al–Si–Fe alloy. Standard mechanical properties test samples were prepared from the sand cast 25 mm diameter by 45 mm rods. Thermal ageing was done for 6 h at 200 °C. The ageing characteristics of these alloys were evaluated using tensile properties, hardness values, impact energy and microstructure as criteria. The thermal aged samples exhibited higher yield strength, tensile strength and hardness values as the weight percent of magnesium increased up to 5 wt% in the Al–Si–Fe/Mg alloys as compared to as-cast samples. The optimum values were obtained at 5 wt. % Mg. Lower percent elongation, reduction in area and impact energy values were obtained for age-hardened Al–Si–Fe/Mg alloy samples as compared to as-cast samples. The increases in hardness values and strength during ageing are attributed to the formation of coherent and uniform precipitation in the metal lattice. It was found that the age-hardened showed acceleration in ageing compared to the as-cast alloy. However, the 5 wt% Mg addition to the alloy showed more acceleration to thermal ageing treatment. These results show that better mechanical properties are achievable by subjecting the as-cast Al–Si–Fe/Mg alloys to thermal ageing treatment.

Demir and Gunduz [28] studied the effect of aging on machinability behavior in 6061 Al-alloy was studied in artificially aged conditions and found that an increase in hardness of SHTA (solution heat treated and aged) 6061 Al-alloy with increase in aging time at 180 ºC can be explained by a diffusion assisted mechanism which causes an increase in the density of GP zones, distortion of lattice planes and hindering of dislocation movement by the impurity atoms. The strengthening effect can also be as a result of interference with the motion of dislocation, due to the formation of precipitates. Further increase in aging time decreases the hardness of the alloy. This could be due to coalescence of the precipitates into larger particles which will cause fewer obstacles to the movement of dislocation and hence the hardness starts to decrease. Unlike cutting forces, aging at different times for 180 ºC affected surface

roughness of workpieces considerably. This is due to its highest hardness value as the result of aging and easy disposal of the chips during machining.

Shivanand and Benal [29] studied the improvement in abrasive wear rate of as-cast and heat-treated Al (6061) alloy reinforced with 9% by weight of SiC particulate and 0, 1, 3 and 5% by weight of E-glass fiber subjected to different ageing durations. The liquid melt technique route is used to produce the castings. Castings were machined to the ASTM standards and T6 heat-treatment process is carried out. All the specimens were artificially aged to different durations like 1, 3, 5 and 7 h at a temperature of 175 ºC. It was found that the heat-treatment T65h was the one that provided the matrix greater hardness and therefore it was the one, which shows the heat-treated specimens, are the high wear resistance. The wear rate of the Al-based hybrid composites do not depend on type of reinforcement, but wear rate of the hybrid composites decreases with increasing the weight percentage of reinforcing materials. The abrasive wear resistance of Al-based hybrid composites may be controllably altered by thermal ageing. As-cast hybrid composites and 1 h aged hybrid composites provided relatively low resistance. Maximum wear resistance was achieved when the hybrid composites aged at 5 h condition, when the Al alloy contained a large number of coherent precipitates.

Zhang et al. [30] studied the influence of artificial aging (T6) on evaluation of microstructure changed and hardness of Al-Al_2O_3 composite produced by stir casting route. The Al2O3 particle reinforced previously was coated by electroless coating method to improve wetting system between Al-AC8H and Al_2O_3 when aluminium composites fabricated by stir casting route. The volume fraction of Al_2O_3 which added into Al melts was various from 2% to 22.5%. The stirring process was carried out at 500-700 rpm to achieve vortex in alumnium melt using graphite impeller for 15 minutes. The prepared aluminium composites then heat treated by T6 treatment with different aging time. Microstructure and hardness after T6 treatment were investigated. It was observed that microstructure changed after T6 while hardness increase after T6 due to the Mg2Si precipitation hardening was present in Al matrix as well as Si eutectic accumulated on the surface of Al_2O_3. It was found that the optimum hardness occurred after aging for 3 hours.

Yilmaz and Buytoz [31] studied the effects of volume fraction, Al_2O_3 particle size and effects of porosity in the composites on the abrasive wear resistance of compo-casting Al alloy MMCs have been studied for different abrasive conditions. It was seen that porosity in the composites is proportional to particle content. In addition, process variables like the stirring speed, and the position and diameter of the stirrer affect of the porosity content in a way similar to that observed for particle content. In addition, the abrasive wear rates of composites decreased more rapidly with increase in Al_2O_3 volume fraction in tests performed over 80 grades SiC abrasive paper than in tests conducted over 220 grade SiC abrasive paper. Furthermore, the wear rates decreased with increase in Al_2O_3 size for the composites containing the same amount of Al_2O_3. Hence, it is deduced that aluminium alloy composites reinforced with larger Al_2O_3 particles are more effective against abrasive wear than those reinforced with smaller Al_2O_3 particles. At the same time the results show that the beneficial effects of hard Al_2O_3 particles on wear resistance far surpassed that of the sintered porosity in the compocasting metal-matrix composites (MMCs). Nevertheless, the fabrication of composites containing soft particles such as graphite favors a reduction in the friction coefficient. For this reason graphite and copper were used in the matrix in different amounts to detect their effect on wear resistance. Finally, it was seen that wear rate of the composites decreased considerably with graphite additions.

Christy et al. [32] researched that Al-TiB_2 composite is a metal matrix composite (MMC) that can be manufactured using the in-situ salt-metal reaction. With TiB_2 as the particulate addition the properties of Al 6061 alloy can be greatly improved. A comparison of the mechanical properties and the microstructure of Al 6061 alloy with Al–TiB_2 metal matrix composite containing 12% by weight TiB_2 manufactured through the in-situ process.

Kumar et al. [33] presented the results of the studies conducted regarding hardness, tensile strength and wear resistance properties of Al6061-SiC and Al7075-Al_2O_3 composites. The composites are prepared using the liquid metallurgy technique, in which 2-6 wt.%'age of particulates were dispersed in the base matrix in steps of 2. The obtained cast composites of Al6061-SiC and Al7075-Al_2O_3 and the castings of the base alloys were carefully machined to prepare the test specimens for density, hardness, mechanical, tribological tests and as well as for microstructural studies as per ASTM standards. The SiC and Al_2O_3 resulted in improving the hardness and density of their respective composites. Further, the increased %'age of these

reinforcements contributed in increased hardness and density of the composites. The microphotographs of the composites studied revealed the uniform distribution of the particles in the matrix system. The experimental density values were agreed with that of the theoretical density values of the composites obtained using the rule of mixture for composites. The dispersed SiC in Al6061 alloy and Al_2O_3 in Al7075 alloy contributed in enhancing the tensile strength of the composites. The wear factor K obtained using computerized pin on disc wear tester with counter surface as EN31 steel disc (HRC60) and the composite pin as specimens, demonstrated the superior wear resistance property of the composites.

Reddy and Zitoun [34] used of investment casting process to fabricate 6063/Al_2O_3 metal matrix composites. The tensile properties have been evaluated. The EDS report confirmed the presence of $Al_5Cu_2Mg_8Si_6$, $Al_4CuMg_5Si_4$ and Mg_2Si compounds in the 6063/Al_2O_3 composites. The yield strength and fracture strength increase with increase in volume fraction of Al_2O_3, whereas ductility decreases. The fracture mode is ductile in 10% volume fraction composites and the brittle fracture is observed in 20% and 30% volume fraction composites.

Luangvaraunt et al. [35] fabricated aluminum matrix composites having Al_2O_3 by powder metallurgy method. Mixture of Al-1at.%MnO2 is cold compacted and hot forged to produce high density billet. Annealing of forged billet is subsequently carried out to generate Al_2O_3 in-situ from chemical reaction between Al and MnO2. Phase identification by X-ray diffraction technique verifies formation of Al_2O_3, as reinforcement phase, along with formation of MnO and Al6Mn phases, after annealing. MnO is the product of incomplete reduction of MnO2 by Al, while formation of Al6Mn is due to the release of manganese to the aluminum matrix beyond the limit of solubility. Tensile strength and ductility of the obtained Al/Al_2O_3 composite reaches 120 MPa and 8%, respectively, for forged billet which are anneal at 600°C for 30 h. annealing at higher temperature and for longer time results in decrease of tensile strength.

Chou et al. [36] proposed that porous aluminum oxide (Al_2O_3) formed by sintering in air at 1200^0C for 2 h. A356, 6061, and 1050 aluminum alloys were infiltrated into the preforms in order to fabricate Al_2O_3/A356, Al_2O_3/6061, and Al_2O_3/1050 composites, respectively, with different volumes of aluminum alloy content by squeeze casting. The volume contents of aluminum alloy in the composites were 10–40 vol.%. For the corresponding composites, the

hardness decreased dramatically from 610 to 213, 201, and 153HV, the four-points bending strength of the composites increased from 397 to 443, 435.1, and 418.7MPa, and the fracture toughness increased from 4.97 to 11.35, 11.15, and 10.98MPa m1/2 of Al_2O_3/A356, Al_2O_3/6061, and Al_2O_3/1050 composites, respectively. From SEM microstructural analysis, the porous ratio and the relative density of the composites were the most important factors to affect the mechanical properties and the three different toughening mechanisms, i.e. crack bridging, crack deflection, and crack branching in the composites.

Deshmanya and Purohit [37] presented the details of modeling the impact strength of Al7075 matrix reinforced with Al_2O_3 particulates in terms of Charpy-V in the forged condition. Stir-casting was used to produce the composites. Previous work by the authors showed that size and weight fraction of Al_2O_3 particulates were the most influential parameters in deciding the impact strength in the as-cast condition. Hence, in this work in addition to these, forging temperature and reduction in area are used to evaluate the effect of forging on the impact strength of forged composites. Factorial design of experiments with the four selected parameters, viz., size of reinforcement, weight percent, forging temperature and reduction in area, maintained at five levels is used to develop the model.

Nripjit et al. [38] presented that Al-Cu-Si (Al_2O_3)p composite containing 5% Al_2O_3 with particle size 0.220 µm were fabricated by modified stir casting technique. The addition of Al_2O_3 in A.384.1, Al Alloy was found to increase hardness, proof stress and ultimate tensile strength. The fabricated composites showed higher peak hardness and lower peak ageing time as compared to the unreinforced Al alloy. In addition, ageing is found to increase the strength, micro and macro-hardness of the fabricated composites. The reinforced composite samples with different particle sizes of Al_2O_3 i.e. 0.220, 0.106 and 0.053 µm were also fabricated to further investigate the interfacial characteristics. It is observed that the samples with small particle size exhibited clustering, whereas, the larger particles were found to mix up homogeneously in Al alloy matrix.

Das et al. [39] had studied the abrasive wear behavior of aluminium metal matrix composite reinforced with alumina and zircon sand particles have been carried out. Microstructures of the composites in as-cast condition show uniform distribution of particles and reveal better bonding

in the case of zircon particles reinforced composite compared to that in alumina particles reinforced composite. Abrasive wear resistance of both the composites improves with the decrease in particle size. It is observed that the alumina particle reinforced composite shows relatively poor wear resistance property compared to zircon-reinforced composite.

Daouda and Reif [40] had studied the influence of Al_2O_3 particulates on the precipitation and hardening behaviour of the A356 Al– Al_2O_3 composites**.** It was found that the $MgAl_2O_4$ spinel formed at the interface led to Mg depletion in the matrix and subsequently to lesser age hardening in the composites. Therefore, it was necessary for the composite matrix to have a higher Mg concentration prior to casting to achieve the same level of hardening in the composite as in the unreinforced. The hardening kinetics is enhanced by Al_2O_3 particulates because the precipitation preferentially develops on the dislocation lines that increased due to coefficient of thermal expansion mismatch between the matrix and reinforcement.

Narayan et al. [41] studied on dry sliding wear behaviour of Al alloy 2024 Al_2O_3 particle metal matrix composites and have shown that the Al 2014, 15 vol% Al_2O_3 composite shows better seizure resistance than does the unreinforced alloy in the peak aged condition and also in the as-extruded condition the wear resistance of the unreinforced alloy is better than that of composite.

Liu et al. [42] studied the Effects of different impact angles such as 45°and 90°on the erosion-abrasion properties of Al-Mn alloy and its composites reinforced with Al_2O_3 particulates were studied by rotating erosion-abrasion test, and the failure mechanism were analyzed. The results showed that the as-cast Al-Mn alloy is composed of aluminium-manganese solid solution, MnAl6 and Al11Mn4 phase, while the δ-Al_2O_3 particles are included in the composites besides the aforementioned microstructures. The cumulative mass loss of the Al-Mn alloy and its composites at 45° are both more than those at 90°, however, the loss of the composites are lower than those of the Al-Mn alloy, suggesting that the former possesses more excellent erosion-abrasion resistance properties.

Li et al. [43] analyzed, Al-2%Mn alloy matrix composites reinforced with Al_2O_3 particulates was fabricated by stirring cast, and the composites, by using a variety of analytical techniques, such as XRD, SEM, EDS, Brinell hardness tester, ring-on-block tribometer, and erosion-

corrosion tester. The results showed that the Al_2O_3,δcomposites in as cast condition is mainly composed of Al, MnAl6 and Al11Mn4 phase, and the Al_2O_3 particles are dispersed uniformly in the Al matrix. Compared with the base aluminium and the Al-2%Mn alloy, the HB hardness of the composites is increased significantly, and the wear loss is far less under the SO4•Cl-Na•Ca• Mg corrosive alkalescent aqueous solution lubricated condition. The erosive-corrosive wear rates of the composites are lower than those of the Al-2%Mn alloy irrespective of the rotational speed or the size of grinding particles. The Al_2O_3 particulates reinforced Al-2%Mn alloy matrix composites possesses a good wear-resistance and erosion-corrosion resistance due to its higher hardness.

Pruthviraj [44] described the fabrication and testing of zinc aluminium – based metal matrix composites (MMCs) reinforced with silicon carbide particles cast in sand moulds containing metallic (copper, steel and cast iron), chills respectively. SiC particles (of size 50-100µm) are added to the matrix. The dispersoid added was in steps of 3 wt. % (from 3 wt.% to 12 wt.%). The resulting composites cast were tested for their strength, hardness and wear resistance. Micro structural studies indicate good and uniform bonding between the matrix and the dispersoid. Strength and hardness increase by up to 9 wt.% of the SiC content and is highly dependent on the location of the casting from where the test specimens are taken. In addition, the wear resistance (dry and slurry wear) is significantly affected by the strength and hardness of the composite developed. It was inferred that a small amount of SiC particles are sufficient to cause a fairly large change in mechanical properties.

Kok and Ozdin [45] analyzed sliding wear tests on 10, 20 and 30wt.% Al_2O_3 particles reinforced 2024 aluminium alloy composites fabricated by a vortex method were carried out by using a pin-on-disc abrasion test apparatus where the sample slid against SiC abrasive papers of 20 (600 grit), 46 (320 grit) and 60µm (240 grit) under the loads of 2N and 5N at the room conditions, and the effects of sliding distance, Al_2O_3 particle content and size, SiC abrasive grit size and wear load on the wear properties of the composites were systematically investigated. For determination of the wear mechanisms of the composites, the worn surfaces were examined using scanning electron microscopy (SEM). It has been found that the wear resistance of the composites was significantly larger than that of the aluminium alloy, and increased with increasing Al_2O_3 particles content and size, and decreased with increasing the sliding distance,

the wear load and the abrasive grit size. The effect of Al_2O_3 particle size on the wear resistance was more significant than that of the particle content.

Curle and Ivanchev [46] rheocasted of plates in Al alloy 359 reinforced with SiC at 11%, 27% and 50% (volume fractions) exhibits the capability of the council for scientific and industrial research-rheocasting system sin rheo-processing and high pressure die casting of SiC metal matrix composites. The metal matrix consisting of nearly spherical proeutectic α(Al) globules was produced. Spheroidization of fibrous eutectic silicon took place upon heat treatment of the as-cast metal matrix composites (MMCs). Hardness increases as the volume fractions of SiC increases. Wear rates of the MMCs in the F and T6 heat treatment conditions were assessed with a metallographic preparation machine. It is found that the 11% SiC MMC wear rate is higher on SiC abrasives compared with the 50% SiC MMC wear rate due to wear of the aluminum matrix. This trend is reversed on diamond abrasives due to pull-out of the irregular shaped composite particles. The 50% SiC MMC suffers from composite particle fracture porosity after high pressure die casting.

Wang et al. [47] studied the effects of Al_2O_3 particle size on the arc erosion behavior of the ceramic-reinforced Al_2O_3/Cu composite, Al_2O_3/Cu composites with different sizes of Al_2O_3 particles were prepared by powder metallurgy, the effect of Al_2O_3 particle size on the characteristics of arc motion was studied, and the mechanism of arc erosion of Al_2O_3/Cu composites was discussed as well. The results show that with decrease in the size of Al_2O_3 particles, the erosion area increases significantly and the erosion pits become shallower. The vacuum breakdown is preferred to appear in the area between Al_2O_3 particle and the copper matrix.

Umanath et al. [48] fabricated an Al6061alloy with mixtures of SiC and Al_2O_3 particles by stir casting method and their wear resistance and Co-efficient of Friction has been investigated as a function of applied load and Volume fraction of the particles. The dry sliding wear properties of the hybrid composites and that of Al6061 unreinforced alloy at room temperature were investigated by using Pin-on-disk wear testing machine at a constant sliding velocity of 2.09 m/s and sliding distance of 1884m over a various loads of 29.43N, 39.24N and 49.05N (3, 4 and 5 kgf) for particle volume fraction ranging from 5-25%. The results showed that, the

reinforcement of the metal matrix with SiC and Al_2O_3 particulates up to a volume fraction of 25% reduces the wear rate at room temperature. The results also showed that the wear of the test specimens increase with the increasing load and sliding distance. The coefficient of friction slightly decreases with increasing volume content of reinforcements. Micro hardness of the specimens at the room temperature was also measured before and after the wear tests by Vickers hardness testing machine. The micro hardness of the hybrid composite test specimens increases with increasing volume fraction of particulates reinforcement. The optical micrographs taken for the micro structure analysis of the hybrid composite specimens showed that the SiC and Al_2O_3 particulates are uniformly distributed in the matrix. The wear surfaces were examined by scanning electron microscopy, which showed that the large grooved regions and cavities with ceramic particles were found on the worn surface of the composite alloy. This indicates an abrasive wear mechanism which is essentially a result of hard ceramic particles exposed on the worn surface.

Lashgari et al. [49] presented the influence of T6 heat treatment (solution treatment at 540ºC for 5 h, quenching in hot water and artificial aging at 170ºC for 8 h) on the microstructure, tensile properties and dry sliding wear behavior of A356–10%B_4C cast composites. The composite ingots were made by stir casting process. The matrix alloy and composite were characterized by optical microscope, scanning electron microscope equipped with energy dispersive X-ray spectroscopy, tensile tests and conventional pin-on-disk experiment. The obtained results showed that in Al–B_4C composite, T6 treatment was a dominant factor on the hardness improvement in comparison with hardness increasing due to the addition of B_4C hard particles. In addition, T6 treatment can contribute to the strong bonding between B_4C and matrix alloy and also it can change eutectic silicon morphology from acicular to near spherical. This case can lead to higher strength and wear properties of heat treated metal matrix composites in comparison with unheat treated state. Observation of worn surfaces indicated detachment of mechanically mixed layer which can primarily due to the delamination wear mechanism under higher applied load.

Li et al. [50] studied the effect of post-spray heat treatment at 250ºC, 350ºC and 450ºC for 2 h on the microstructure and properties of CS Al5356/TiN composites was examined in this study. The results show that the heat treatment has little effect on the distribution of TiN particles in

the matrix of all the composites. The pure Al5356 deposit presents large pores between the deposited particles after heat treatment, which is a common phenomenon for CS metallic coatings having an apparent increasing porosity during annealing. The adhesion between the deposit and substrate could be enhanced through atom diffusion, especially at elevated temperatures. However, the microhardness of all the deposits is significantly reduced after heat treatment because of the release of work-hardening effect within the as-sprayed metallic particles.

Zhu et al. [51] analyzed the microstructural evolution and high temperature wear characteristics of aluminum matrix composites fabricated by reaction of Al–ZrO_2–B elemental powders were explored. The amount of the Al_3Zr phase in the composites decreased with the increase of the B/ZrO_2 mole ratio. When the B/ZrO_2 mole ratio reached 2, the Al3Zr components almost diminished and the resultant composites consisted of primarily fine α-Al_2O_3 and ZrB_2 particles. At test temperature of 373 K and the applied load of 20 N, the wear rate of the composites increased and arrived at the maximum value before decreasing with the further increase of sliding velocity. However, when the test temperature was reached to 473 K, the wear rate decreased constantly with the increase of sliding velocity. With the increase of B/ZrO_2 molar ratio, both the wear rate and the friction coefficient of the composites decreased, while the subsurface deformation zone increases.

2.2 Summary of Literature

A lot of work has been done in aluminium matrix composite at different types of reinforcements, different sizes and manufactured either by stir casting or by sintering technique then aged at various temperature and time durations. Alloy composition and its condition influence the wear rate. Heat treatment of all composites and Al alloys improved abrasive wear resistance. With increase in temperature hardness and wear resistance also increases and hardness will increase initially with ageing time and after a peak value it tends to decrease. In case of the hybrid composites the wear rate do not depend on type of reinforcement, but wear rate of the hybrid composites decreases with increasing the weight percentage of reinforcing

materials. The abrasive wear resistance of Al-based hybrid composites will be controllably altered by thermal ageing.

CHAPTER 3

PILOT EXPERIMENT &DESIGN OF STUDY

3.1 PILOT EXPERIMENTATION

The effects of Al_2O_3 (2.5%, 5%, 10% & 15%) in LM6 investigated through the pilot experimentation. After, prepared the composites with stir casting method wear resistance was calculated.

A pin-on-disc tribometer is used to perform the wear experiment. The alloy and composite samples are cleaned thoroughly with acetone. Each sample is then weighed using a Digital balance having an accuracy of ±0.1 mg. After that the sample is mounted on the pin holder of the tribometer ready for wear test. For all experiments, the sliding speed is adjusted to 1 m/s.

The specific wear rates for the materials were obtained by

$$W = \Delta w / L\rho F$$

Where W denotes specific wear rates in mm^3/N-m, Δw is the weight loss measured in grams, L is the sliding distance in meters, ρ is the density of the worn material in g/mm^3, and F is the applied load in N. Weight loss of the alloy and composite samples in grams is shown in Tables 3.1 and Table 3.2.

Table 3.1: Data of cumulative wear loss of alloy

Length (mm)	Diameter (mm)	Velocity (m/S)	Track Diameter(mm)	Weight (Kg)	Time (sec)
50	8	1.6	60	2	1800

Sample No.	Specimen Name LM6+Al_2O_3	Initial Weight (gm)	Final Weight (gm)	Weight Loss (gm)
1	2.5% Al_2O_3	5.84633	5.82111	0.02522
2	5% Al_2O_3	6.16840	6.15064	0.01776
3	10% Al_2O_3	5.89106	5.87688	0.01418

4	15% Al_2O_3	6.67453	6.66168	0.01285
5	Base Alloy LM6	6.64630	6.62088	0.02542

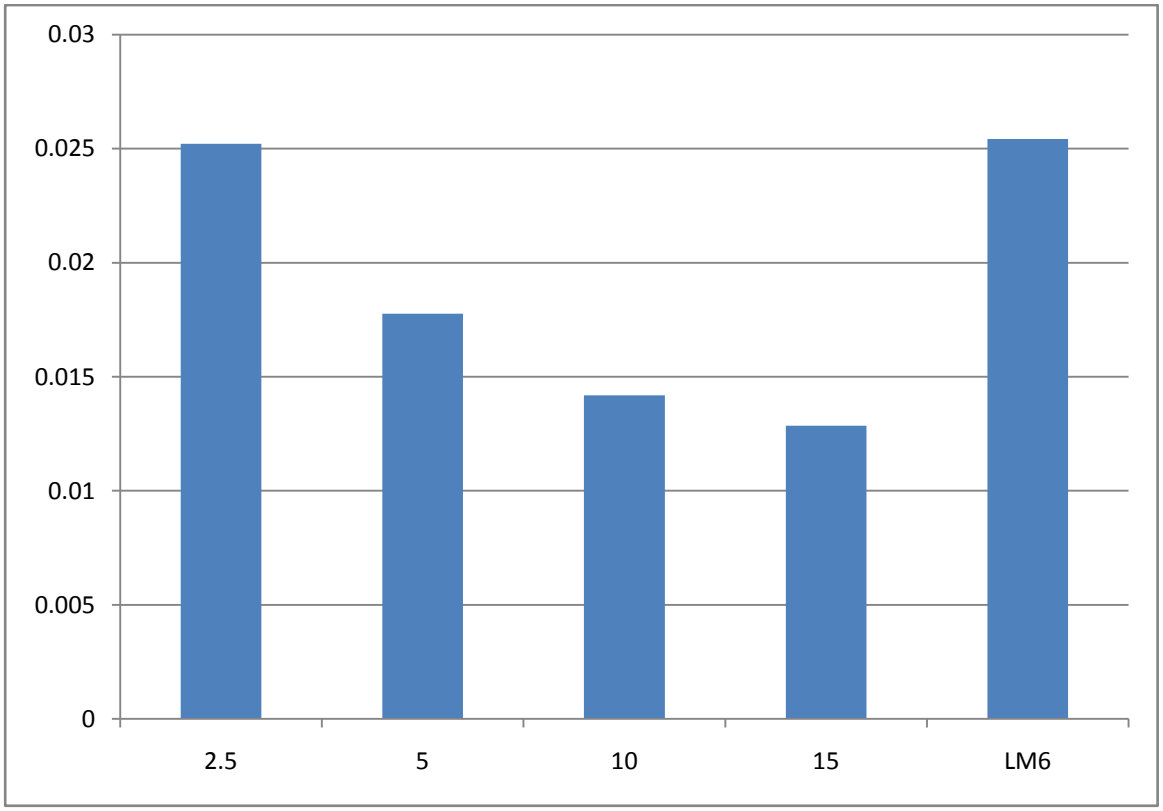

Figure 3.1: Weight loss of alloy and composites

The graph in Figure 3.1 shows the cumulative weight loss of alloy specimen after addition of alumina produced with help of stir casting technique. After addition of reinforced material the sliding wear decreases significantly or we can say that weight loss is decreasing as the alumina addition is increasing as compared to matrix metal. .

Table 3.2: Data of cumulative wear loss of composite

Time(seconds) / Wear loss (μm)	300	600	900	1200	1500	1800
Sample1 (LM6+2.5% Al_2O_3)	106.38	140.48	170.43	201.33	229.99	257.79
Sample 2(LM6+ 5% Al_2O_3)	102.75	144.87	171.64	193.91	224.99	262.86
Sample 3(LM6+10% Al_2O_3)	66.91	100.93	131.48	163.01	193.39	218.24
Sample 4(LM6+ 15% Al_2O_3)	55.23	91.35	107.61	125.25	179.93	199.04
Sample 5(LM6)	68.98	142.66	192.01	232.02	268.04	302.2

3.2 METHODOLOGY

The full factorial design is referred as the technique of defining and investigating all possible conditions in an experiment involving multiple factors while the fractional factorial design investigates only a fraction of all the combinations. Although these approaches are widely used, they have certain limitations: they are inefficient in time and cost when the number of the variables is large; they require strict mathematical treatment in the design of the experiment and in the analysis of results; the same experiment may have different designs thus produce different results; further, determination of contribution of each factors is normally not permitted in this kind of design. The Taguchi method has been proposed to overcome these limitations by simplifying and standardizing the fractional factorial design. The methodology involves identification of controllable and uncontrollable parameters and the establishment of a series of experiments to find out the optimum combination of the parameters which has greatest

influence on the performance and the least variation from the target of the design. The effect of various parameters (workpiece material, electrode, dielectric, pulse on time, pulse off time, current and powder) and some of the effects of interactions between the main factors were also be studied using parameterization approach developed by Taguchi [52].

3.3 PROCEDURE OF EXPERIMENTAL DESIGN

The whole procedure of Taguchi method is as under. [53]

1. Establishment of objective function.
2. Selection of factors and/or interactions to be evaluated.
3. Identifications of uncontrollable factors and test conditions.
4. Selection of number of levels for the controllable and uncontrollable factors.
5. Calculation total degree of freedom needed
6. Select the appropriate Orthogonal Array (OA).
7. Assignment of factors and/or interactions to columns.
8. Execution of experiments according to trial conditions in the array.
9. Analyze results.
10. Confirmation experiments

3.4 ESTABLISHMENT OF OBJECTIVE FUNCTION

The objective of the study is to evaluate the main effects of stir speed, composition percentage and method of cooling, micro hardness and getting maximum hardness from different combinations of composition of alumina. Analyze for microstructure to study the change in material properties as a result of the experimentation. XRD was completed to understand the form and amount of deposition on the surface of the work piece.

3.5 DEGREE OF FREEDOM (dof)

The number of factors and their interactions and level for factors determine the total degree of freedom required for the entire experimentation. The degree of freedom for each factor is given by the number of levels minus one.

dof for each factor : k-1

Where k is the number of level for each factor

dof for interactions between factors : $(k_A-1) \times (k_B-1)$

Where k_A and k_B are number of level for factor A and B

3.6 SELECTION OF FACTORS AND INTERACTION

The determination of which factors to investigate depends on the responses of interest. The factors affects the responses were identified using cause and effect analysis, brainstorming and pilot experimentation. The lists of factors studied with their levels are given in the Table 3.3.

Table 3.3: Factors interested and their levels

S. No	Factors	Levels		
		Level-1	Level-2	Level-3
1	Composition% (A)	2.5	5.0	7.5
2	Type of Cooling (B)	Air	Furnace	Brine Solution
3	Stirr Speed (C)	220	440	580

3.7 ORTHOGONAL ARRAY

OA plays a critical part in achieving the high efficiency of the Taguchi method. OA is derived from factorial design of experiment by a series of very sophisticated mathematical algorithms including combinatorics, finite fields, geometry and error- correcting codes. The algorithms ensure that the OA to be constructed in a statistically independent manner that each level has an

equal number of occurrences within each column; and for each level within one column, each level within any other column will occurs an equal number of times as well. Then, the columns are called orthogonal to each other. OAs are available with a variety of factors and levels in the Taguchi method. Since each column is orthogonal to the others, if the results associated with one level of a specific factor are much different at another level, it is because changing that factor from one level to the next has strong impact on the quality characteristic being measured. Since the levels of the other factors are occurring an equal number of times for each level of the strong factor, any effect by these other factors will be ruled out. The Taguchi method apparently has the following strengths:

1. Consistency in experimental design and analysis.
2. Reduction of time and cost of experiments.
3. Robustness of performance without removing the noise factors.

The selection of orthogonal array depends on:

- The number of factors and interactions of interest
- The number of levels for the factors of interest

Taguchi's orthogonal arrays are experimental designs that usually require only a fraction of the full factorial combinations. The arrays are designed to handle as many factors as possible in a certain number of runs compared to those dictated by full factorial design. The columns of the arrays are balanced and orthogonal. This means that in each pair of columns, all factor combinations occur same number of times. Orthogonal designs allow estimating the effect of each factor on the response independently of all other factors. Once the degrees of freedom are known, the next step, selecting the orthogonal array (OA) is easy. The number of treatment conditions is equal to the number of rows in the orthogonal array and it must be equal to or greater than the degrees of freedom. The interactions to be evaluated will require an even larger orthogonal array. Once the appropriate orthogonal array has been selected, the factors and interactions can be assigned to the various columns. [52]

In this experiment, there are three parameters at three levels each. The degrees of freedom (DOF) of a three level parameter is 2 (number of levels - 1), hence total DOF for the experiment is 6. The DOF of an orthogonal array selected for an experiment should be more

than the total DOF for that experiment. The difference should also not be very high, otherwise the cost and effort involved in conducting the extra experiments is wasted. Out of the standard orthogonal arrays available in Taguchi design, L9 orthogonal array has 8 degrees of freedom and it can accommodate three levels of up to four parameters, so it has been selected for this work. The array has been shown in Table 3.4

Table 3.4: L9 Experimental Design

Trial no	Composition % (A)	Cooling (B)	Speed(rpm) (C)
1	2.5	Air Cooling	220
2	2.5	Furnace Cooling	440
3	2.5	Brine Solution Cooling	580
4	5.0	Air Cooling	440
5	5.0	Furnace Cooling	580
6	5.0	Brine Solution Cooling	220
7	7.5	Air Cooling	580
8	7.5	Furnace Cooling	220
9	7.5	Brine Solution Cooling	440

3.8 ANALYSIS OF RESULTS

Signal-to-noise ratio

The parameters that influence the output can be categorized into two classes, namely controllable (or design) factors and uncontrollable (or noise) factors. Controllable factors are those factors whose values can be set and easily adjusted by the designer.

Uncontrollable factors are the sources of variation often associated with operational environment. The best settings of control factors as they influence the output parameters are determined through experiments. From the analysis point of view, there are three possible categories of the response characteristics explained below.

r is the number of tests in a trial (noise of repetitions regardless of noise levels)

$\sum_{i=1}^{r} y^2{}_i$ = summation of all response values under each trial

MSD = Mean square deviation

y_j = Observed value of the response characteristic

y_o = nominal or target value of the results

The three different response characteristics are given by the following.

1) Higher is Better. The S/N for higher the better is given by:

$(S/N)_{HB} = -10 \log (MSD_{HB})$

Where $MSD_{HB} = \frac{1}{r}\sum_{j=1}^{r}\left(\frac{1}{y_j^{\,2}}\right)$ equation 3.1.

MSD_{HB} = Mean Square Deviation for higher-the-better response.

2) Nominal is Better. The S/N for nominal is better is:

$(S/N)_{NB} = -10 \log (MSD_{NB})$

Where $MSD_{NB} = \frac{1}{r}\sum_{j=1}^{r}\left(y_j - y_0\right)^2$ equation 3.2.

3) Lower is Better. In this design situation, the heart rate, and oxygen uptake consumed is the type of ‘‘lower is better’’, which is a logarithmic function based on the mean square deviation (MSD), given by

$$S/N_{LB} = -10\log(MSD) = -10\log[(\frac{1}{r}\sum_{i=1}^{r} y^2{}_i)$$

Where $MSD_{LB} = \frac{1}{r}\sum_{j=1}^{r}\left(y_j{}^2\right)$ equation 3.3.

Signal to noise ratio for response characteristics

The parameters that influence the output can be categorized in two categories, controllable factors and uncontrollable factors. The control factors that may contribute to reduced variation can be quickly identified by looking at the amount of variation present in response. The uncontrollable factors are the sources of variation often associated with operational environment. For this experimental work, response characteristics have given in the Table 3.5.

Table 3.5: Response Characteristics

Response name	Response type	Units
Micro Hardness	Higher the better	MVN
Wear resistance	Lower the better	mm^3/min

Measurement of F-value of Fisher's F ratio

The principle of the *F* test is that the larger the *F* value for a particular parameter, the greater the effect on the performance characteristic due to the change in that process parameter. *F* value is defined as:

$$F = \frac{MS\ for\ the\ term}{MS\ for\ the\ error\ term}$$

Depending on F-value, percentage contribution is calculated of each factor and interaction.

Computation of average performance:

Average performance of a factor at certain level is the influence of the factor at this level on the mean response of the experiments.

Analysis of variance

The knowledge of the contribution of individual factors is critically important for the control of the final response. The analysis of variance (ANOVA) is a common statistical technique to determine the percent contribution of each factor for results of the experiment. It calculates parameters known as sum of squares (*SS*), pure *SS*, degree of freedom (dof), variance, F-ratio and percentage of each factor. Since the procedure of ANOVA is a very complicated and employs a considerable of statistical formula, only a brief description of is given as following.

The Sum of Squares (SS) is a measure of the deviation of the experimental data from the mean value of the data.

Let '*A*' be a factor under investigation

$$SS_T = \sum_{i=1}^{N} (y_i - \overline{T})^2$$

Where N = Number of response observations, $\overline{T}$ is the mean of all observations y_i is the i, *th* response

Factor Sum of Squares (SS_A) - Squared deviations of factor (*A*) averages from overall average

$$SS_A = \left[\sum_{i=1}^{k_A} \left(\frac{A_i^2}{n_{Ai}} \right) \right] - \frac{T^2}{N}$$

equation 3.4.

Where

A_i =Average of all obseravtions under A_i level = A_i / n_{Ai}

T = sum of all observations

$\overline{T}$ = Average of all observations = T / N

n_{Ai} = Number of obsernations under A_i level

Error Sum of Squares (SS_e) - Squared deviations of observations from factor (A) averages

$$SS_e = \sum_{j=1}^{k_A} \sum_{i=1}^{n_{Ai}} \left(y_i - \overline{A}_j \right)^2$$

equation 3.5.

Sum of Squares ($SS_{A\times B}$) for interactions

$$SS_{A\times B} = \left[\sum_{i=1}^{c} \left(\frac{(A\times B)_i^2}{n_{(A\times B)i}} \right) \right] - \frac{T^2}{N} - SS_A - SS_B$$

equation 3.6.

3.9 EXPERIMENTAL SET UP

Composite is made up of two materials aluminium alloy LM6 and reinforced with Al_2O_3 particles of grain size 30-50 μm by stir casting route. Aluminum alloy is used as matrix in the synthesis of composite. Chemical composition of used alloy is given in table 3.6.

Table 3.6: Composition of LM6 Aluminium alloy

	% composition
Copper	0.1 Max
Magnesium	0.10 Max
Silicon	10.0 - 13.0
Iron	0.6 Max
Manganese	0.5 Max
Nickel	0.1 Max
Zinc	0.1 Max
Lead	0.1 Max
Tin	0.05 Max
Titanium	0.2 Max
Aluminum	Reminder

3.10 EXPERIMENTAL PROCEDURE

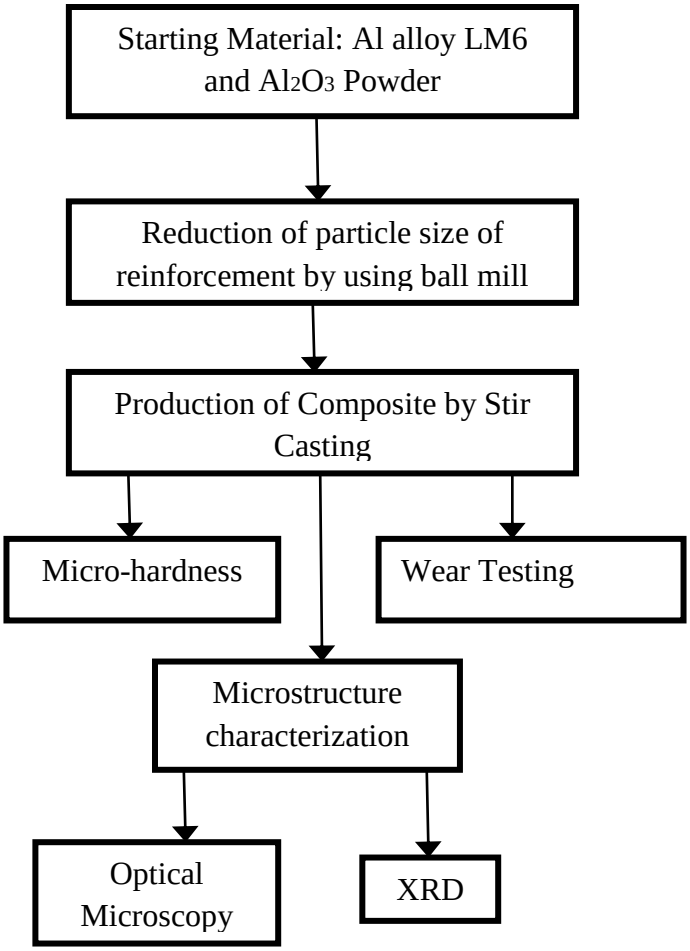

Figure 3.1: Experimental techniques followed

3.11 BALL MILL PROCESSING

Ball mill is a grinder for reducing hard materials to powder. A ball mill grinds material by rotating a cylinder with steel grinding balls/ceramic balls causing the balls to fall back into the cylinder and onto the material to be ground. The cylinder rotates at a relatively slow speed, allowing the balls to cascade through the mill base, thus grinding or dispersing the materials. The rotation is usually between 4 to 20 revolutions per minute, depending upon the diameter of the mill. The larger is the diameter, the slower the rotation. If the peripheral speed of the mill is

too great, it begins to act like a centrifuge and the balls do not fall back, but stay on the perimeter of the mill. The point where the mill becomes a centrifuge is called the "Critical Speed", and ball mills usually operate at 65% to 75% of the critical speed.

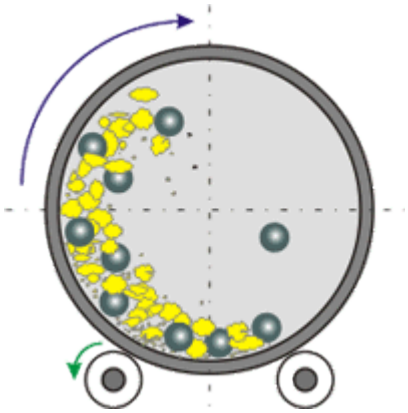

Figure 3.2: Ball Mill

Ball mills are generally used to grind material 1/4 inch and finer, down to the particle size of 20 to 75 microns. To achieve a reasonable efficiency with ball mills, they must be operated in a closed system, with oversize material continuously being recirculated back into the mill to be reduced. Various classifiers, such as screens, cyclones and air classifiers are used for classifying the discharge from ball mills.

3.12 MUFFLE FURNACE

Stir casting setup consist of digital control muffle furnace (fig. 4.3) and a stirrer (fig.4.4) made of graphite connected to electric motor with speed range of 22-840 rpm. SiC particles were artificially oxidized in air at 1000 ◦C for 150 min to form a layer of SiO_2 on them and improve their wettability with molten aluminium. This treatment helps the incorporation of the particles while reducing undesired interfacial reactions. Batches of the matrix alloy were melted in a clay-bonded graphite crucible of 1.5 kg capacity using a small muffle furnace. The temperature of the alloy was first raised to about 800 °C and then stirred at 540 rpm using an impeller fabricated from graphite and driven by a variable ac motor.

Figure 3.3: Muffle furnace

The temperature of the furnace was gradually lowered until the melt reached a temperature in the liquid solid range while stirring was continued. Then the stirrer was positioned just below the surface of the slurry and the oxidized particles were added uniformly at a rate of 20 g/min over a time period of approximately 3–5 min and speed is lowered to 260 rpm. At the end of charging the slurry was allowed to mix in the semisolid state isothermally for another 15 min while the stirrer was positioned near the bottom of the crucible.

Figure 3.4 Graphite stirrer

Figure 3.5: Crucible

3.13 SYNTHESIS OF COMPOSITE

The synthesis of composite is done by stir casting route. The parameters which are important in this work are stirrer design, preheating temperature for particulate and stirring speed. These parameters are discussed below.

3.13.1 Stirrer Design

It is very important parameter for stir casting process. It is essentially requires for vortex formation for the uniformly dispersion of particles. There is different type of stirrer some 90º form the shaft and some are bent at 45º. There is a no uniform dispersion of particles in case of no vortex formation.

3.13.2 Particle Preheating Temperature

Preheating of particulate is necessary to avoid moisture from the particulate otherwise there is chance of agglomeration of particulate due moisture and gases. Along this SiC particles are heated at 1000ºC to form a oxide layer on the SiC particles which make it chemically more stable and by the oxide layer formation wettability will increase so particles will effectively embedded in aluminium matrix and less number of porosities in casting. After oxide layer formation preheating of particulate is done on temperature of 400° C.

3.13.3 Stirring Speed

In stir casting process stirring is very important parameter for consideration. In the process stirring speed was 240 rpm which was effectively producing vortex without any spattering. Stirring speed is decided by fluidity of metal speed, dispersion of particulates are not proper because of ineffective vortex.

3.14 MICROHARDNESS TESTER

Micro hardness testing is a method for measuring the hardness of a material on a microscopic scale. A precision diamond indenter is impressed into the material at loads from a few grams to 1 kilogram. The impression length, measured microscopically, and the test load are used to calculate a hardness value.

Figure 3.6: Micro hardness Tester

The indentations are typically made using either a square-based pyramid indenter (Vickers hardness scale) or an elongated, rhombohedral-shaped indenter. The tester applies the selected test load using dead weights. The length of the hardness impressions are precisely measured with a light microscope using either a video image or computer software. A hardness number is then calculated using the test load, the impression length, and a shape factor for the indenter type used for the test.

3.15 X-Ray Diffraction (XRD)

X-ray diffraction (XRD) is a rapid analytical technique primarily used for phase identification of a crystalline material and can provide information on unit cell dimensions. The analyzed material is finely ground, homogenized, and average bulk composition is determined. X-ray diffraction is based on constructive interference of monochromatic X-rays and a crystalline sample. These X-rays are generated by a cathode ray tube, filtered to produce monochromatic radiation, collimated to concentrate, and directed toward the sample.

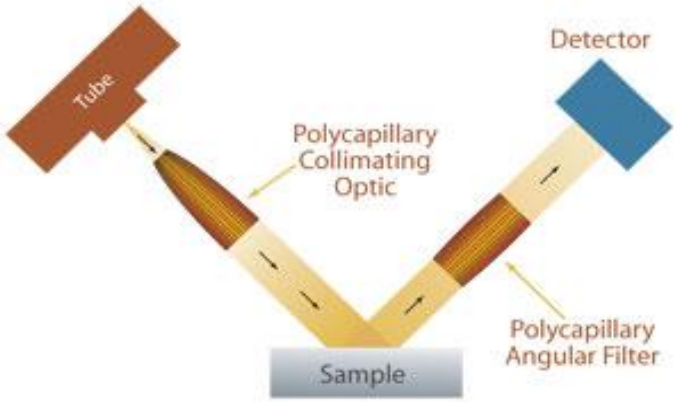

Figure 3.7: X-ray diffraction mechanisms

The interaction of the incident rays with the sample produces constructive interference (and a diffracted ray) when conditions satisfy Bragg's Law ($n\lambda=2d \sin \theta$). This law relates the wavelength of electromagnetic radiation to the diffraction angle and the lattice spacing in a crystalline sample. These diffracted X-rays are then detected, processed and counted. By scanning the sample through a range of 2θangles, all possible diffraction directions of the lattice should be attained due to the random orientation of the powdered material. Conversion of the diffraction peaks to d-spacings allows identification of the mineral because each mineral has a set of unique d-spacings. Typically, this is achieved by comparison of d-spacings with standard reference patterns. All diffraction methods are based on generation of X-rays in an X-ray tube. These X-rays are directed at the sample, and the diffracted rays are collected. A key component of all diffraction is the angle between the incident and diffracted rays. X-ray

diffractometers consist of three basic elements: an X-ray tube, a sample holder, and an X-ray detector. X-rays are generated in a cathode ray tube by heating a filament to produce electrons, accelerating the electrons toward a target by applying a voltage, and bombarding the target material with electrons. When electrons have sufficient energy to dislodge inner shell electrons of the target material, characteristic X-ray spectra are produced. These X-rays are collimated and directed onto the sample. As the sample and detector are rotated, the intensity of the reflected X-rays is recorded. When the geometry of the incident X-rays impinging the sample satisfies the Bragg Equation, constructive interference occurs and a peak in intensity occurs. A detector records and processes this X-ray signal and converts the signal to a count rate which is then output to a device such as a printer or computer monitor. The geometry of an X-ray diffractometer is such that the sample rotates in the path of the collimated X-ray beam at an angle θ while the X-ray detector is mounted on an arm to collect the diffracted X-rays and rotates at an angle of 2θ.

3.16 WEAR TEST

Sliding wear tests were conducted in pin-on-disc wear testing apparatus under constant applied load of 2kg at a fixed sliding speed of 1 m/s against EN32 steel disc. The pin samples were 30 mm in length and 8 mm in diameter. The surfaces of the pin sample ground using emery paper prior to test. In ordered to ensure effective contact of fresh surface with the steel disc, the fresh samples were subjected to sliding on emery paper of 240 grit size. During sliding, the load is applied on the specimen through cantilever mechanism and the specimens brought in intimate contact with the rotating disc at a track radius of 100 mm. The samples were cleaned with acetone and weighed (up to an accuracy of 0.01 mg using microbalance) prior to and after each test. The wear rate was calculated from the weight loss technique and expressed in terms of volume loss per unit sliding distance.

Figure 3.8: Wear testing machine

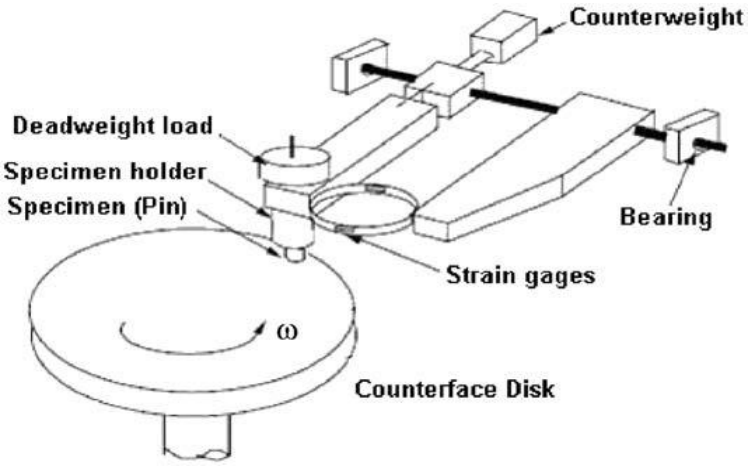

Figure 3.9: Pin-on-disk apparatus.

CHAPTER 4

RESULTS AND ANALYSIS OF MICROHARDNESS

4.1 INTRODUCTION

The effect of the parameters i.e. variation in the composition of Al_2O_3 (A), Stirring speed (B), type of cooling (C) were evaluated using ANOVA and factorial design analysis. By using the above parameters the composites were prepared by stir casting process. A confidence interval of 95% has been used for the analysis. One repetition for each of 9 trials was completed so as to measure Signal to Noise ratio (S/N ratio).

4.2 RESULTS FOR MICRO HARDNESS

The result of micro hardness at bottom surface and upper surface of the composites for all 9 experiments are calculated to know the mean micro hardness of the composite. Table 4.1 shows

Table 4.1 Results for micro hardness

Trail no.	Composition % (A)	Cooling (B)	Speed (rpm) (C)	Mean micro hardness (HVN)	S/N Ratio
1	2.5	Air Cooling	220	19.8550	25.9574
2	2.5	Furnace Cooling	440	20.0436	26.0395
3	2.5	Brine Solution Cooling	580	20.0156	26.0274
4	5.0	Air Cooling	440	38.9780	31.8164
5	5.0	Furnace Cooling	580	45.2987	33.1217
6	5.0	Brine Solution Cooling	220	43.9693	32.8630
7	7.5	Air Cooling	580	59.9248	35.5521
8	7.5	Furnace Cooling	220	65.4096	36.3128
9	7.5	Brine Solution Cooling	440	61.5090	35.7788

the factorial design and the mean micro hardness of the composites. Firstly few readings are taken at bottom surface and few on upper surface then mean micro hardness of the both the surfaces are taken to know the overall micro hardness. The micro hardness measurement is depending on the diameter of indentation on the samples. The indents formed in the pyramid shaped indenter were measured with Quantimet software using a load of 100g for 20 seconds.

4.3 ANALYSIS OF VARIANCE- MICRO HARDNESS OF THE COMPOSITES

The results for mean micro hardness of composites for each of the 9 treatment conditions with repetition are given in Table 4.1. The results were analyzed using ANOVA for identifying the significant factors affecting the performance at 95% confidence interval. ANOVA Table 4.2 shows that factors, namely composition (p= 0.001), cooling (p= 0.046) were found to be significant factors. Stirring speed was found insignificant. Table 4.3 shows ranks of various factors in terms of their relative significance. Composition has the highest rank, signifying the highest contribution in micro hardness and stirring speed has the lowest rank and was observed to be insignificant in micro hardness of composites. Main effect plots are shown in the Figure 4.1 which shows that micro hardness increases with increase in composition of Al_2O_3 in LM6. The micro hardness increases with increase in composition and change in cooling. The micro hardness was found to be high when composition is about 7.5% and cooling is furnace cooling. During furnace or slow cooling the structure obtained is denser as compared to brine an air cooling. Due to the addition of the Al_2O_3 the bonding strength of the metal increased. As the interfacial bonding was increased the micro hardness is also improved as compared to the parent metal (LM6).

Table 4.2: ANOVA for micro hardness of the composites

Sources	DOF	Seq SS	Adj MS	F	P
Composition% (A)	2	2690.43	1345.22	1899.48	0.001
Cooling (B)	2	24.10	12.05	17.01	0.046
Speed (C)	2	12.65	6.33	8.93	0.101
Residual Error	2	1.42	0.71		
Total	8	2728.60			
e pooled	4	14.07	3.5175		

Table 4.3: Response table for means of micro hardness of composites

Level	Composition %	Cooling	Speed
1	19.97	39.59	43.08
2	42.75	41.83	40.18
3	62.28	43.58	41.75
Delta	42.31	4.00	2.90
Rank	1	2	3

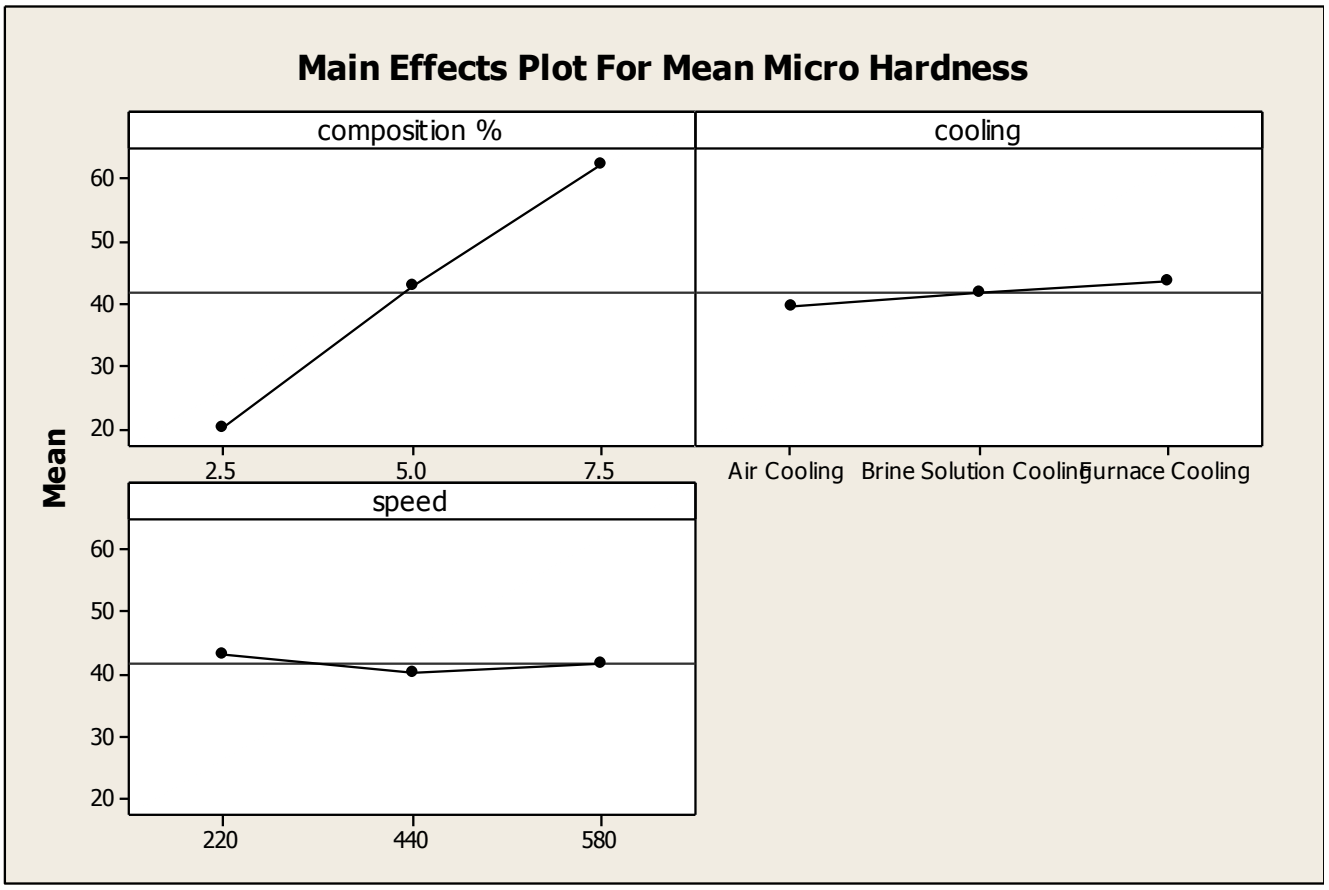

Figure 4.1: Main effect plots for mean micro harness of Aluminum metal matrix composites

4.4 RESULTS FOR S/N RATIO – MICRO HARDNESS OF COMPOSITES

The S/N ratio consolidated several repetitions into one value and is an indication of the amount of variation present in the process. The S/N ratios have been calculated to identify the major

contributing factors that cause variation in micro hardness of composites. Micro hardness is a "Higher the better" type response is given by a logarithmic function based on the mean square deviation:

$(S/N)_{HB} = -10 \log (MSD_{HB})$

Where $MSD_{HB} = \frac{1}{r}\sum_{j=1}^{r}\left(\frac{1}{y_j^{\,2}}\right)$

MSD_{HB} = Mean Square Deviation for higher-the-better response.

Table 4.4 shows the ANOVA results for S/N ratio of micro hardness of composites at 95% confidence interval. The factor, namely, composition was found to be significant on the basis of the p- value and the other factors cooling, stirring time were found to insignificant for micro hardness of composites. Table 4.5 shows rank importance to various factors in terms of their relative significance. The highest rank to composition signifying the highest contribution to micro hardness and stirring speed has the lowest rank and was observed to be insignificant for micro hardness. Main effect plots of S/N ratio for micro hardness of are shown in the Figure 4.2.

Table 4.4: ANOVA for S/N ratio of micro hardness of composites

Source	DOF	Seq SS	Adj MS	F	P
Composition% (A)	2	151.701	75.8506	1836.94	0.001
Cooling (B)	2	0.785	0.3926	9.51	0.095
Speed (C)	2	0.397	0.1983	4.80	0.172
Residual Error	2	0.083	0.0413		
Total	8	152.966			
e pooled	6	1.265	0.2108		

Table 4.5: Response table for S/N ratio of micro hardness of composites

Level	Composition%	Cooling	Speed
1	26.01	31.11	31.71
2	32.60	31.56	31.21
3	35.88	31.82	31.57
Delta	9.87	0.72	0.50
Rank	1	2	3

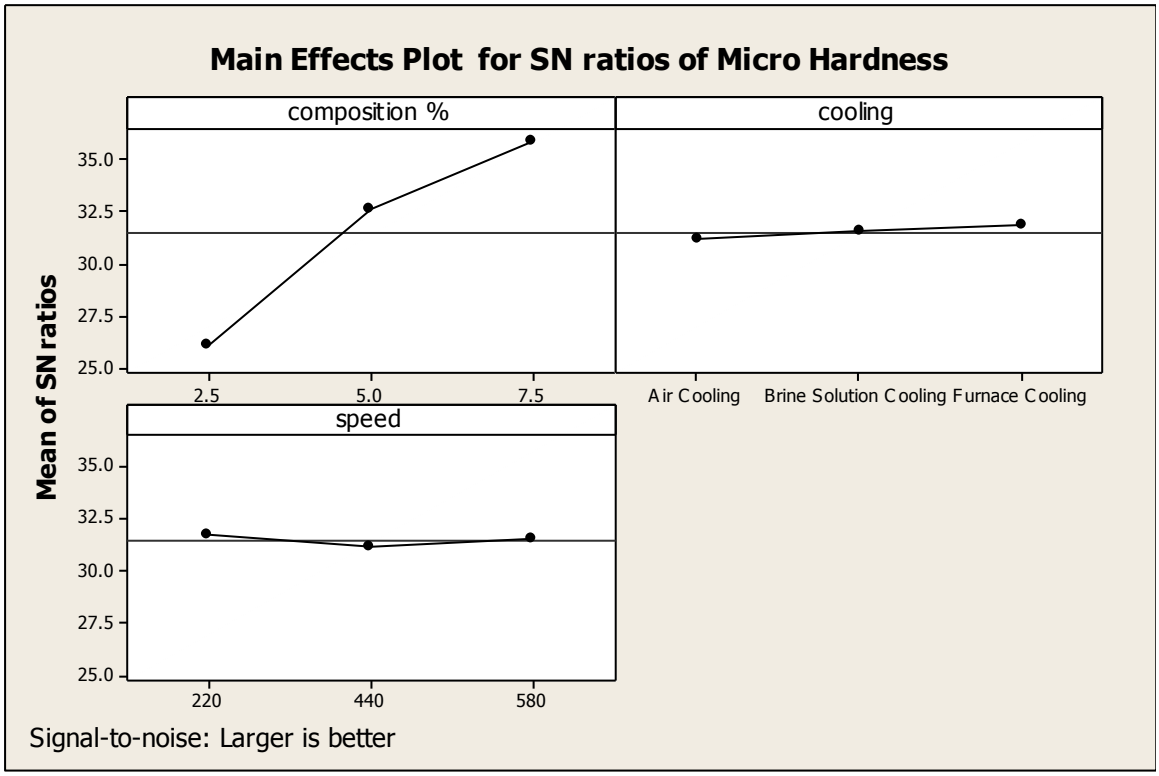

Figure 4.2: Main effect plot for S/N ratio of micro hardness of composites

4.5 OPTIMAL DESIGN

In this experimental analysis, main effect plot in figure 4.1 shows the mean micro hardness of the composites. From the Table 4.6 it is concluded that highest micro hardness of composites was observed when composition was 7.5% and the furnace cooling was chosen in the treatment conditions. In S/N ratio the highest micro hardness is achieved at 7.5 % composition. The Table

4.6 shows that the factors composition and cooling were found to be significant as their value of 'p' less than 0.05.

Table 4.6: Significant factors for micro hardness of composites

Factors	Affecting mean		Affecting variation (S/N ratio)	
	Contribution	Best level	Contribution	Best level
Composition (A)	Significant	Level 3 -7.5%	Significant	Level 3 - 7.5%
Cooling (B)	Significant	Level 3 – FC	Insignificant	-
Stirring speed (C)	Insignificant	-	Insignificant	-

Estimating the mean

In experimental analysis, the Micro hardness is a higher average response is better (HB) characteristic. Depending on the characteristic, different treatment combinations has chosen to obtain satisfactory results. After conducting the experiments the optimum treatment condition within the experiments determined on the basis of prescribed combination of factor levels is determined to one of those in the experiment

Mean value of micro hardness

$\mu_{A3XB3} = \overline{A_3} + \overline{B_3} - \overline{T}$

μ_{A3XB3} = 62.2811+48.5839- 41.6670 = 69.198HVN

Confidence Interval around the Estimated Mean

The confidence interval is a maximum and minimum value between which the true average should fall at some stated percentage of confidence. The estimate of the mean μ is only a point estimate based on the averages of results obtained from the experiment. Statistically this provides a 50% chance of the true averages being greater than μ and a 50% chance of the true average being less than μ

Confidence Interval around the estimated micro hardness at deposited region:

$$CI_1 = \sqrt{\frac{F_{\alpha,\nu_1,\nu_2} V_e}{n_{eff}}}$$ Where $F_{\alpha\nu_1\nu_2} = F\ ratio$

$\alpha = risk$ (0.05) $confidence = 1-\alpha$

$\nu_1 = dof\ \ for\ mean\ which\ is\ always = 1$

$\nu_2 = dof\ \ for\ error = \nu_e$

n_{eff} = Number of tests under that condition using the participating factors

$$n_{eff} = \frac{N}{1+dof_{A,B}} = \frac{9}{1+2+2} = 1.8$$

$$CI = \sqrt{\frac{F_{\alpha,\nu_1,\nu_2} V_e}{n_{eff}}} = \sqrt{\frac{0.2 \times 3.5175}{1.8}} = 0.625$$

So the confidence interval around the mean micro hardness of composites is given by 69.198±0.625 HVN

CHAPTER 5

RESULTS AND ANALYSIS OF WEAR RATE

5.1 INTRODUCTION

The effect of parameters i.e. composition of Al_2O_3, type of cooling and stirring speed were evaluated using ANOVA and factorial design analysis. A confidence interval of 95% has been used for the analysis. One repetition for each of 9 trials was completed so as to measure signal to noise ratio (S/N ratio). Wear testing was performed on pin on disc machine manufactured by 'DUCOM'. Wear testing was done in three stages. To check the effect of the parameters i.e. composition of Al_2O_3, type of cooling and stirring speed on the composite's wear resistance dry sliding friction wear testing is performed. In first stage of wear testing was performed by keeping the 'Time' as a variable. In second stage the variable was 'sliding distance' and in third stage the variable was 'load'.

5.2 RESULTS FOR WEAR RATE WITH TIME

The results for wear rate with time for each of the 9 treatment conditions with repetition are given in Table 5.1. The effect of the various parameters was noted to see the effect on the wear properties of composites. Wear rate is calculated at the different time i.e. 5, 10, 15, 20, 25, and 30 minutes. The wear rate is calculated from the loss in height of pin during performance trial:

$$\text{Wear rate} = \frac{wear\ \ volume}{sliding\ \ distance}\ \text{mm}^3/\text{sec}$$

$$\text{Wear volume} = = \pi r^2 \text{h}$$

Where

r = radius of pin (5mm)

h = commutative height loss of pin after sliding over disc

And

$$\text{Sliding distance} = \frac{\pi DN}{60} \times t$$

Where

D = Diameter of the track (60mm)

N = RPM of the disc (510)

5.3 WEAR RATE AT 5 MINUTES

The effects of the parameters i.e. composition, type of cooling and stirring speed were evaluated on the composites having 2.5%, 5% and 7.5% reinforcement particles of average size 40 micron on the wear rate.

Table 5.1: Results for Wear rate at 5 minutes

Trail no.	Composition of Al_2O_3	Type of cooling	Stirring speed(rpm)	Wear at 5 minute	Mean	S/N ratio
1	2.5	Air Cooling	220	0.006436	0.006436	43.8277
2	2.5	Furnace Cooling	440	0.005921	0.005921	44.5521
3	2.5	Brine Solution Cooling	580	0.006121	0.006121	44.2636
4	5.0	Air Cooling	440	0.004061	0.004061	47.8273
5	5.0	Furnace Cooling	580	0.003552	0.003552	48.9905
6	5.0	Brine Solution Cooling	220	0.003702	0.003702	48.6313
7	7.5	Air Cooling	580	0.001749	0.001749	55.1442
8	7.5	Furnace Cooling	220	0.001502	0.001502	56.4666
9	7.5	Brine Solution Cooling	440	0.001544	0.001544	56.2271

5.3.1 Analysis Of Variance – Wear at 5 Minutes

The results were analyzed using ANOVA for identifying the significant factors affecting the performance measures. The Analysis of Variance (ANOVA) for the wear at 95% confidence interval is given in Table 5.2. Table 5.3 shows the ranks of various factors in the terms of their relative significance. Composition has the highest rank, signifying highest contribution to minimize the wear rate and stirring speed has the lowest rank and was observed to be insignificant in affecting MRR. Main effect plot for the mean MRR is shown in the Figure 5.1 which shows the variation of wear rate with the input parameters. As can be seen that wear rate decreases as the composition of Al_2O_3 increases. Even in the case of cooling furnace cooling gives best result as compared to brine solution and air cooling.

Table 5.2: ANOVA for wear rate at 5 minutes

Sources	DF	Seq SS	Adj MS	F	P
Composition%	2	0.000031	0.000016	1924.32	0.001
Cooling	2	0.000001	0.000001	17.40	0.044
Speed	2	0.000000	0.000000	0.49	0.672
Residual error	2	0.000001	0.000000		
Total	8	0.000034			
e pooled	4	0.000001	0.0000002		

Table 5.3: Response table for means of wear rate at 5 minutes

Level	Composition	Cooling	Speed
1	0.006159	0.004082	0.003880
2	0.003772	0.003789	0.003842
3	0.001598	0.003658	0.003807
Delta	0.004561	0.000424	0.000073
Rank	1	2	3

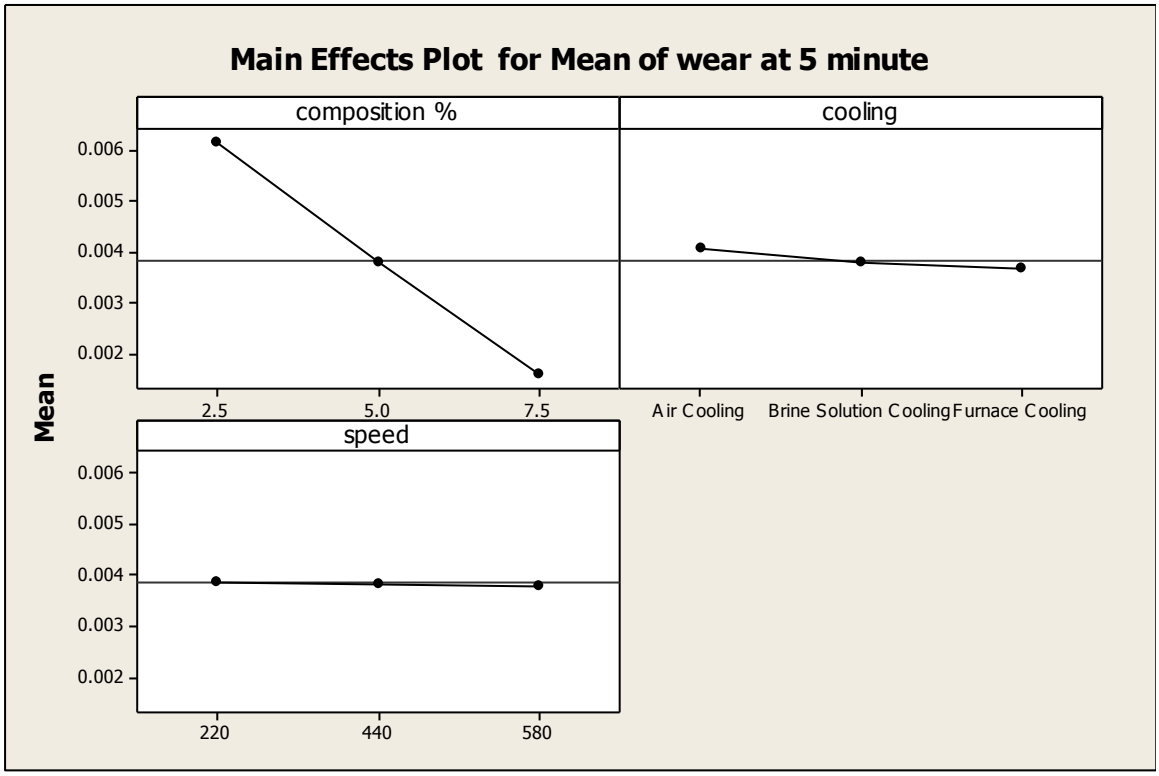

Figure 5.1: Main effect plot for Mean wear rate at 5 minutes

5.3.2 Results for S/N Ratio – Wear Rate at 5 Minutes

The S/N ratios have been calculated to identify the major contributing factors that cause variation in wear rate. Wear rate is a "Lower is better", type response and is given by a logarithmic function based on the mean square deviation (MSD) given by:

$$S/N_{LB} = -10\log(MSD) = -10\log[(\frac{1}{r}\sum_{i=1}^{r} y^2{}_i)$$

Table 5.4 shows the ANOVA results for S/N ratio of wear rate at 95% confidence interval. According the F test, composition was observed to be the most significant factor affecting the wear rate, followed by type cooling and stirring speed. The rank of importance of various factors in the terms of their relative significance is given in the Table 5.5. The composition has the highest rank, signifying highest contribution to lowering down the wear and stirring speed has the lowest rank and was observed be insignificant in affecting wear. Main effect plot and interaction plot of S/N ratio for wear rate after 5 minute are shown in the Figure 5.3 and Figure 5.4 respectively.

Table 5.4: ANOVA for S/N of wear rate at 5 minutes

Source	DF	Seq SS	Adj MS	F	P
Composition%	2	211.544	105.772	2362.49	0.006
Cooling	2	1.832	0.916	20.46	0.047
Speed	2	0.047	0.024	0.53	0.656
Residual error	2	0.090	0.045		
Total	8	213.513			
E pool	4	0.137	0.03425		

Table 5.5: Response table for S/N ratio of wear rate at 5 minutes

Level	Composition%	Cooling	Speed
1	44.21	48.93	49.64
2	48.48	49.71	49.54
3	55.95	50.00	49.47
Delta	11.73	1.07	0.18
Rank	1	2	3

5.3.3 Optimal Design

Table 5.6: Significant factors for wear rate at 5 minutes of composites

Factors	Affecting mean		Affecting variation (S/N ratio)	
	Contribution	Best level	Contribution	Best level
Composition (A)	Significant	Level 3-7.5%	Significant	Level 3-7.5%
Cooling (B)	Significant	Level 3-FC	significant	Level 3-FC
Stirring speed (C)	Insignificant	-	Insignificant	-

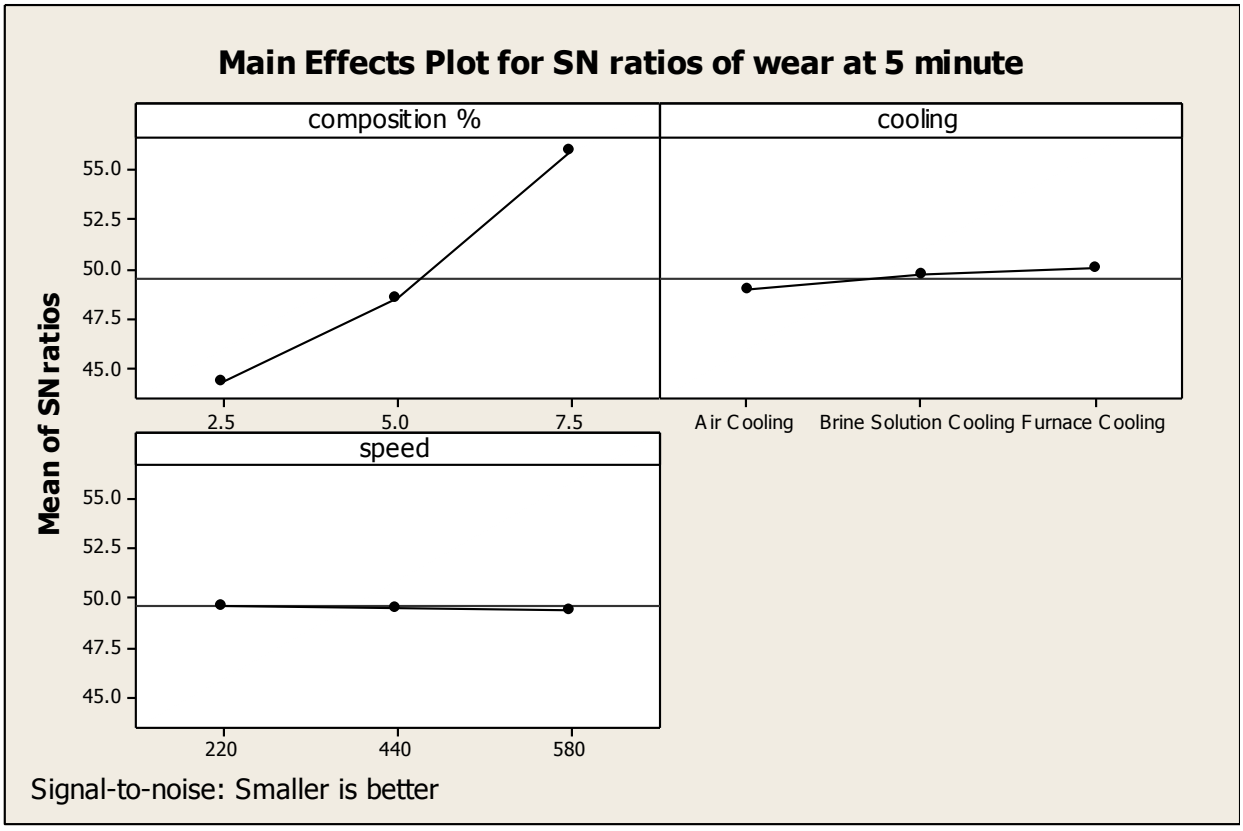

Figure 5.2: Main effects plot of wear rate at 5 minutes for S/N ratio

Estimating the mean

Mean value of wear rate at 5 min. of composites

$\mu_{A_3B_3} = \overline{A_3} + \overline{B_3} - \overline{T}$

$\mu_{A_3B_3}$ = 0.001598 + 0.003658 - 0.003843 =0.001413

Confidence Interval around the Estimated Mean

Confidence Interval around the estimated wear rate at 5 minutes of composites:

$CI_1 = \sqrt{\frac{F_{\alpha,v_1,v_2} V_e}{n_{eff}}}$ Where $F_{\alpha v_1 v_2} = F\ ratio$

$\alpha = risk$ (0.05) $\quad\quad$ $confidence = 1-\alpha$

$\nu_1 = dof$ *for mean which is always* $= 1$

$\nu_2 = dof$ *for error* $= \nu_e$

n_{eff} = Number of tests under that condition using the participating factors

$$n_{eff} = \frac{N}{1+dof_{A,B}} = \frac{9}{1+2+2} = 1.8$$

$$CI = \sqrt{\frac{F_{\alpha,\nu_1,\nu_2} V_e}{n_{eff}}} = \sqrt{\frac{0.2 \times 2.5 \times 10^{-7}}{1.8}} = 0.000167$$

So the confidence interval around the wear rate at 5 min of composites is given by 0.001413±0.000167 mm^3/m

5.4 WEAR RATE AT 10 MINUTES

The effects of the parameters i.e. composition, type of cooling and stirring speed were evaluated on the composites having 2.5%, 5% and 7.5% reinforcement particles of average size 40 micron on the wear rate.

Table 5.7: Results for wear rate at 10 minutes

Trail no.	Composition of Al2O3	Type of cooling	Stirring speed	Wear at 10 minute	Mean	S/N ratio
1	2.5	Air Cooling	220	0.0049020	0.0049020	46.1925
2	2.5	Furnace Cooling	440	0.0056190	0.0056190	45.0068
3	2.5	Brine Solution Cooling	580	0.0051850	0.0051850	45.7050
4	5.0	Air Cooling	440	0.0043190	0.0043190	47.2923

5	5.0	Furnace Cooling	580	0.0054181	0.0054181	45.3230
6	5.0	Brine Solution Cooling	220	0.0047360	0.0047360	46.4917
7	7.5	Air Cooling	580	0.0039360	0.0039360	48.0989
8	7.5	Furnace Cooling	220	0.0049920	0.0049920	46.0345
9	7.5	Brine Solution Cooling	440	0.0049020	0.0049020	46.1925

5.4.1 Analysis of Variance – Wear at 10 Minutes

The results were analyzed using ANOVA for identifying the significant factors affecting the performance measures. The Analysis of Variance (ANOVA) for the wear at 95% confidence interval is given in Table 5.7. The principle of the F-test is that the larger the F value for a particular parameter, the greater the effect on the performance characteristic due to the change in that process parameter.

Table 5.8: ANOVA for wear rate at 10 minutes

Sources	DF	Seq SS	Adj MS	F	P
Composition%	2	0.000001	0.000016	53.90	0.018
Cooling	2	0.000002	0.000000	78.86	0.013
Speed	2	0.000000	0.000000	1.75	0.364
Residual error	2	0.000001	0.000000		
Total	8	0.000004			
e pooled	4	0.000001	0.00000025		

Table 5.9: Response table for means of wear rate at 10 minutes

Level	Composition	Cooling	Speed
1	0.005413	0.005213	0.005024
2	0.004974	0.005343	0.005026
3	0.004555	0.004386	0.004891
Delta	0.000859	0.000957	0.000135
Rank	2	1	3

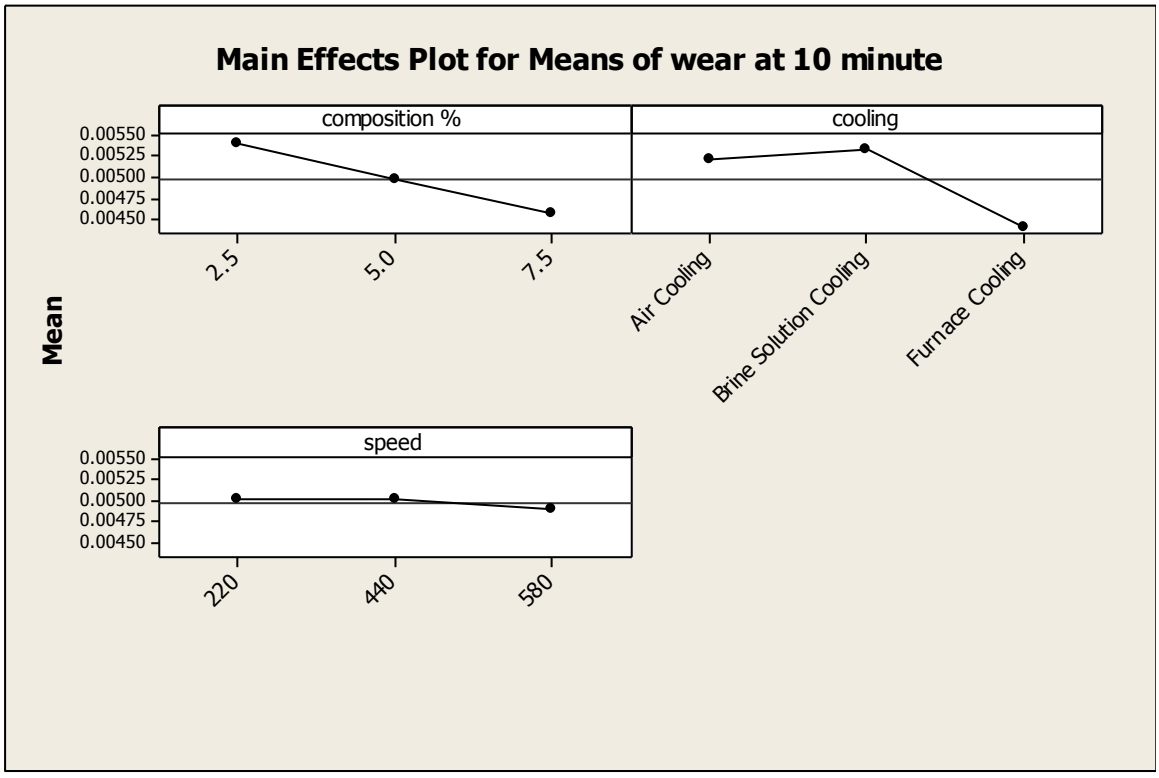

Figure 5.3: Main effect plot for Mean wear rate at 10 minutes

5.4.2 Results for S/N Ratio – Wear Rate at 10 Minutes

Table 5.4 shows the ANOVA results for S/N ratio of wear rate at 95% confidence interval. According the F test, composition was observed to be the most significant factor affecting the wear rate, followed by type cooling and stirring speed. The rank of importance of various factors in the terms of their relative significance is given in the Table 5.5. The

composition has the highest rank, signifying highest contribution to lowering down the wear and stirring speed has the lowest rank and was observed be insignificant in affecting wear. Main effect plot and interaction plot of S/N ratio for wear rate after 10 minute are shown in the Figure 5.3 and Figure 5.4 respectively.

Table 5.10: ANOVA for S/N of wear rate at10 minutes

Source	DF	Seq SS	Adj MS	F	P
Composition%	2	3.4843	1.74213	29.23	0.033
Cooling	2	5.3626	2.68132	44.99	0.022
Speed	2	0.1246	0.06229	1.05	0.489
Residual error	2	0.1192	0.05959		
Total	8	9.0906			
E pool	4	0.2438	0.06095		

Table 5.11: Response table for S/N ratio of wear rate at 10 minutes

Level	Composition%	Cooling	Speed
1	45.35	45.68	49.09
2	46.11	45.45	45.98
3	46.88	47.19	46.26
Delta	1.52	1.74	0.29
Rank	2	1	3

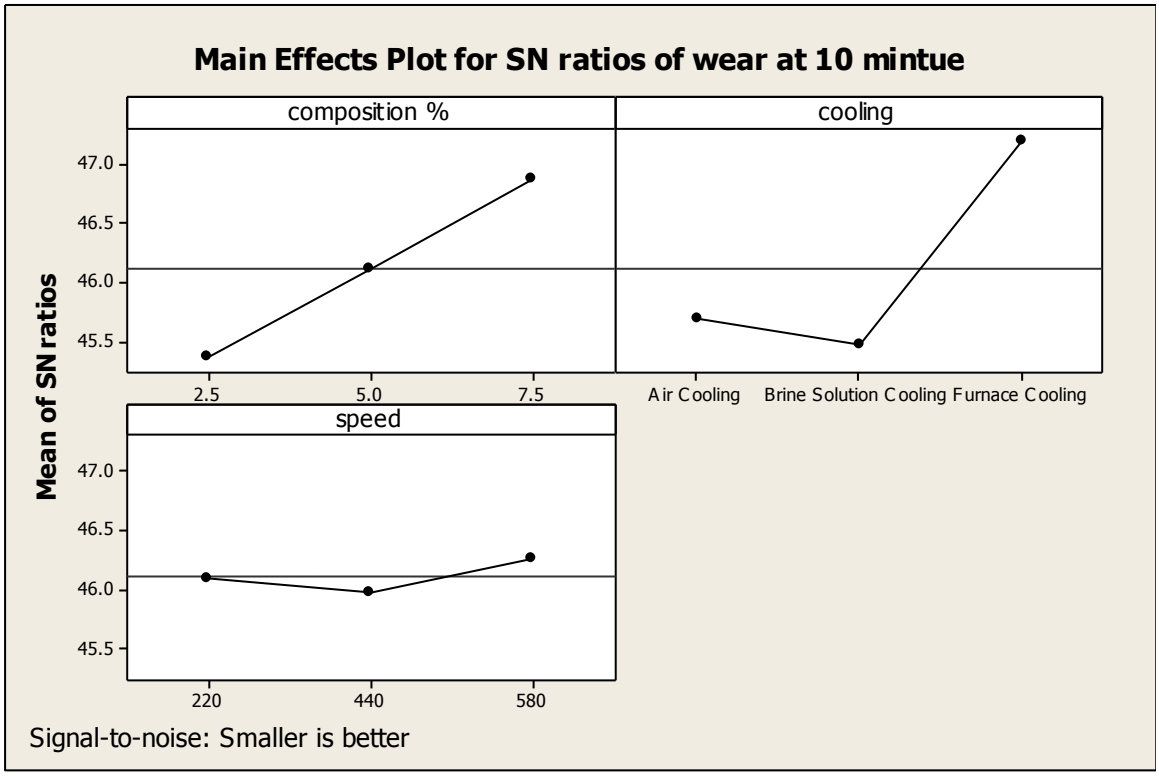

Figure 5.4: Main effects plot of wear rate at 10 minutes for S/N ratio

5.4.3 Optimal Design

Table 5.12: Significant factors for wear rate at 5 minutes of composites

Factors	Affecting mean		Affecting variation (S/N ratio)	
	Contribution	Best level	Contribution	Best level
Composition (A)	Significant	Level 3 -7.5%	Significant	Level 3 -7.5%
Cooling (B)	Significant	Level 3- FC	significant	Level 3- FC
Stirring speed (C)	Insignificant	-	Insignificant	-

Estimating the mean

Mean value of wear rate at 10 min. of composites

$\mu_{A_3B_3} = \overline{A_3} + \overline{B_3} - \overline{T}$

$\mu_{A_3B_3}$ = 0.00461 + 0.00534 - 0.00489 =0.00506

So the confidence interval around the wear rate at 10 min of composites is given by 0.00506±0.000167 mm^3/m

5.5 WEAR RATE AT 15 MINUTES

The effects of the parameters i.e. composition, type of cooling and stirring speed were evaluated on the composites having 2.5%, 5% and 7.5% reinforcement particles of average size 40 micron on the wear rate.

Table 5.13 results of wear rate at 15 minutes

Trail no.	Composition of Al2O3	Type of cooling	Stirring speed	Wear at 15 minute	Mean	S/N ratio
1	2.5	Air Cooling	220	0.0059913	0.0059913	44.4495
2	2.5	Furnace Cooling	440	0.0070807	0.0070807	42.9985
3	2.5	Brine Solution Cooling	580	0.0081467	0.0081467	41.7804
4	5.0	Air Cooling	440	0.0054467	0.0054467	45.2774
5	5.0	Furnace Cooling	580	0.0065467	0.0065467	43.6796
6	5.0	Brine Solution Cooling	220	0.0077360	0.0077360	42.2297
7	7.5	Air Cooling	580	0.0047127	0.0047127	46.5347
8	7.5	Furnace Cooling	220	0.0058573	0.0058573	44.6460
9	7.5	Brine Solution Cooling	440	0.0059913	0.0059913	44.4495

5.5.1 Analysis of Variance – Wear at 15 Minutes

The results were analyzed using ANOVA for identifying the significant factors affecting the performance measures. The Analysis of Variance (ANOVA) for the wear at 95% confidence interval is given in Table 5.13. As can be seen that wear rate decreases as the composition of

Al2O3 increases. Even in the case of cooling furnace cooling gives best result as compared to brine solution and air cooling.

Table 5.14: ANOVA for wear rate at 15 minutes

Sources	DF	Seq SS	Adj SS	Adj MS	F	P
Composition%	2	0.000002	0.000002	0.000001	99.43	0.010
Cooling	2	0.000012	0.000012	0.000006	593.64	0.002
Speed	2	0.000000	0.000000	0.000000	0.85	0.540
Residual error	2	0.000001	0.000000	0.000000		
Total	8	0.000015				
e pooled	4	0.00000025				

Table 5.15: Response table for means of wear rate at 15 minutes

Level	Composition	Cooling	Speed
1	0.007262	0.008199	0.006658
2	0.006713	0.006495	0.006665
3	0.006102	0.005384	0.006754
Delta	0.001160	0.002816	0.000096
Rank	2	1	3

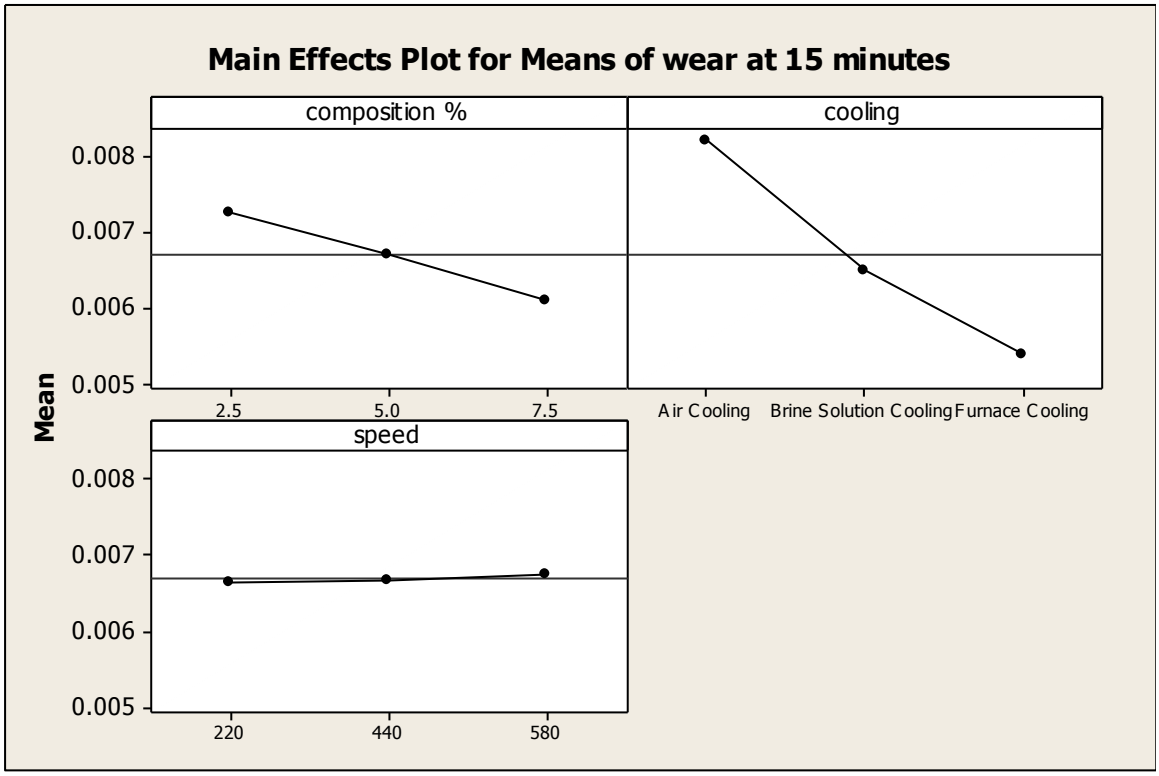

Figure 5.5: Main effect plot for Mean wear rate at 15 minutes

5.5.2 Results for S/N Ratio – Wear Rate at 15 Minutes

Table 5.16: ANOVA for S/N of wear rate at 15 minutes

Source	DF	Seq SS	Adj MS	F	P
Composition%	2	3.8065	1.9032	22.44	0.043
Cooling	2	20.4520	10.2260	120.57	0.008
Speed	2	0.1376	0.0688	0.81	0.552
Residual error	2	0.1696	0.0848		
Total	8	24.5657			
E pool	4	0.3072	0.0768		

Table 5.17: Response table for S/N ratio of wear rate at 15 minutes

Level	Composition%	Cooling	Speed
1	42.88	41.74	43.80
2	43.58	43.77	43.63
3	44.47	45.42	43.50
Delta	1.59	3.69	0.30
Rank	2	1	3

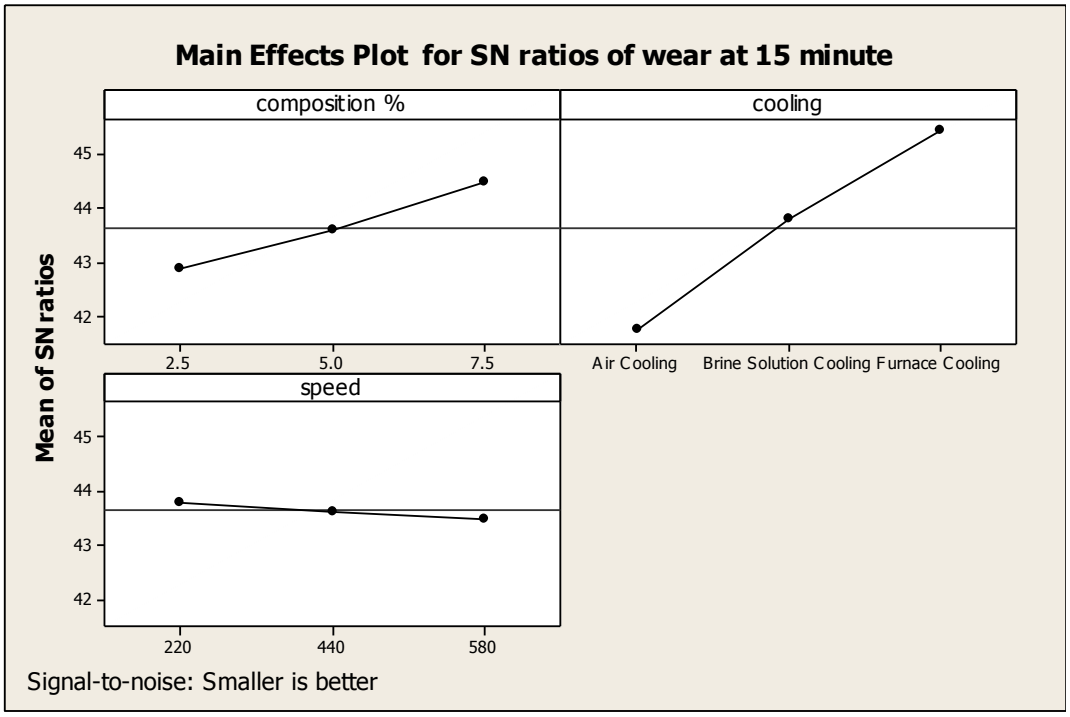

Figure 5.6: Main effects plot of wear rate at 15 minutes for S/N ratio

5.5.3 Optimal Design

Table 5.18: Significant factors for wear rate at 15 minutes of composites

Factors	Affecting mean		Affecting variation (S/N ratio)	
	Contribution	Best level	Contribution	Best level
Composition (A)	Significant	Level 3 -7.5%	Significant	Level 3 -7.5%

Cooling (B)	Significant	Level 3-FC	significant	Level 3-FC
Stirring speed (C)	Insignificant	-	Insignificant	-

Estimating the mean

Mean value of wear rate at 15 min. of composites

$\mu_{A_3B_3} = \overline{A_3} + \overline{B_3} - \overline{T}$

$\mu_{A_3B_3}$ = 0.00552 + 0.00649 - 0.00639 =0.005062

So the confidence interval around the wear rate at 15 min of composites is given by 0.005062±0.000167 mm^3/m

5.6 WEAR RATE AT 20 MINTUE

The effects of the parameters i.e. composition, type of cooling and stirring speed were evaluated on the composites having 2.5%, 5% and 7.5% reinforcement particles of average size 40 micron on the wear rate.

Table 5.19: Results for wear rate at 20 minutes

Trail no.	Composition of Al2O3	Type of cooling	Stirring speed	Wear at 20 minute	Mean	S/N ratio
1	2.5	Air Cooling	220	0.0106210	0.0106210	39.4767
2	2.5	Furnace Cooling	440	0.0080000	0.0080000	41.9382
3	2.5	Brine Solution Cooling	580	0.0075425	0.0075425	42.4497
4	5.0	Air Cooling	440	0.0100190	0.0100190	39.9835
5	5.0	Furnace Cooling	580	0.0076190	0.0076190	42.3620
6	5.0	Brine Solution Cooling	220	0.0071105	0.0071105	42.9620
7	7.5	Air Cooling	580	0.0093530	0.0093530	40.5810
8	7.5	Furnace Cooling	220	0.0069494	0.0069494	43.1611

9	7.5	Brine Solution Cooling	440	0.0065935	0.0065935	43.6177

5.6.1 Analysis of Variance – Wear at 20 Minutes

The results were analyzed using ANOVA for identifying the significant factors affecting the performance measures. The Analysis of Variance (ANOVA) for the wear at 95% confidence interval is given in Table 5.19.

Table 5.20: ANOVA for wear rate at 20 minutes

Sources	DF	Seq SS	Adj MS	F	P
Composition%	2	0.000002	0.000001	66.23	0.015
Cooling	2	0.000015	0.000007	548.26	0.002
Speed	2	0.000000	0.000000	0.17	0.853
Residual error	2	0.000001	0.000000		
Total	8	0.000018			
e pooled	4	0.000001	0.00000025		

Table 5.21: Response table for means of wear rate at 20 minutes

Level	Composition	Cooling	Speed
1	0.008721	0.009998	0.008227
2	0.008250	0.007082	0.008204
3	0.007632	0.007523	0.008172
Delta	0.001089	0.002916	0.000055
Rank	2	1	3

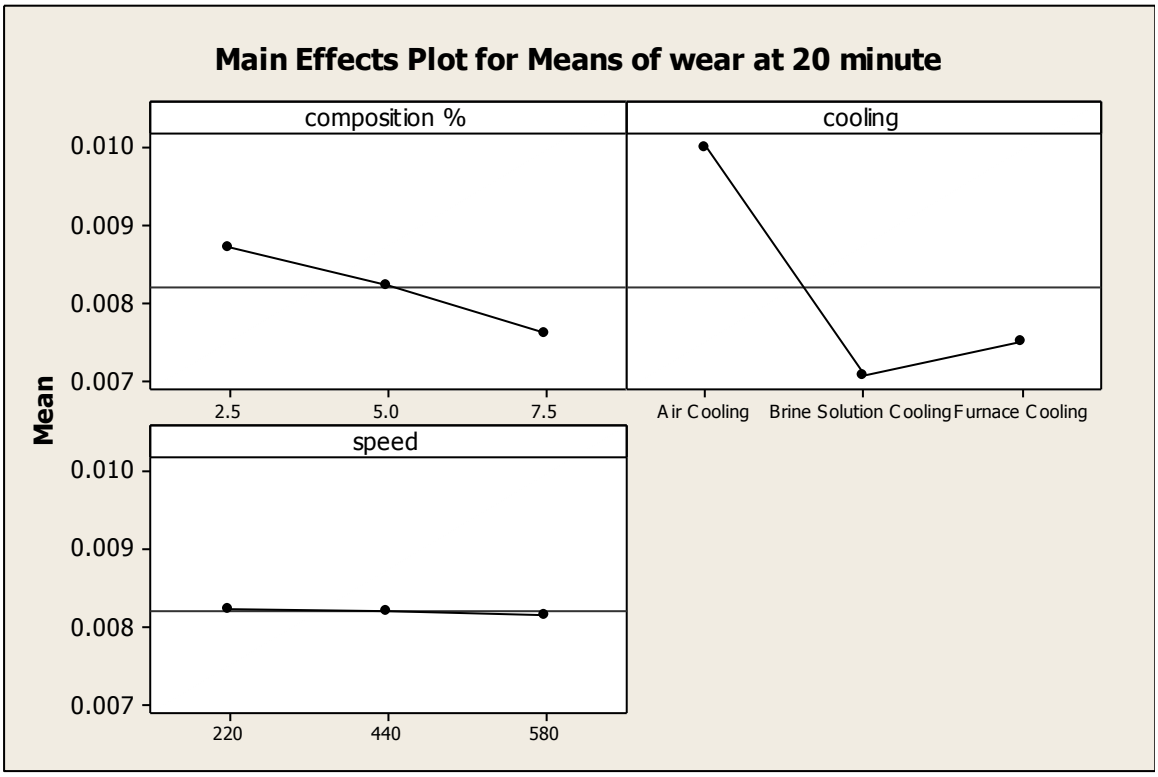

Figure 5.7: Main effect plot for Mean wear rate at 20 minutes

5.6.2 Results for S/N Ratio – Wear Rate at 20 Minutes

Table 5.22: ANOVA for S/N of wear rate at 20 minutes

Source	DF	Seq SS	Adj MS	F	P
Composition%	2	2.0567	1.02834	570.51	0.002
Cooling	2	15.3673	7.68365	4262.80	0.001
Speed	2	0.0076	0.00378	2.10	0.323
Residual error	2	0.0036	0.00180		
Total	8	17.4351			
E pool	4	0.00112	0.0028		

Table 5.23: Response table for S/N ratio of wear rate at 20 minutes

Level	Composition%	Cooling	Speed
1	41.29	40.01	41.87
2	41.77	43.01	41.85
3	42.45	42.49	41.80
Delta	1.17	3.00	0.07
Rank	2	1	3

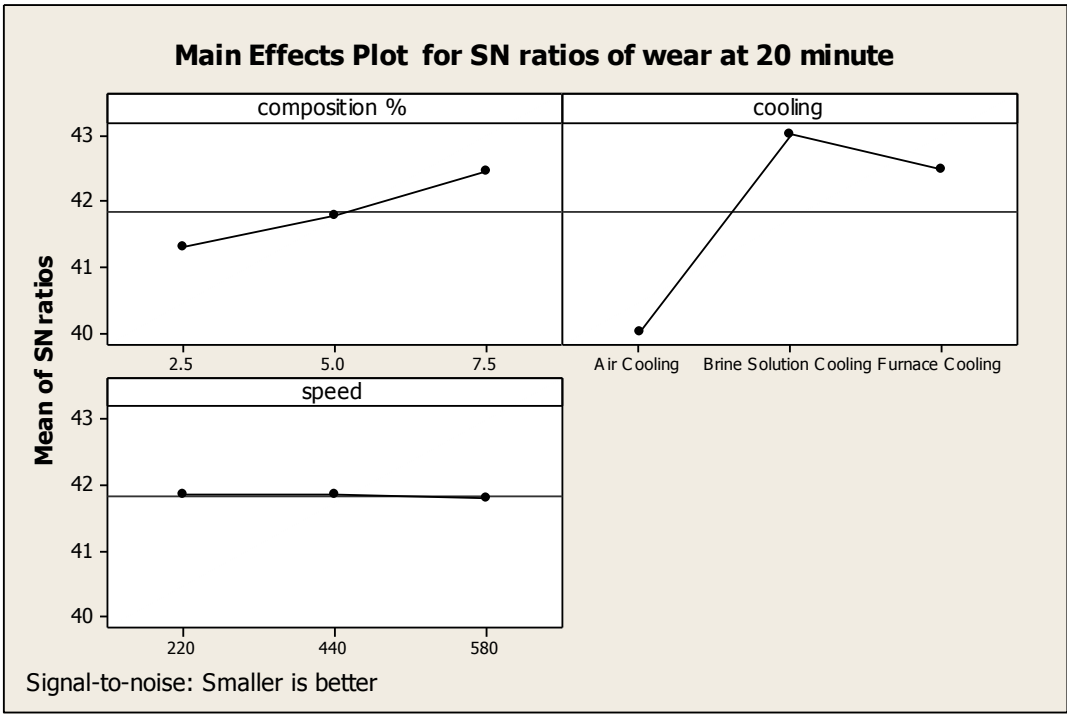

Figure 5.8: Main effects plot of wear rate at 20 minutes for S/N ratio

5.6.3 Optimal Design

Table 5.24: Significant factors for wear rate at 20 minutes of composites

Factors	Affecting mean		Affecting variation (S/N ratio)	
	Contribution	Best level	Contribution	Best level
Composition (A)	Significant	Level 3-7.5%	Significant	Level 3-7.5%
Cooling (B)	Significant	Level 2-BSC	significant	Level 2-BSC
Stirring speed (C)	Insignificant	-	Insignificant	-

Estimating the mean

Mean value of wear rate at 20 min. of composites

$\mu_{A_3B_3} = \overline{A_3} + \overline{B_2} - \overline{T}$

$\mu_{A_3B_2}$ = 0.00763 + 0.00708 - 0.00820 =0.00651

So the confidence interval around the wear rate at 20 min of composites is given by 0.00651±0.000167 mm^3/m

5.7 WEAR RATE AT 25 MINUTES

The effects of the parameters i.e. composition, type of cooling and stirring speed were evaluated on the composites having 2.5%, 5% and 7.5% reinforcement particles of average size 40 micron on the wear rate.

Table 5.25: Results for wear rate at 25 minutes

Trail no.	Composition of Al2O3	Type of cooling	Stirring speed	Wear at 20 minute	Mean	S/N ratio
1	2.5	Air Cooling	220	0.0111112	0.0111112	39.0848
2	2.5	Furnace Cooling	440	0.0090000	0.0090000	40.9151
3	2.5	Brine Solution Cooling	580	0.0092608	0.0092608	40.6670
4	5.0	Air Cooling	440	0.0105360	0.0105360	39.5465
5	5.0	Furnace Cooling	580	0.0083360	0.0083360	41.5808
6	5.0	Brine Solution Cooling	220	0.0084484	0.0084484	41.4645
7	7.5	Air Cooling	580	0.0098628	0.0098628	40.1200
8	7.5	Furnace Cooling	220	0.0075575	0.0075575	42.4324
9	7.5	Brine Solution Cooling	440	0.0077484	0.0077484	42.2158

5.7.1 Analysis]of Variance – Wear at 25 Minutes

The results were analyzed using ANOVA for identifying the significant factors affecting the performance measures. The Analysis of Variance (ANOVA) for the wear at 95% confidence interval is given in Table 5.25.

Table 5.26: ANOVA for wear rate at 25 minutes

Sources	DF	Seq SS	Adj MS	F	P
Composition%	2	0.000003	0.000001	656.07	0.002
Cooling	2	0.000009	0.000004	1998.15	0.001
Speed	2	0.000000	0.000000	4.36	0.187
Residual error	2	0.000001	0.000000		
Total	8	0.000012			
e pooled	4	0.000001	0.00000025		

Table 5.27: Response table for means of wear rate at 25 minutes

Level	Composition	Cooling	Speed
1	0.009791	0.010503	0.009039
2	0.009107	0.008486	0.009095
3	0.008390	0.008298	0.009153
Delta	0.001401	0.002206	0.000114
Rank	2	1	3

\

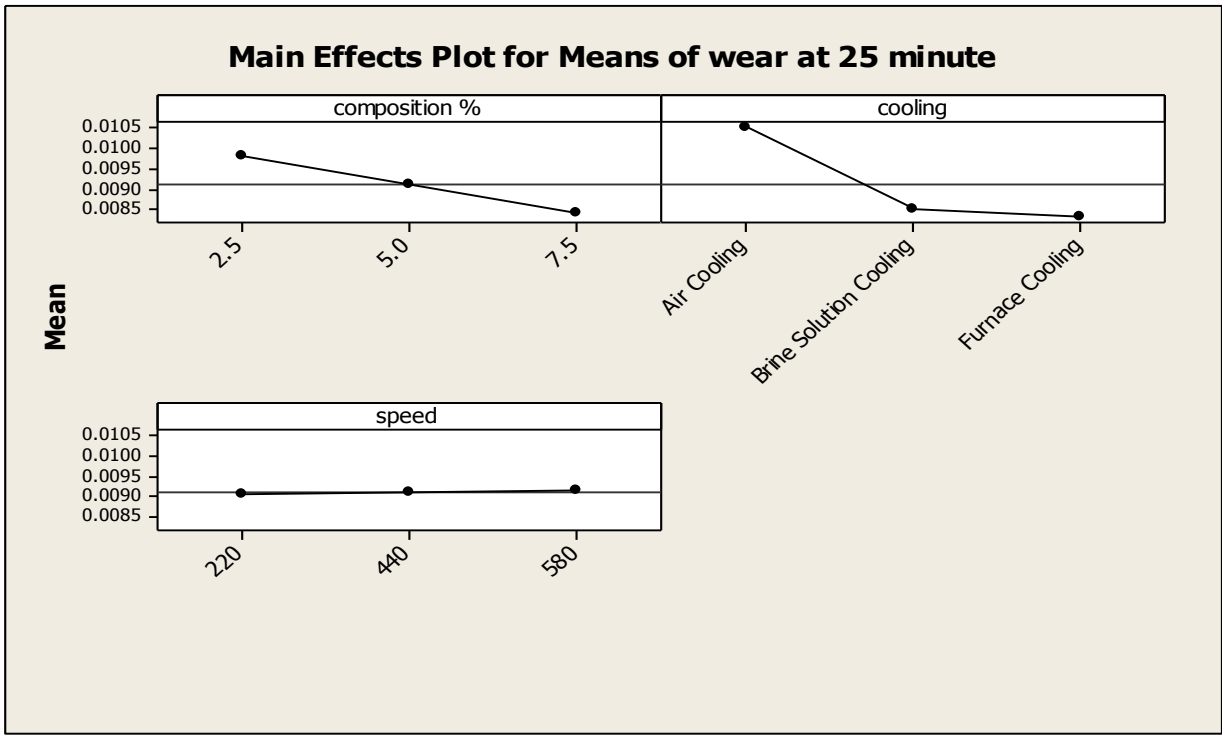

Figure 5.9: Main effect plot for Mean wear rate at 25 minutes

5.7.2 Results for S/N Ratio – Wear Rate After 25 Minutes

Table 5.28: ANOVA for S/N of wear rate at 25 minutes

Source	DF	Seq SS	Adj MS	F	P
Composition%	2	2.8068	1.40341	113.52	0.009
Cooling	2	7.7568	3.87839	313.72	0.003
Speed	2	0.0628	0.03140	2.54	0.282
Residual error	2	0.0247	0.01236		
Total	8	10.6511			
E pool	4	0.0875	0.021875		

Table 5.29: Response table for S/N ratio of wear rate at 25 minutes

Level	Composition%	Cooling	Speed
1	40.22	39.58	40.99
2	40.86	41.45	40.89
3	41.59	41.64	40.79
Delta	1.37	2.06	0.20
Rank	2	1	3

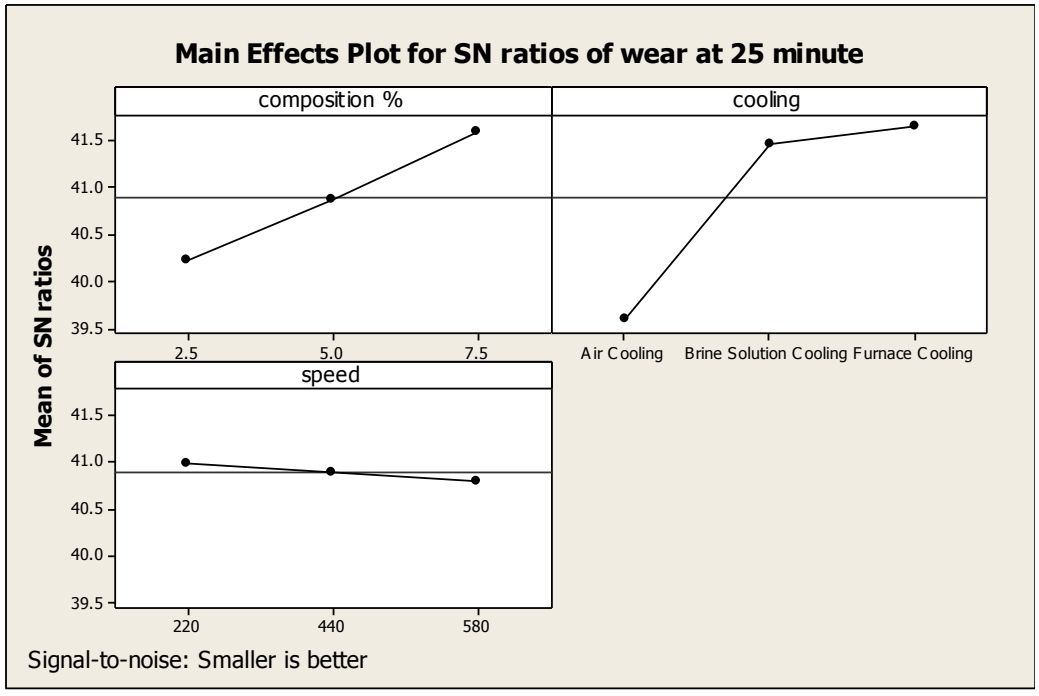

Figure 5.10: Main effects plot of wear rate at 25 minutes for S/N ratio

5.7.3 Optimal Design

Table 5.30: Significant factors for wear rate at 25 minutes of composites

Factors	Affecting mean		Affecting variation (S/N ratio)	
	Contribution	Best level	Contribution	Best level
Composition (A)	Significant	Level 3-7.5%	Significant	Level 3-7.5%

Cooling (B)	Significant	Level 3-FC	significant	Level 3-FC
Stirring speed (C)	Insignificant	-	Insignificant	-

Estimating the mean

Mean value of wear rate at 25 min. of composites

$\mu_{A_3B_3} = \overline{A_3} + \overline{B_3} - \overline{T}$

$\mu_{A_3B_3}$ = 0.00839 + 0.00829 - 0.00909 =0.00759

So the confidence interval around the wear rate at 25 min of composites is given by 0.00759±0.000167 mm^3/m

5.8 WEAR RATE AT 30 MINUTES

The effects of the parameters i.e. composition, type of cooling and stirring speed were evaluated on the composites having 2.5%, 5% and 7.5% reinforcement particles of average size 40 micron on the wear rate.

Table 5.31 results for wear rate at 30 minutes

Trail no.	Composition of Al_2O_3	Type of cooling	Stirring speed	Wear at 30 minute	Mean	S/N ratio
1	2.5	Air Cooling	220	0.0206974	0.0206974	33.6817
2	2.5	Furnace Cooling	440	0.0120000	0.0120000	38.4164
3	2.5	Brine Solution Cooling	580	0.0157434	0.0157434	36.0580
4	5.0	Air Cooling	440	0.0199093	0.0199093	34.0189
5	5.0	Furnace Cooling	580	0.0111083	0.0111083	39.0870
6	5.0	Brine Solution Cooling	220	0.0151991	0.0151991	36.3636
7	7.5	Air Cooling	580	0.0181637	0.0181637	34.8159
8	7.5	Furnace Cooling	220	0.0104085	0.0104085	39.6522

9	7.5	Brine Solution Cooling	440	0.0143357	0.0143357	36.8716

5.8.1 Analysis Of Variance – Wear at 30 Minutes

The results were analyzed using ANOVA for identifying the significant factors affecting the performance measures. The Analysis of Variance (ANOVA) for the wear at 95% confidence interval is given in Table 5.31

Table 5.32: ANOVA for wear rate at 30 minutes

Sources	DF	Seq SS	Adj MS	F	P
Composition%	2	0.000005	0.000003	42.26	0.023
Cooling	2	0.000106	0.000053	870.63	0.001
Speed	2	0.000000	0.000000	2.89	0.257
Residual error	2	0.000001	0.000000		
Total	8	0.000112			
e pooled	4	0.000001	0.00000025		

Table 5.33: Response table for means of wear rate at 30 minutes

Level	Composition	Cooling	Speed
1	0.01615	0.01959	0.01544
2	0.01541	0.01509	0.01541
3	0.01430	0.01117	0.01501
Delta	0.00184	0.00842	0.00043
Rank	2	1	3

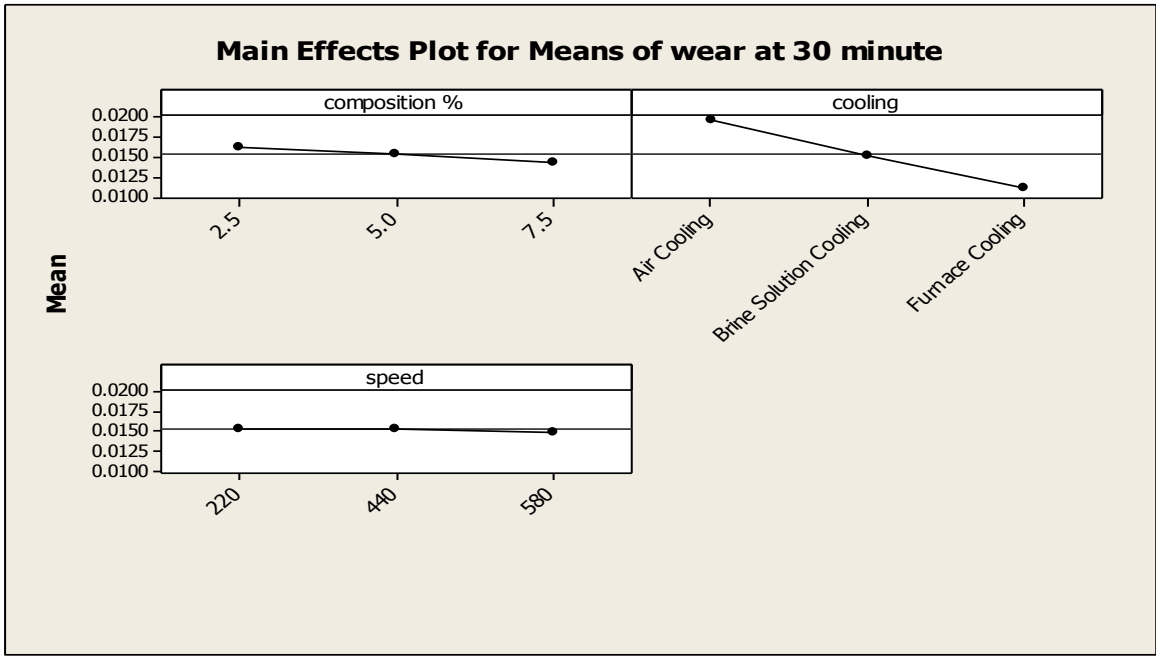

Figure 5.11: Main effect plot for Mean wear rate at 30 minutes

5.8.2 Results of S/N Ratio – Wear Rate at 30 Minutes

Table 5.34: ANOVA for S/N of wear rate at 30 minutes

Source	DF	Seq SS	Adj MS	F	P
Composition%	2	1.7065	0.8533	556.29	0.002
Cooling	2	35.7827	17.8914	11664.38	0.000
Speed	2	0.0722	0.0361	23.54	0.041
Residual error	2	0.0031	0.0015		
Total	8	37.5645			
E pool	2	0.0031	0.00155		

Table 5.35: Response table for S/N ratio of wear rate at 30 minutes

Level	Composition%	Cooling	Speed
1	36.05	34.17	36.57
2	36.49	36.43	36.44
3	37.11	39.05	36.65
Delta	1.06	4.88	0.22
Rank	2	1	3

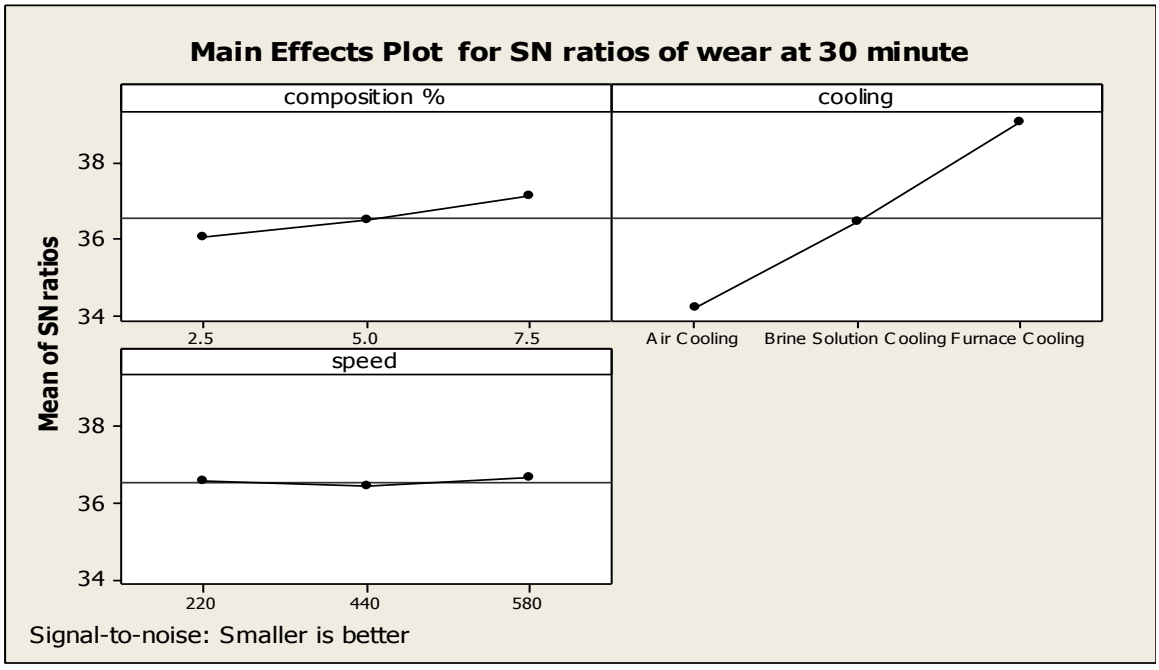

Figure 5.12: Main effects plot of wear rate at 30 minutes for S/N ratio

5.8.3 Optimal Design

Table 5.36: Significant factors for wear rate at 30 minutes of composites

Factors	Affecting mean		Affecting variation (S/N ratio)	
	Contribution	Best level	Contribution	Best level
Composition (A)	Significant	Level 3-7.5%	Significant	Level 3-7.5%
Cooling (B)	Significant	Level 3-FC	significant	Level 3-FC
Stirring speed (C)	Insignificant	-	Insignificant	Level 3-580

Estimating the mean

Mean value of wear rate at 30 min. of composites

$\mu_{A_3B_3} = \overline{A_3} + \overline{B_3} - \overline{T}$

$\mu_{A_3B_3}$ = 0.01430 + 0.01117 - 0.015285 =0.010185

So the confidence interval around the wear rate at 30 min of composites is given by 0.010185±0.000167 mm^3/m

5.9 RESULTS OF WEAR RATE WITH TIME

The effect of the various parameters i.e. composition, cooling and stirring speed on wear rate of the composites prepared by L9 treatment were compared by using ANOVA. The wear rate was compared at different times i.e. 5min, 10, 15, 20, 25, and 30 min. From the above various plots for means and S/N ratios, the effect of the parameters were compared. The parameters having 'p' value less than 0.05 are significant and the other having values of 'p' more than '0.05' are insignificant. From the response table the rank of the different parameters are decided according to their effect on the wear rate. It has been seen that the two factors i.e. composition and type of cooling were significant on the each time and the parameter stirring speed was insignificant.

It has been seen that in composition level 3 '7.5%' was always best in all the cases and in the case of cooling the 'furnace cooling' was best in the all of the cases except at 20 min. at 20 min brine solution cooling was the best cooling. But if overall results were evaluated then furnace cooling was best. The parameter stirring speed was insignificant all the times.

At 7.5% composition the amount of the reinforcement particles is more in MMC. During furnace cooling the structure obtained is denser than that of air cooling and furnace cooling. Because of the presence of the Al2O3 particles in cooling the bonding strength is more so the strength of the MMC is more due to which the less wear rate was achieved. Even the strength of the Al2O3 particles is far superior which helps to decrease the wear rate.

When the wear rate of MMC's is compared with time then the wear rate is increase as the time is increased. The wear was less at 5 min and maximum when time was 30 min.

5.10 WEAR RATE WITH SLIDING DISTANCE

After analysis of wear behavior with time, wear rate with respect to sliding distance was calculated. Wear rate was calculated on various sliding distances i.e. 500, 1000, 1500, 2000, 2500, and 3000. Effect of the parameters i.e. composition of Al_2O_3, type of cooling and stirring speed were analyzed on the wear rate w.r.t sliding distance.

$$\text{Wear rate} = \frac{wear\ \ volume}{sliding\ \ distance}\ \text{mm}^3/\text{sec}$$

$$\text{Wear volume} = = \pi r^2 \text{h}$$

Where

r = radius of pin (5mm)

h = commutative height loss of pin after sliding over disc

And

$$\text{Sliding distance} = \frac{\pi DN}{60} \times t$$

Where

D = Diameter of the track (60mm)

N = RPM of the disc (510)

5.11 WEAR RATE AT 500 SLIDING DISTANCE

The effects of the parameters i.e. composition, type of cooling and stirring speed were evaluated on the composites having 2.5%, 5% and 7.5% reinforcement particles of average size 40 micron on the wear rate.

Table 5.37: Results for wear rate at 500 sliding distance

Trail no.	Composition of Al2O3	Type of cooling	Stirring speed	Wear at 500 SD	Mean	S/N ratio
1	2.5	Air Cooling	220	0.950144	0.950144	0.44421
2	2.5	Furnace Cooling	440	0.589000	0.589000	4.59769
3	2.5	Brine Solution Cooling	580	0.948520	0.948520	0.45907
4	5.0	Air Cooling	440	0.889020	0.889020	1.02177
5	5.0	Furnace Cooling	580	0.540484	0.540484	5.34434
6	5.0	Brine Solution Cooling	220	0.878634	0.878634	1.12384
7	7.5	Air Cooling	580	0.774870	0.774870	2.21542
8	7.5	Furnace Cooling	220	0.471222	0.471222	6.53550
9	7.5	Brine Solution Cooling	440	0.765608	0.765608	2.31987

5.11.1 Analysis Of Variance – Wear at 500 Sliding Distance

The results were analyzed using ANOVA for identifying the significant factors affecting the performance measures. The Analysis of Variance (ANOVA) for the wear at 95% confidence interval is given in Table 5.37.

Table 5.38: ANOVA for wear rate after 500 sliding distance

Sources	DF	Seq SS	Adj MS	F	P
Composition%	2	0.038516	0.019258	47.24	0.021
Cooling	2	0.223496	0.111748	274.13	0.004
Speed	2	0.000544	0.000272	0.67	
Residual error	2	0.000815	0.000408		
Total	8	0.263371			

e pooled	4	0.001359	0.0003397		

Table 5.39: Response table for means of wear rate after 500 sliding distance

Level	Composition	Cooling	Speed
1	0.8292	0.8713	0.7667
2	0.7694	0.8643	0.7479
3	0.6706	0.5336	0.7546
Delta	0.1587	0.3378	0.0188
Rank	2	1	3

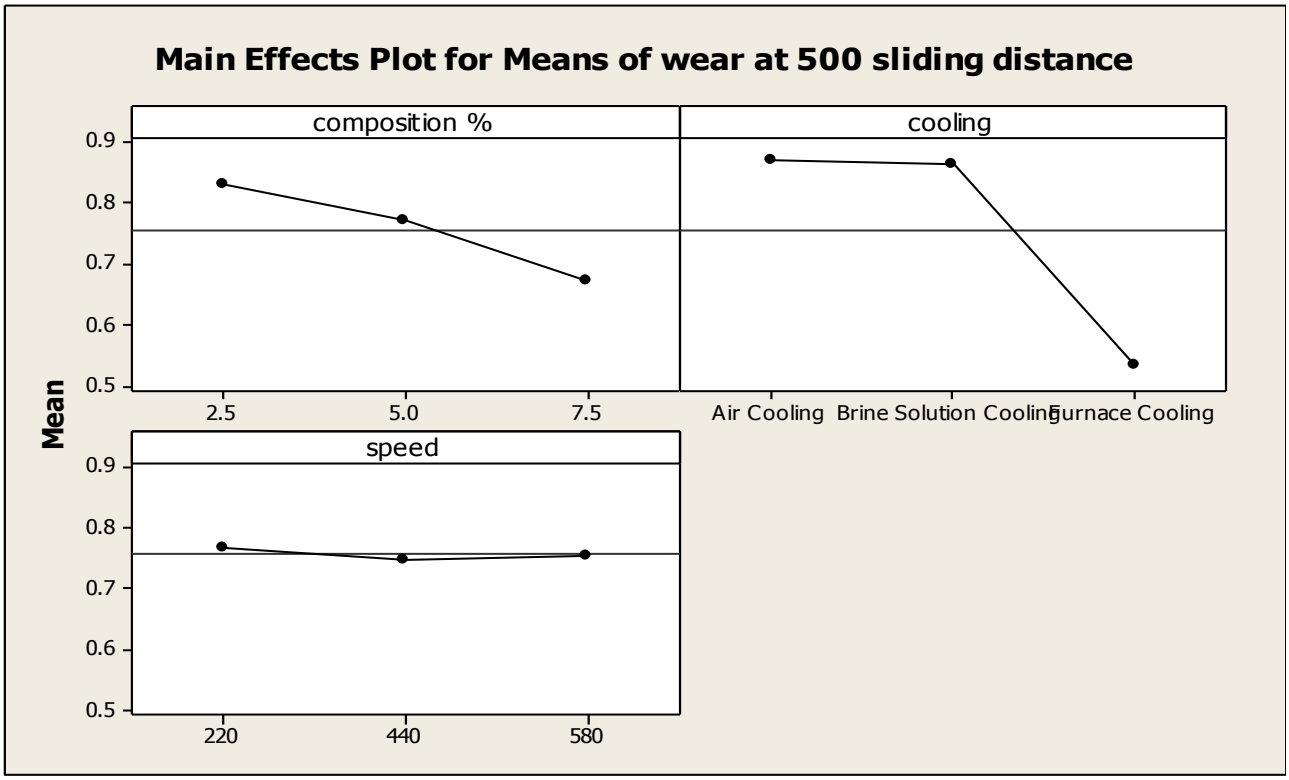

Figure 5.13: Main effect plot for Mean wear rate 500 sliding distance

5.11.2 Results for S/N Ratio – Wear Rate at 500 Sliding Distance

Table 5.40: ANOVA for S/N of wear rate at 500 sliding distance

Source	DF	Seq SS	Adj MS	F	P
Composition%	2	5.3113	2.6556	1081.90	0.001
Cooling	2	35.7683	17.8841	7285.96	0.000
Speed	2	0.0045	0.0022	0.92	0.522
Residual error	2	0.0049	0.0025		
Total	8	41.0889			
E pool	4	0.0094	0.00235		

Table 5.41: Response table for S/N ratio of wear rate

Level	Composition%	Cooling	Speed
1	1.834	1.227	2.701
2	2.497	1.301	2.646
3	3.690	5.493	2,673
Delta	1.857	4.265	0.055
Rank	2	1	3

5.11.3 Optimal Design

Table 5.42: Significant factors for wear rate at 500 SD of composites

Factors	Affecting mean		Affecting variation (S/N ratio)	
	Contribution	Best level	Contribution	Best level
Composition (A)	Significant	Level 3-7.5%	Significant	Level 3-7.5%
Cooling (B)	Significant	Level 3-FC	significant	Level 3-FC
Stirring speed (C)	Insignificant	-	Insignificant	-

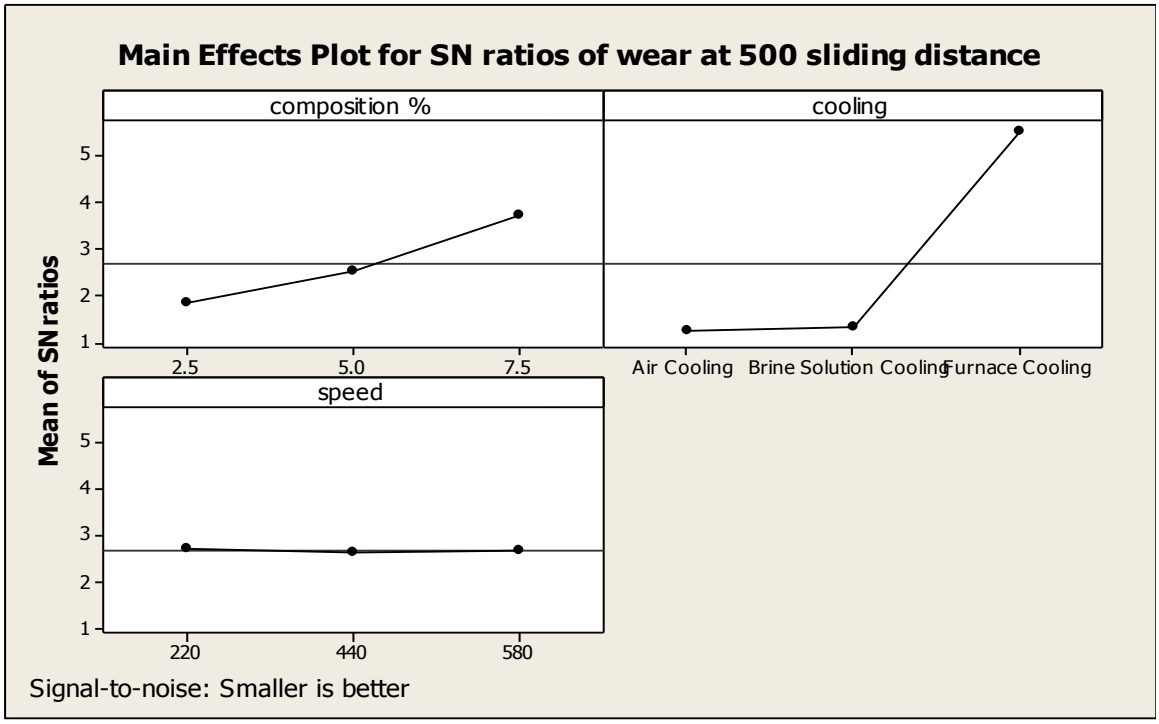

Figure 5.14: Main effects plot of wear rate at 500 sliding distance for S/N ratio

Estimating the mean

Mean value of wear rate of composites at 500 sliding distance

$\mu_{A_3B_3} = \overline{A_3} + \overline{B_3} - \overline{T}$

$\mu_{A_3B_3}$ = 0.670566 + 0.533569 - 0.756389 =0.447746

Confidence Interval around the Estimated Mean

Confidence Interval around the estimated wear rate of composites at 500 sliding distance:

$$CI_1 = \sqrt{\frac{F_{\alpha,v_1,v_2} V_e}{n_{eff}}} \quad \text{Where} \quad F_{\alpha v_1 v_2} = F\ ratio$$

$\alpha = risk\ (0.05)$ $\qquad$ $confidence = 1-\alpha$

$v_1 = dof\ \ for\ mean\ which\ is\ always = 1$

$\nu_2 = dof \ \ for\, error = \nu_e$

n_{eff} = Number of tests under that condition using the participating factors

$$n_{eff} = \frac{N}{1 + dof_{A,B}} = \frac{9}{1+2+2} = 1.8$$

$$CI = \sqrt{\frac{F_{\alpha,\nu_1,\nu_2} V_e}{n_{eff}}} = \sqrt{\frac{0.2 \times 0.0003397}{1.8}} = 0.006144$$

So the confidence interval around the wear rate of composites at 500 sliding distance is given by 0.447746±0.006144 mm^3/m

5.12. WEAR RATE AT 1000 SLIDING DISTANCE

The effects of the parameters i.e. composition, type of cooling and stirring speed were evaluated on the composites having 2.5%, 5% and 7.5% reinforcement particles of average size 40 micron on the wear rate.

Table 5.43 Results for wear rate at 1000 sliding distance

Trail no.	Composition of Al2O3	Type of cooling	Stirring speed	Wear at 1000 SD	Mean	S/N ratio
1	2.5	Air Cooling	220	0.695974	0.695974	3.14814
2	2.5	Furnace Cooling	440	0.518170	0.518170	5.71055
3	2.5	Brine Solution Cooling	580	0.580707	0.580707	4.72086
4	5.0	Air Cooling	440	0.649941	0.649941	3.74252
5	5.0	Furnace Cooling	580	0.452754	0.452754	6.88276
6	5.0	Brine Solution Cooling	220	0.531983	0.531983	5.48205

7	7.5	Air Cooling	580	0.578952	0.578952	4.74714
8	7.5	Furnace Cooling	220	0.395019	0.395019	8.06763
9	7.5	Brine Solution Cooling	440	0.493700	0.493700	6.13073

5.12.1 Analysis of Variance – Wear at 1000 Sliding Distance

The results were analyzed using ANOVA for identifying the significant factors affecting the performance measures. The Analysis of Variance (ANOVA) for the wear at 95% confidence interval is given in Table 5.43.

Table 5.44: ANOVA for wear rate after 1000sliding distance

Sources	DF	Seq SS	Adj MS	F	P
Composition%	2	0.017844	0.008922	341.52	0.003
Cooling	2	0.052404	0.026202	1003.00	0.001
Speed	2	0.000451	0.000226	8.63	0.104
Residual error	2	0.000052	0.000026		
Total	8	0.070751			
e pooled	4	0.000503	0.000125		

Table 5.45: Response table for means of wear rate at 1000 sliding distance

Level	Composition	Cooling	Speed
1	0.5983	0.6416	0.5410
2	0.5449	0.5355	0.5539
3	0.4892	0.4553	0.5375
Delta	0.1091	0.1863	0.0165
Rank	2	1	3

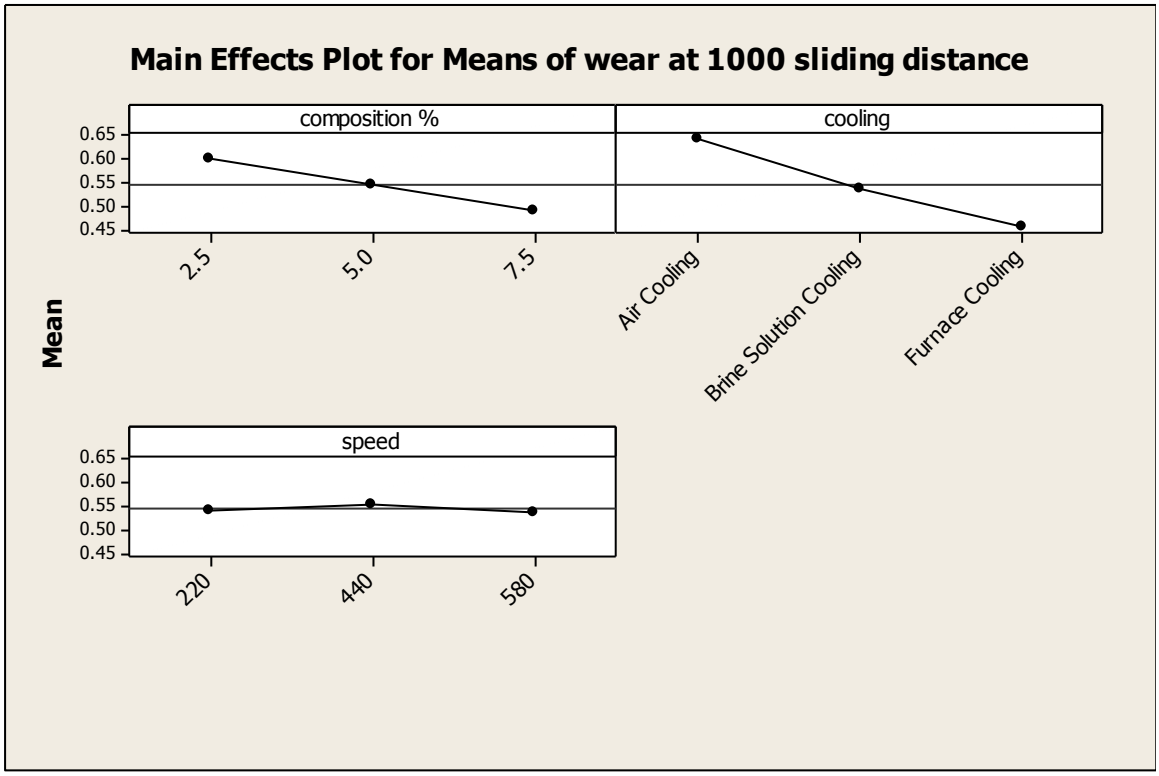

Figure 5.15: Main effect plot for Mean wear rate at 1000 sliding distance

5.12.2 Results of S/N Ratio – Wear Rate at 1000 Sliding Distance

Table 5.46: ANOVA for S/N of wear rate at 1000 sliding distance

Source	DF	Seq SS	Adj MS	F	P
Composition%	2	4.8043	2.40213	80.78	0.012
Cooling	2	13.5771	6.78853	228.29	0.004
Speed	2	0.2166	0.10832	3.64	0.215
Residual error	2	0.0595	0.02974		
Total	8	18.6574			
E pool	4	0.2761	0.06902		

Table 5.47: Response table for S/N ratio of wear rate at 1000 sliding distance

Level	Composition%	Cooling	Speed
1	4.527	3.879	5.566
2	5.369	5.445	5.195
3	6.315	6.887	5.450
Delta	1.789	3.008	0.371
Rank	2	1	3

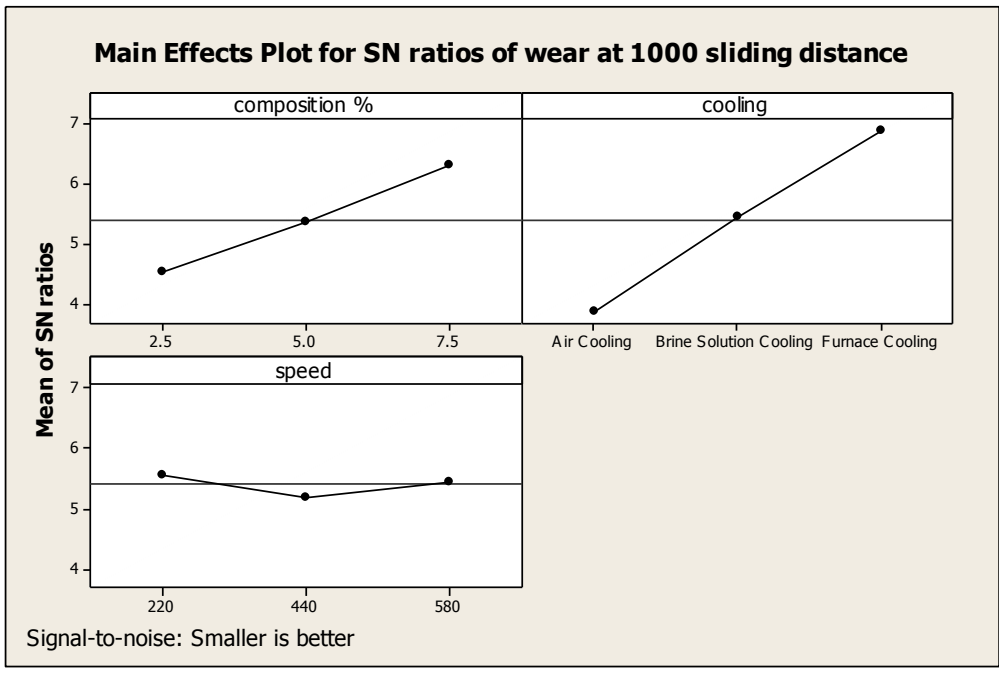

Figure 5.16: Main effects plot of wear rate at 1000 sliding distance for S/N ratio

5.12.3. Optimal Design

Table 5.48: Significant factors for wear rate at 1000 sliding distance of composites

Factors	Affecting mean		Affecting variation (S/N ratio)	
	Contribution	Best level	Contribution	Best level
Composition (A)	Significant	Level 3-7.5%	Significant	Level 3-7.5%
Cooling (B)	Significant	Level 3-FC	significant	Level 3-FC
Stirring speed (C)	Insignificant	-	Insignificant	-

Estimating the mean

Mean value of wear rate of composites at 1000 sliding distance

$\mu_{A_3B_3} = \overline{A_3} + \overline{B_3} - \overline{T}$

$\mu_{A_3B_3}$ = 0.489224 + 0.455314 - 0.544133 =0.400405

Confidence Interval around the Estimated Mean

Confidence Interval around the estimated wear rate of composites at 1000 sliding distance:

$CI_1 = \sqrt{\frac{F_{\alpha,\nu_1,\nu_2} V_e}{n_{eff}}}$ Where $F_{\alpha\nu_1\nu_2} = F\ ratio$

$\alpha = risk$ (0.05) $confidence = 1-\alpha$

$\nu_1 = dof\ \ for\ mean\ which\ is\ always = 1$

$\nu_2 = dof\ \ for\ error = \nu_e$

n_{eff} = Number of tests under that condition using the participating factors

$$n_{eff} = \frac{N}{1+dof_{A,B}} = \frac{9}{1+2+2} = 1.8$$

$$CI = \sqrt{\frac{F_{\alpha,\nu_1,\nu_2} V_e}{n_{eff}}} = \sqrt{\frac{0.2 \times 0.000125}{1.8}} = 0.0037267$$

So the confidence interval around the wear rate of composites at 1000 sliding distance is given by 0.400405±0.0037267 mm^3/m

5.13 WEAR RATE AT 1500 SLIDING DISTANCE

The effects of the parameters i.e. composition, type of cooling and stirring speed were evaluated on the composites having 2.5%, 5% and 7.5% reinforcement particles of average size 40 micron on the wear rate.

Table 5.49 Results for wear rate at 1500 sliding distance

Trail no.	Composition of Al2O3	Type of cooling	Stirring speed	Wear at 1500 SD	Mean	S/N ratio
1	2.5	Air Cooling	220	0.664893	0.664893	3.54496
2	2.5	Furnace Cooling	440	0.579854	0.579854	4.73363
3	2.5	Brine Solution Cooling	580	0.594715	0.594715	4.51383
4	5.0	Air Cooling	440	0.639268	0.639268	3.88634
5	5.0	Furnace Cooling	580	0.547016	0.547016	5.24000
6	5.0	Brine Solution Cooling	220	0.577001	0.577001	4.77646
7	7.5	Air Cooling	580	0.596253	0.596253	4.49139
8	7.5	Furnace Cooling	220	0.504660	0.504660	5.94002
9	7.5	Brine Solution Cooling	440	0.511047	0.511047	5.83078

5.13.1 Analysis Of Variance – Wear at 1500 Sliding Distance

The results were analyzed using ANOVA for identifying the significant factors affecting the performance measures. The Analysis of Variance (ANOVA) for the wear at 95% confidence interval is given in Table 5.49.

Table 5.50: ANOVA for wear rate at 1500 sliding distance

Sources	DF	Seq SS	Adj MS	F	P
Composition%	2	0.008940	0.004470	58.97	0.017
Cooling	2	0.013588	0.006794	89.63	0.011
Speed	2	0.000045	0.000022	0.30	0.772
Residual error	2	0.000152	0.000076		
Total	8	0.022725			
e pooled	4	0.000197	0.0000492		

Table 5.51: Response table for means of wear rate at 1500 sliding distance

Level	Composition	Cooling	Speed
1	0.6132	0.6335	0.5822
2	0.5878	0.5609	0.5767
3	0.5373	0.5438	0.5793
Delta	0.0758	0.0896	0.0055
Rank	2	1	3

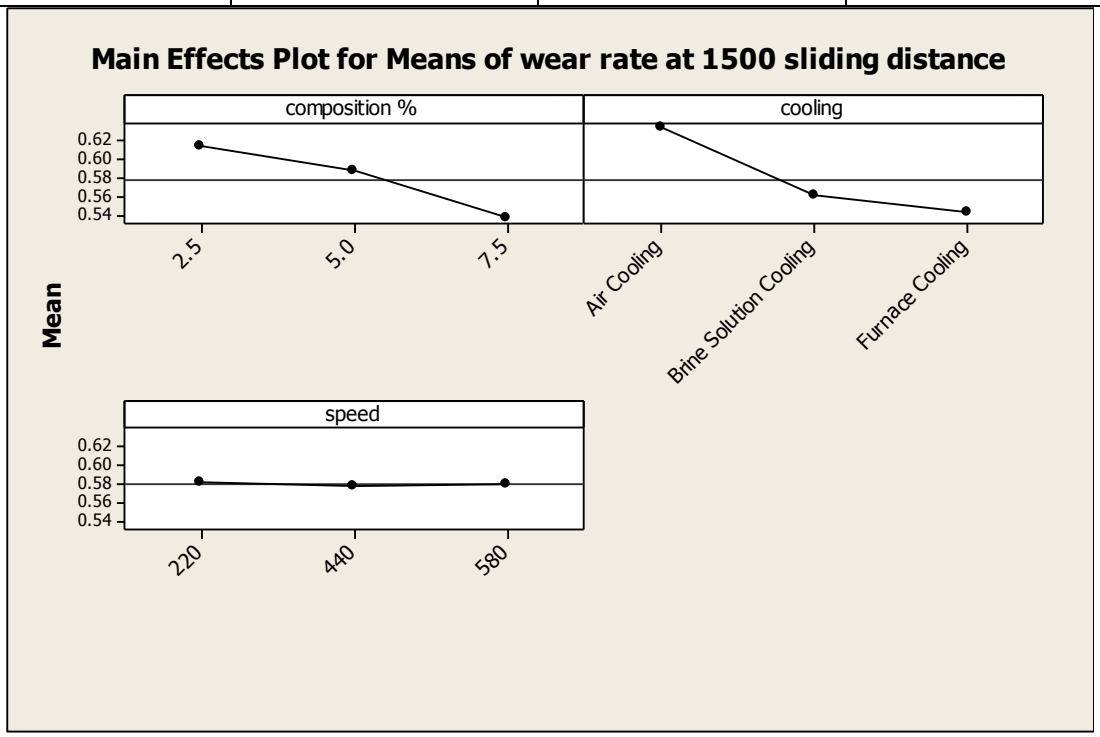

Figure 5.17: Main effect plot for Mean wear rate

5.13.2 Results of S/N Ratio – Wear Rate at 1500 Sliding Distance

Table 5.52: ANOVA for S/N of wear rate at 1500 sliding distance

Source	DF	Seq SS	Adj MS	F	P
Composition%	2	2.09322	1.04661	33.17	0.029
Cooling	2	2.97618	1.48809	47.16	0.021
Speed	2	0.00871	0.00435	0.14	0.879
Residual error	2	0.06311	0.03155		
Total	8	5.14121			
E pool	4	0.07182	0.01795		

Table 5.53: Response table for S/N ratio of wear rate at 1500 sliding distance

Level	Composition%	Cooling	Speed
1	4.264	3.974	4.754
2	4.634	5.040	4.817
3	5.421	5.305	4.748
Delta	1.157	1.330	0.069
Rank	2	1	3

5.13.3 Optimal Design

Table 5.54: Significant factors for wear rate at 1500 sliding distance of composites

Factors	Affecting mean		Affecting variation (S/N ratio)	
	Contribution	Best level	Contribution	Best level
Composition (A)	Significant	Level 3-7.5%	Significant	Level 3-7.5%
Cooling (B)	Significant	Level 3-FC	significant	Level 3-FC
Stirring speed (C)	Insignificant	-	Insignificant	-

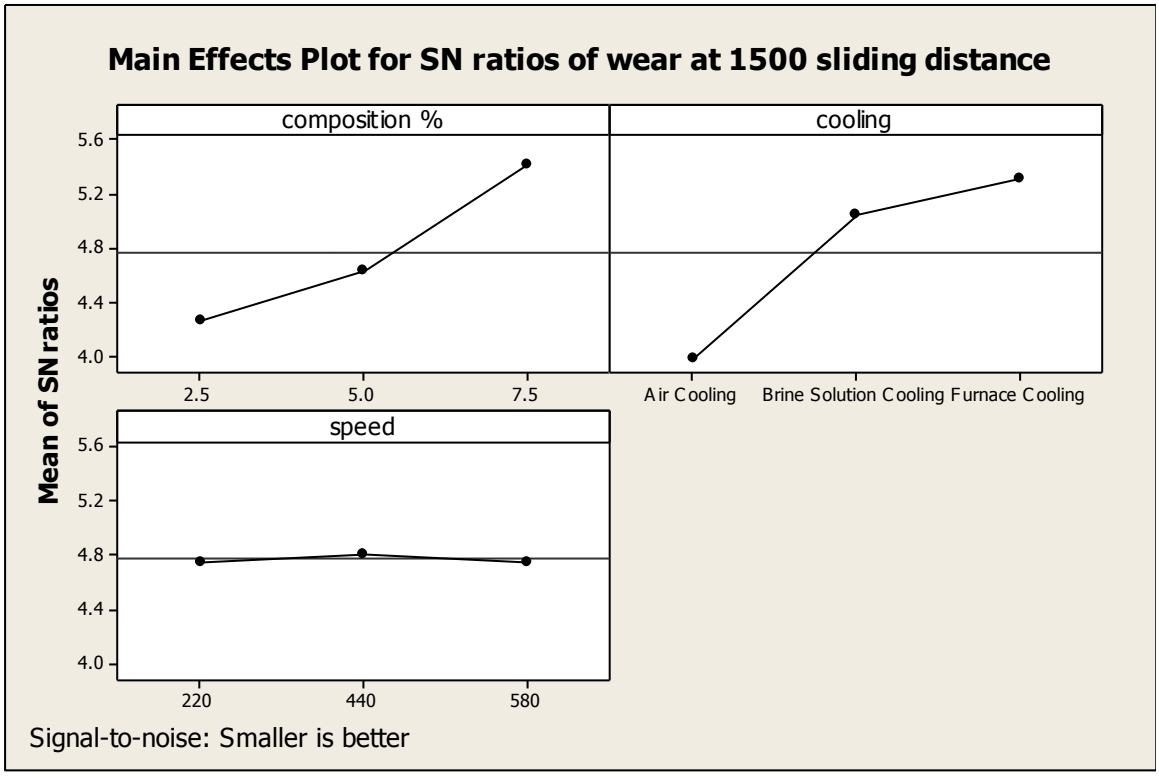

Figure 5.18: Main effects plot of wear rate for S/N ratio

Estimating the mean

Mean value of wear rate of composites at 1500 sliding distance

$\mu_{A_3B_3} = \overline{A_3} + \overline{B_3} - \overline{T}$

$\mu_{A_3B_3}$ = 0.53732 + 0.543843 - 0.579412 =0.501751

Confidence Interval around the Estimated Mean

Confidence Interval around the estimated wear rate of composites at 1500 sliding distance:

$$CI_1 = \sqrt{\frac{F_{\alpha,v_1,v_2} V_e}{n_{eff}}} \quad \text{Where} \quad F_{\alpha v_1 v_2} = F\ ratio$$

$\alpha = risk\ (0.05) \qquad confidence = 1-\alpha$

$v_1 = dof\ \ for\ mean\ which\ is\ always = 1$

$\nu_2 = dof \ \ for\, error = \nu_e$

n_{eff} = Number of tests under that condition using the participating factors

$$n_{eff} = \frac{N}{1 + dof_{A,B}} = \frac{9}{1+2+2} = 1.8$$

$$CI = \sqrt{\frac{F_{\alpha,\nu_1,\nu_2} V_e}{n_{eff}}} = \sqrt{\frac{0.2 \times 0.0000492}{1.8}} = 0.0023381$$

So the confidence interval around the wear rate of composites at 1500 sliding distance is given by 0.501751±0.0023381 mm^3/m

5.14 WEAR RATE AT 2000 SLIDING DISTANCE

The effects of the parameters i.e. composition, type of cooling and stirring speed were evaluated on the composites having 2.5%, 5% and 7.5% reinforcement particles of average size 40 micron on the wear rate.

Table 5.55 Results for wear rate at 2000 sliding distance

Trail no.	Composition of Al2O3	Type of cooling	Stirring speed	Wear at 2000 SD	Mean	S/N ratio
1	2.5	Air Cooling	220	0.658652	0.658652	3.62688
2	2.5	Furnace Cooling	440	0.527621	0.527621	5.55356
3	2.5	Brine Solution Cooling	580	0.517438	0.517438	5.72283
4	5.0	Air Cooling	440	0.638170	0.638170	3.90127
5	5.0	Furnace Cooling	580	0.496889	0.496889	6.07481
6	5.0	Brine Solution Cooling	220	0.487438	0.487438	6.24161

7	7.5	Air Cooling	580	0.588353	0.588353	4.60724
8	7.5	Furnace Cooling	220	0.465974	0.465974	6.63277
9	7.5	Brine Solution Cooling	440	0.458902	0.458902	6.76560

5.14.1 Analysis of Variance – Wear at 2000 Sliding Distance

The results were analyzed using ANOVA for identifying the significant factors affecting the performance measures. The Analysis of Variance (ANOVA) for the wear at 95% confidence interval is given in Table 5.55

Table 5.56: ANOVA for wear rate at 2000 sliding distance

Sources	DF	Seq SS	Adj MS	F	P
Composition%	2	0.006091	0.003045	109.03	0.009
Cooling	2	0.037119	0.018559	664.42	0.002
Speed	2	0.000081	0.000041	1.46	0.407
Residual error	2	0.000056	0.000028		
Total	8	0.043347			
e pooled	4	0.000137	0.0000343		

Table 5.57: Response table for means of wear rate at 2000 sliding distance

Level	Composition	Cooling	Speed
1	0.5679	0.6284	0.5374
2	0.5408	0.4879	0.5416
3	0.5044	0.4968	0.5342
Delta	0.0635	0.1405	0.0073
Rank	2	1	3

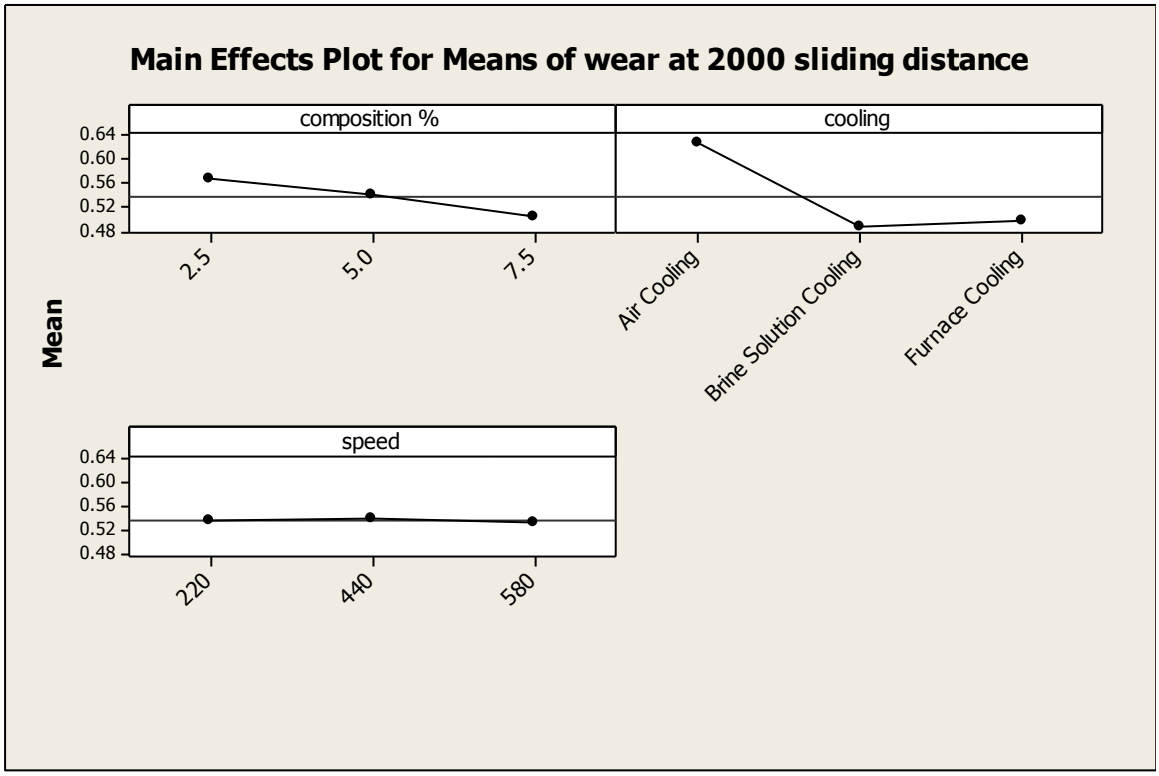

Figure 5.19: Main effect plot for Mean wear rate at 2000 sliding distance

5.14.2 Results of S/N Ratio – Wear Rate at 2000 Sliding Distance

Table 5.58: ANOVA for S/N of wear rate at 2000 sliding distance

Source	DF	Seq SS	Adj MS	F	P
Composition%	2	1.6165	0.80827	208.84	0.005
Cooling	2	9.0260	4.51301	1166.05	0.001
Speed	2	0.0136	0.00679	1.75	0.363
Residual error	2	0.0077	0.00387		
Total	8	10.6639			
E pool	4	0.0213	0.00533		

Table 5.59: Response table for S/N ratio of wear rate at 2000 sliding distance

Level	Composition%	Cooling	Speed
1	4.968	4.045	5.500
2	5.406	6.243	5.407
3	6.002	6.087	5.468
Delta	1.034	2.198	0.094
Rank	2	1	3

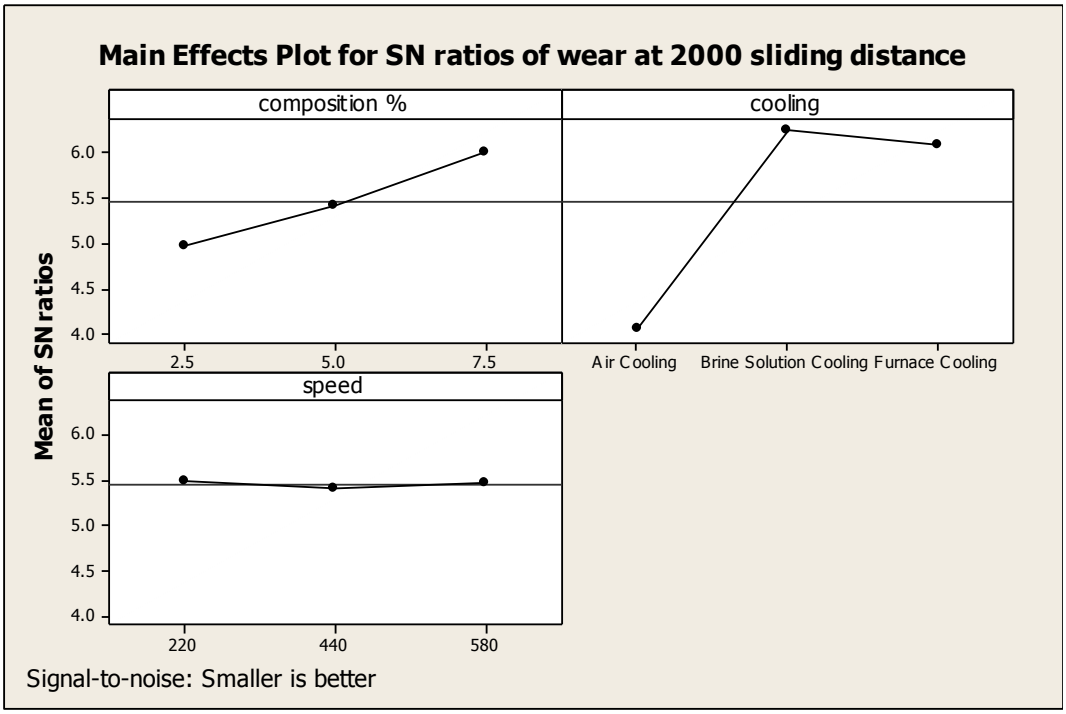

Figure 5.20: Main effects plot of wear rate at 2000 sliding distance for S/N ratio

5.14.3 Optimal Design

Table 5.60: Significant factors for wear rate at 2000 SD of composites

Factors	Affecting mean		Affecting variation (S/N ratio)	
	Contribution	Best level	Contribution	Best level
Composition (A)	Significant	Level 3-7.5%	Significant	Level 3-7.5%
Cooling (B)	Significant	Level 2-BSC	significant	Level 2-BSC
Stirring speed (C)	Insignificant	-	Insignificant	-

Estimating the mean

Mean value of wear rate of composites at 2000 sliding distance

$\mu_{A_3B_2} = \overline{A_3} + \overline{B_2} - \overline{T}$

$\mu_{A_3B_2}$ = 0.504409 + 0.487926 - 0.537715 =0.45462

Confidence Interval around the Estimated Mean

Confidence Interval around the estimated wear rate of composites at 2000 sliding distance:

$CI_1 = \sqrt{\frac{F_{\alpha,\nu_1,\nu_2} V_e}{n_{eff}}}$ Where $F_{\alpha\nu_1\nu_2} = F\ ratio$

$\alpha = risk$ (0.05) $confidence = 1-\alpha$

$\nu_1 = dof\ \ for\ mean\ which\ is\ always = 1$

$\nu_2 = dof\ \ for\ error = \nu_e$

n_{eff} = Number of tests under that condition using the participating factors

$$n_{eff} = \frac{N}{1+dof_{A,B}} = \frac{9}{1+2+2} = 1.8$$

$$CI = \sqrt{\frac{F_{\alpha,\nu_1,\nu_2} V_e}{n_{eff}}} = \sqrt{\frac{0.2 \times 0.0000343}{1.8}} = 0.00195$$

So the confidence interval around the wear rate of composites at 2000 sliding distance is given by 0.45462±0.00195 mm^3/m

5.15 WEAR RATE AT 2500 SLIDING DISTANCE

The effects of the parameters i.e. composition, type of cooling and stirring speed were evaluated on the composites having 2.5%, 5% and 7.5% reinforcement particles of average size 40 micron on the wear rate.

Table 5.61 Results for wear rate at 2500 sliding distance

Trail no.	Composition of Al_2O_3	Type of cooling	Stirring speed	Wear at 2500 SD	Mean	S/N ratio
1	2.5	Air Cooling	220	0.529218	0.529218	5.52731
2	2.5	Furnace Cooling	440	0.534243	0.534243	5.44522
3	2.5	Brine Solution Cooling	580	0.492096	0.492096	6.15900
4	5.0	Air Cooling	440	0.474532	0.474532	6.47469
5	5.0	Furnace Cooling	580	0.502096	0.502096	5.98426
6	5.0	Brine Solution Cooling	220	0.454922	0.454922	6.84126
7	7.5	Air Cooling	580	0.451780	0.451780	6.90145
8	7.5	Furnace Cooling	220	0.529218	0.529218	5.52731
9	7.5	Brine Solution Cooling	440	0.534243	0.534243	5.44522

5.15.1 ANALYSIS OF VARIANCE – WEAR AFTER 2500 SLIDING DISTANCE

The results were analyzed using ANOVA for identifying the significant factors affecting the performance measures. The Analysis of Variance (ANOVA) for the wear at 95% confidence interval is given in Table 5.61

Table 5.62: ANOVA for wear rate at 2500 sliding distance

Sources	DF	Seq SS	Adj MS	F	P
Composition%	2	0.007874	0.003937	153.05	0.006
Cooling	2	0.003552	0.001776	69.04	0.014
Speed	2	0.000297	0.000148	5.77	0.148
Residual error	2	0.000051	0.000026		
Total	8	0.011775			
e pooled	4	0.000348	0.000087		

Table 5.63: Response table for means of wear rate at 2500 sliding distance

Level	Composition	Cooling	Speed
1	0.5418	0.5314	0.4958
2	0.5003	0.4852	0.5081
3	0.4696	0.4951	0.5078
Delta	0.0722	0.0462	0.0123
Rank	1	2	3

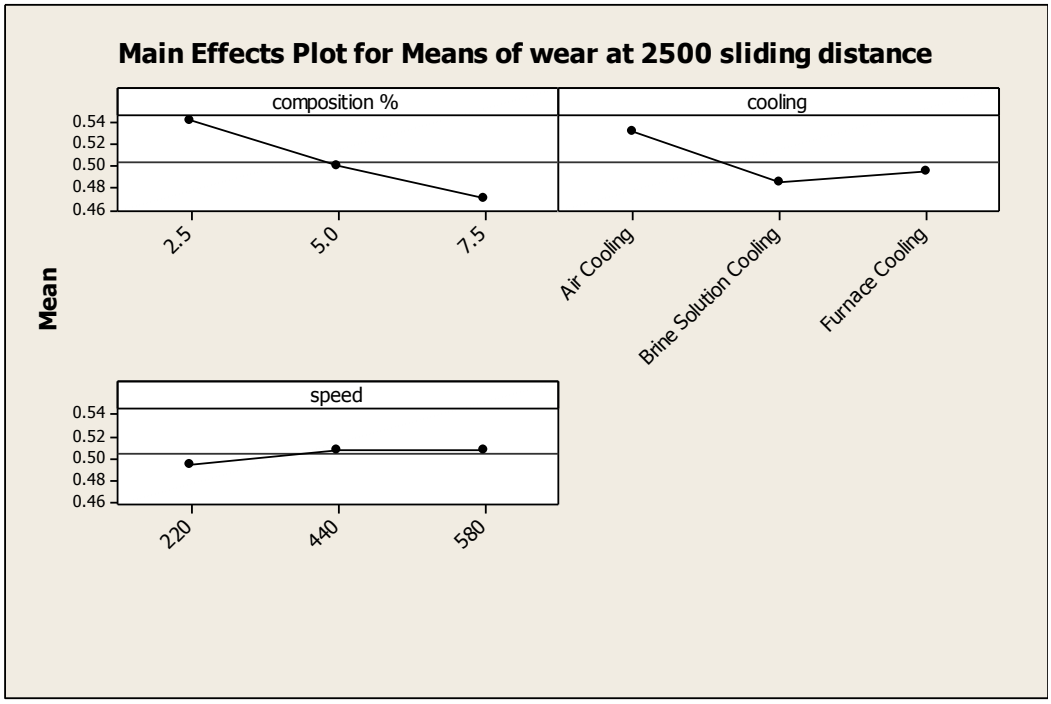

Figure 5.21: Main effect plot for Mean wear rate at 2500 sliding distance

5.15.2 Results of S/N Ratio – Wear Rate at 2500 Sliding Distance

Table 5.64: ANOVA for S/N of wear rate at 2500 sliding distance

Source	DF	Seq SS	Adj MS	F	P
Composition%	2	2.35551	1.17776	114.30	0.009
Cooling	2	1.06590	0.53295	51.72	0.019
Speed	2	0.10541	0.05270	5.11	0.164
Residual error	2	0.02061	0.01030		
Total	8	3.54742			
E pool	4	0.12602	0.031505		

Table 5.65: Response table for S/N ratio of wear rate at 2500 sliding distance

Level	Composition%	Cooling	Speed
1	5.326	5.500	6.129
2	6.026	6.301	5.909
3	6.576	6.127	5.890
Delta	1.250	0.801	0.238
Rank	1	2	3

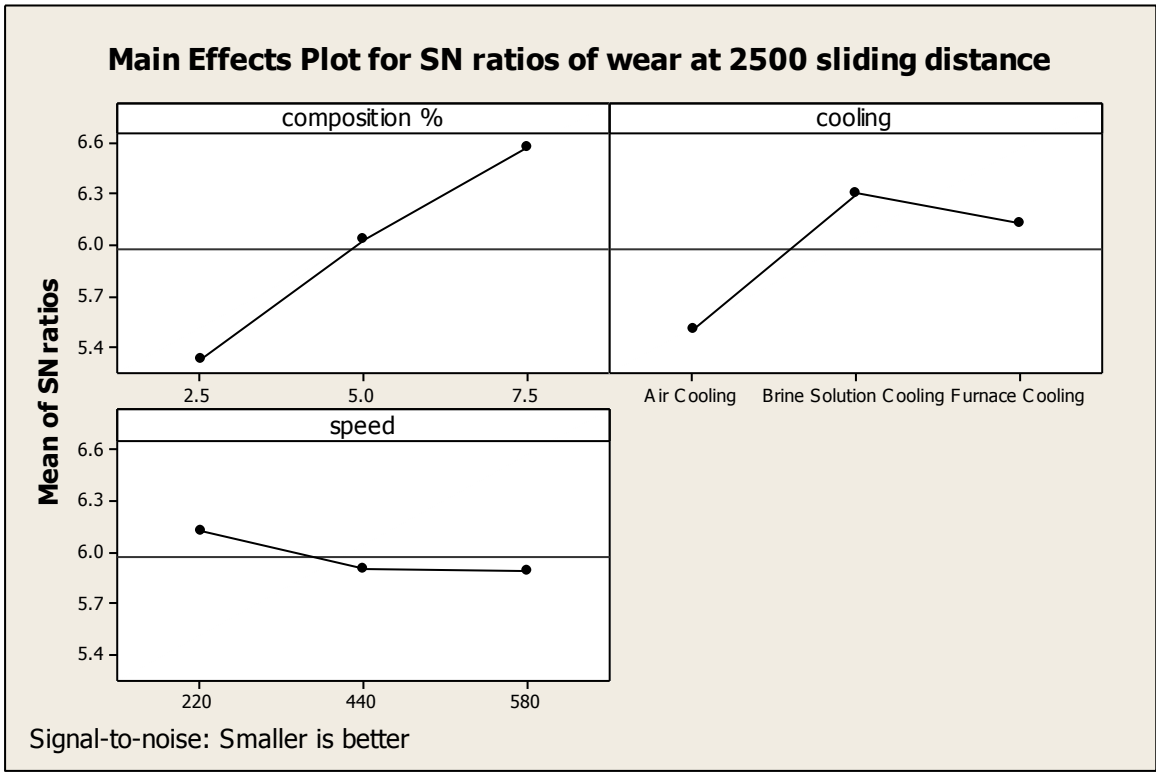

Figure 5.22: Main effects plot of wear rate at 2500 sliding distance for S/N ratio

5.15.3 Optimal Design

Table 5.66: Significant factors for wear rate at 2500 SD of composites

Factors	Affecting mean		Affecting variation (S/N ratio)	
	Contribution	Best level	Contribution	Best level
Composition (A)	Significant	Level 3-7.5%	Significant	Level 3-7.5%

Cooling (B)	Significant	Level 2-BSC	significant	Level 2-BSC
Stirring speed (C)	Insignificant	-	Insignificant	-

Estimating the mean

Mean value of wear rate of composites at 2500 sliding distance

$\mu_{A_3B_2} = \overline{A_3} + \overline{B_2} - \overline{T}$

$\mu_{A_3B_2}$ = 0.504409 + 0.487926 - 0.537715 =0.45462

Confidence Interval around the Estimated Mean

Confidence Interval around the estimated wear rate of composites at 2500 sliding distance:

$CI_1 = \sqrt{\frac{F_{\alpha,v_1,v_2} V_e}{n_{eff}}}$ Where $F_{\alpha v_1 v_2} = F\ ratio$

$\alpha = risk$ (0.05) $confidence = 1-\alpha$

$v_1 = dof\ \ for\ mean\ which\ is\ always = 1$

$v_2 = dof\ \ for\ error = v_e$

n_{eff} = Number of tests under that condition using the participating factors

$$n_{eff} = \frac{N}{1+dof_{A,B}} = \frac{9}{1+2+2} = 1.8$$

$$CI = \sqrt{\frac{F_{\alpha,v_1,v_2} V_e}{n_{eff}}} = \sqrt{\frac{0.2 \times 0.000087}{1.8}} = 0.003109$$

So the confidence interval around the wear rate of composites at 2500 sliding distance is given by 0.498573±0.003109 mm^3/m

5.16 WEAR RATE AT 3000 SLIDING DISTANCE

The effects of the parameters i.e. composition, type of cooling and stirring speed were evaluated on the composites having 2.5%, 5% and 7.5% reinforcement particles of average size 40 micron on the wear rate.

Table 5.67 Results for wear rate at sliding distance 3000 sliding distance

Trail no.	Composition of Al_2O_3	Type of cooling	Stirring speed	Wear at 3000 SD	Mean	S/N ratio
1	2.5	Air Cooling	220	0.477546	0.477546	6.41969
2	2.5	Furnace Cooling	440	0.492593	0.492593	6.15024
3	2.5	Brine Solution Cooling	580	0.456179	0.456179	6.81730
4	5.0	Air Cooling	440	0.442357	0.442357	7.08454
5	5.0	Furnace Cooling	580	0.477804	0.477804	6.41500
6	5.0	Brine Solution Cooling	220	0.437438	0.437438	7.18167
7	7.5	Air Cooling	580	0.450785	0.450785	6.92060
8	7.5	Furnace Cooling	220	0.477546	0.477546	6.41969
9	7.5	Brine Solution	440	0.492593	0.492593	6.15024

		Cooling				

5.16.1 Analysis of Variance – Wear at 3000 Sliding Distance

The results were analyzed using ANOVA for identifying the significant factors affecting the performance measures. The Analysis of Variance (ANOVA) for the wear at 95% confidence interval is given in Table 5.67.

Table 5.68: ANOVA for wear rate at 3000 sliding distance

Sources	DF	Seq SS	Adj MS	F	P
Composition%	2	0.001522	0.000761	70.35	0.014
Cooling	2	0.002282	0.001141	105.46	0.009
Speed	2	0.000284	0.000142	13.10	0.071
Residual error	2	0.000022	0.000011		
Total	8	0.004110			
e pooled	4	0.000306	0.0000765		

Table 5.69: Response table for means of wear rate at 3000 sliding distance

Level	Composition	Cooling	Speed
1	0.4861	0.4909	0.4607
2	0.4637	0.4569	0.4740
3	0.4553	0.4574	0.4705
Delta	0.0308	0.0340	0.0133
Rank	2	1	3

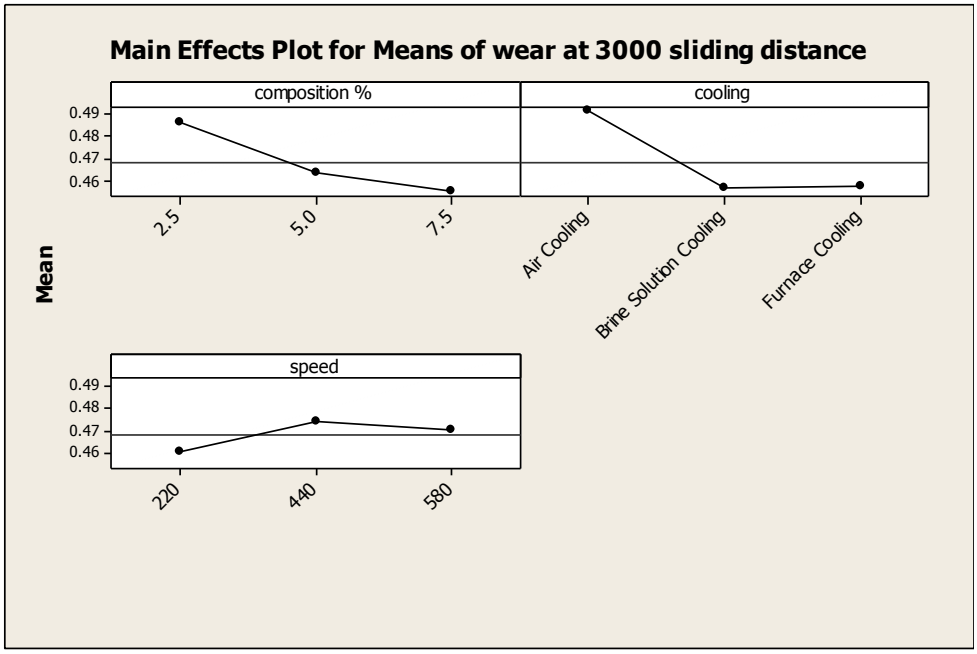

Figure 5.23: Main effect plot for Mean wear rate at 3000 sliding distance

5.16.2 Results For S/N Ratio – Wear Rate at 3000 Sliding Distance

Table 5.70: ANOVA for S/N of wear rate at 3000 sliding distance

Source	DF	Seq SS	Adj MS	F	P
Composition%	2	0.52515	0.262574	82.55	0.012
Cooling	2	0.77533	0.387664	121.88	0.008
Speed	2	0.10924	0.054620	17.17	0.055
Residual error	2	0.00636	0.003181		
Total	8	1.41608			
E pool	4	0.1156	0.0289		

Table 5.71: Response table for S/N ratio of wear rate 3000 sliding distance

Level	Composition%	Cooling	Speed

1	6.267	6.182	6.749
2	6.684	6.808	6.491
3	6.839	6.800	6.551
Delta	0.572	0.627	0.258
Rank	2	1	3

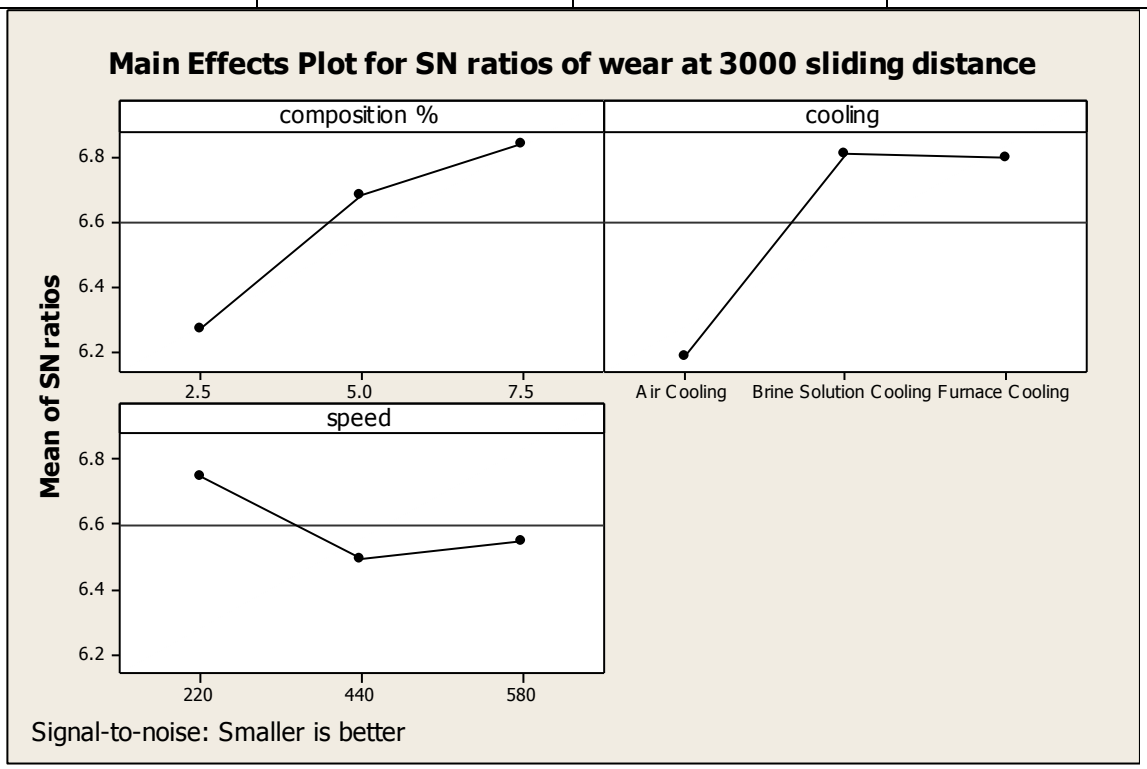

Figure 5.24: Main effects plot of wear rate for S/N ratio

5.16.3 Optimal Design

Table 5.72: Significant factors for wear rate at 3000 sliding distance of composites

Factors	Affecting mean		Affecting variation (S/N ratio)	
	Contribution	Best level	Contribution	Best level
Composition (A)	Significant	Level 3-7.5%	Significant	Level 3-7.5%
Cooling (B)	Significant	Level 2-BSC	significant	Level 2-BSC
Stirring speed (C)	Insignificant	-	Insignificant	-

Estimating the mean

Mean value of wear rate of composites at 3000 sliding distance

$\mu_{A_3B_2} = \overline{A_3} + \overline{B_2} - \overline{T}$

$\mu_{A_3B_2}$ = 0.473641 + 0.46207- 0.467205 =0.468506

Confidence Interval around the Estimated Mean

Confidence Interval around the estimated wear rate of composites at 3000 sliding distance:

$CI_1 = \sqrt{\frac{F_{\alpha,v_1,v_2} V_e}{n_{eff}}}$ Where $F_{\alpha v_1 v_2} = F\ ratio$

$\alpha = risk$ (0.05) $confidence = 1-\alpha$

$v_1 = dof\ \ for\ mean\ which\ is\ always = 1$

$v_2 = dof\ \ for\ error = v_e$

n_{eff} = Number of tests under that condition using the participating factors

$$n_{eff} = \frac{N}{1+dof_{A,B}} = \frac{9}{1+2+2} = 1.8$$

$$CI = \sqrt{\frac{F_{\alpha,v_1,v_2} V_e}{n_{eff}}} = \sqrt{\frac{0.2 \times 0.0000765}{1.8}} = 0.00291$$

So the confidence interval around the wear rate of composites at 3000 sliding distance is given by 0.468506±0.00291 mm^3/m

5.17 RESULTS OF WEAR RATE WITH SLIDING DISTANCE

The effect of the various parameters i.e. composition(A), cooling(B), and stirring speed (C), on wear rate with sliding distance on composites prepared by L9 treatment was compared by using ANOVA. The parameters were compared by using plots for mean and S/N ratio to decide the significant and insignificant factors. Wear rate is a "Lower is better", type response and is given by a logarithmic function based on the mean square deviation (MSD) given by:

$$S/N_{LB} = -10\log(MSD) = -10\log[(\frac{1}{r}\sum_{i=1}^{r} y^2{}_i)$$

Significant and insignificant parameters were decided according to the 'p' value obtained by ANOVA. The factors having 'p' value less than 0.05 are considered as significant factors and the other factors having 'p' value more than 0.05 considered as insignificant.

If the above results of means and S/N ratio compared the two parameters composition(A), and cooling(B), were significant factors for all the sliding distance but the parameter stirring speed (C) was insignificant for all the sliding distances. In both the significant parameters each having three levels, in case of composition(A) from 2.5%, 5% and 7.5% the level 3 composition 7.5% was significant for all the sliding distances. But in case of cooling (B) the results were different for different sliding distances i.e. for sliding distances 500, 1000 and 1500 the significant cooling was level 3 cooling which was 'furnace cooling' and for higher sliding distance like 2000, 2500 and 3000 the 'brine solution cooling' was significant.

Now when the overall wear rate was compared with sliding distance then it was noted that the wear rate of the composite did not increase linearly through the entire applied load range. Under an applied load two different type of wear behavior can be predicted. First the unstable and fluctuating wear at initial stage due to the abrasive nature of sample to the sliding disc. It is observed that wear rate increases initially and then gradually decreases with sliding distances in case of composites. At the initial stage of sliding, the MMC is softer compared to the later stage, as the MMCs gets strain hardened due to the continuous sliding under the applied load after a certain sliding distances.

CHAPTER 6

ANALYSIS OF MICROSTRUCTURE

Microstructure of the composites analyzed to know the difference between the Matrix metal and the composite after stir casting. In case of composites microstructure is also done to see the distribution of reinforcement particles. During this work Al_2O_3 is added as reinforcement in the Aluminium Alloy (LM6) to analyze the change in the properties of the matrix metal. To analyze the microstructure of the composites optical microscope known as Lesica microscope and SEM is used.

6.3 Optical Microscopic Behavior

Optical microstructure is analyzed under the Lesica microscope in Mechanical Engg. Department in Thapar University. For better contrast of the images and to detect easily, firstly samples are prepared. Samples are of rectangular shape and grind on the different grit size emery papers.

Table 6.1: L9 experimental design

Trial	Composition	Cooling	Stirring Speed
1	2.5	Air Cooling	220
2	2.5	Furnace Cooling	440
3	2.5	Brine Solution Cooling	580
4	5.0	Air Cooling	440
5	5.0	Furnace Cooling	580
6	5.0	Brine Solution Cooling	220
7	7.5	Air Cooling	580
8	7.5	Furnace Cooling	220
9	7.5	Brine Solution Cooling	440

The emery papers used are of 100, 220, 320, 600, and 1000 grit size. After grinding on the emery papers samples are polished on polishing machine with use of Alumina paste and water. Then samples were analyzed under the optical microscope to analyze the effect of different parameters i.e. stirring speed, type of cooling and composition on the distribution of the particles. The particle size of the Al_2O_3 particles is 40 micron so a better surface finish and contrast is required to analyze the proper structure of the composites. The composites are prepared L9 orthogonal Array as following way. The specimens are visualized under different magnifications (10X, 20X, 50X). Different figures of optical microstructure are as follows:-

The specimens are visualized under different magnifications (10X, 20X, 50X). Different figures of optical microstructure are as follows:-

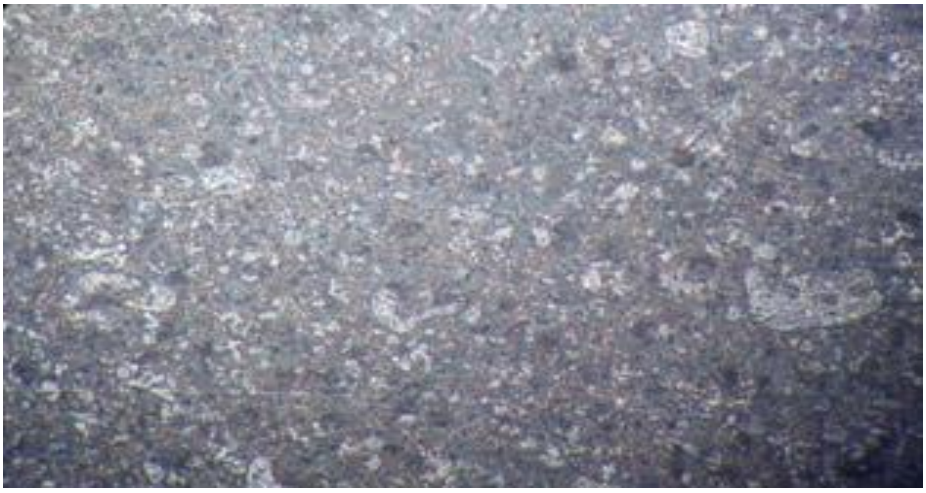

Figure 6.1: Optical micrograph of composite with 5% Al_2O_3 air cooled and 440 stirring speed at 10X

Figure 6.2: Optical micrograph of composite with 5% Al_2O_3 air cooled and 440 stirring speed at 50X

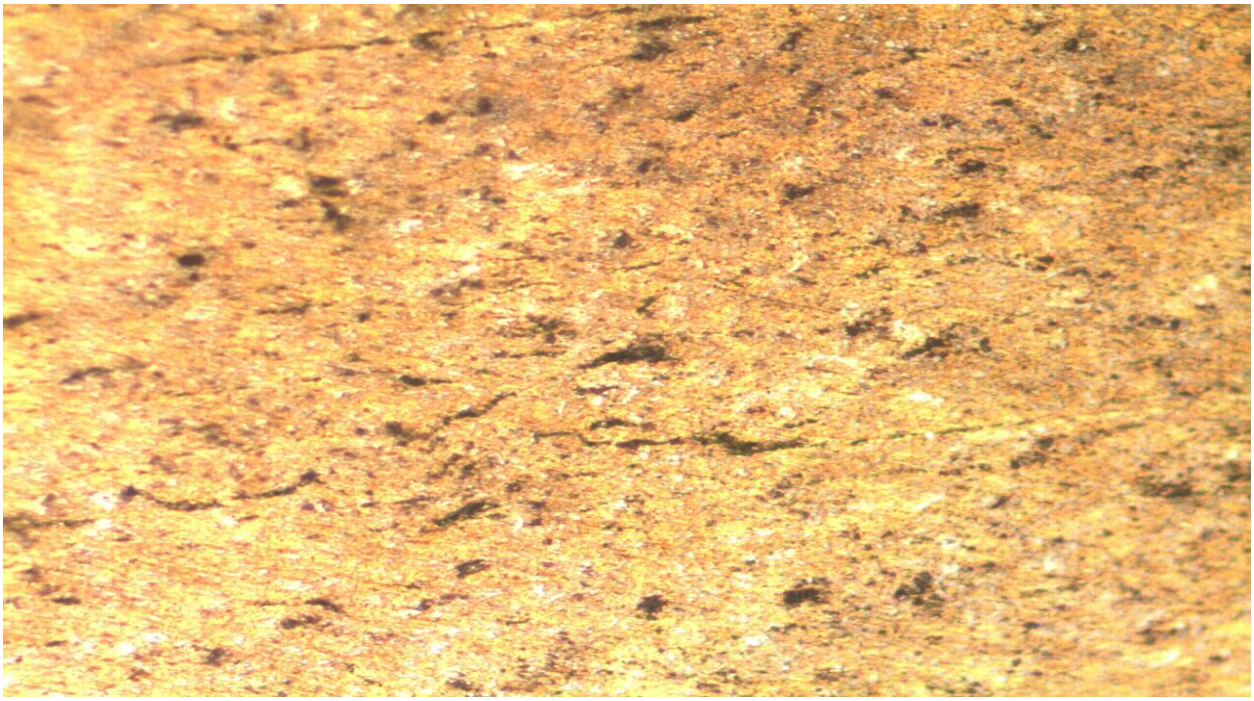

Figure 6.3: Optical micrograph of composite with 5% Al_2O_3 air cooled and 440 stirring speed at 20X

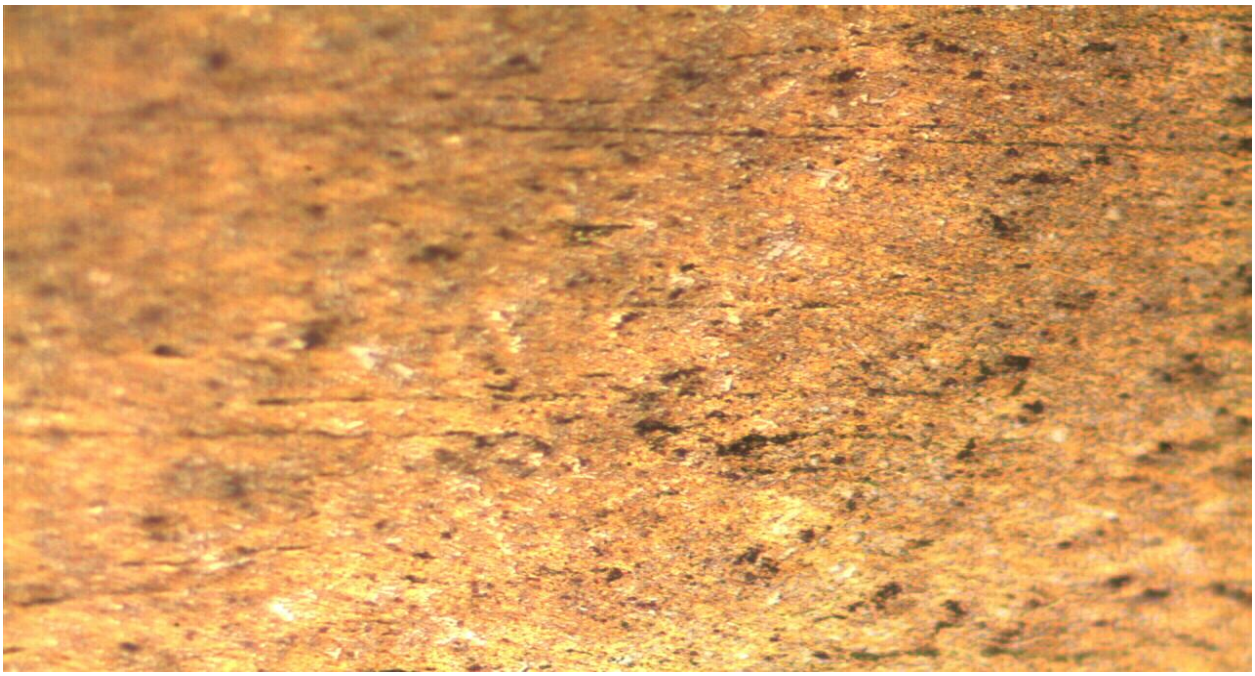

Figure 6.4: Optical micrograph of composite with 5% Al_2O_3 air cooled and 440 stirring speed at 20X

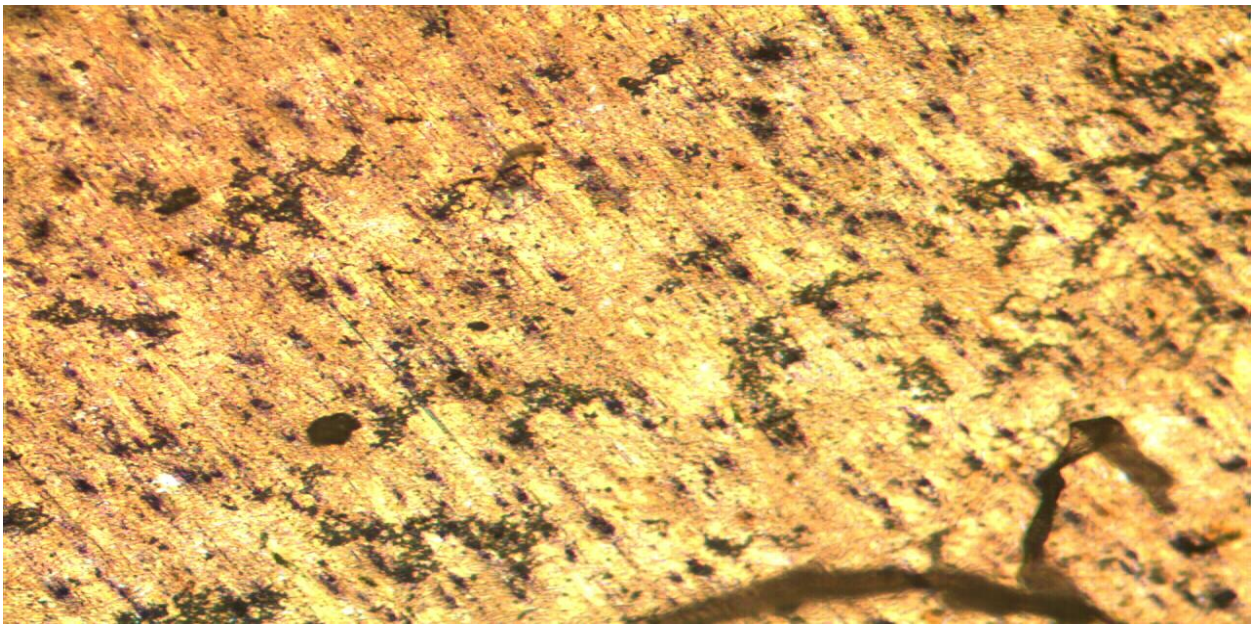

Figure 6.5: Optical micrograph of composite with 5% Al_2O_3 brine solution cooled and 220 stirring speed at 10X

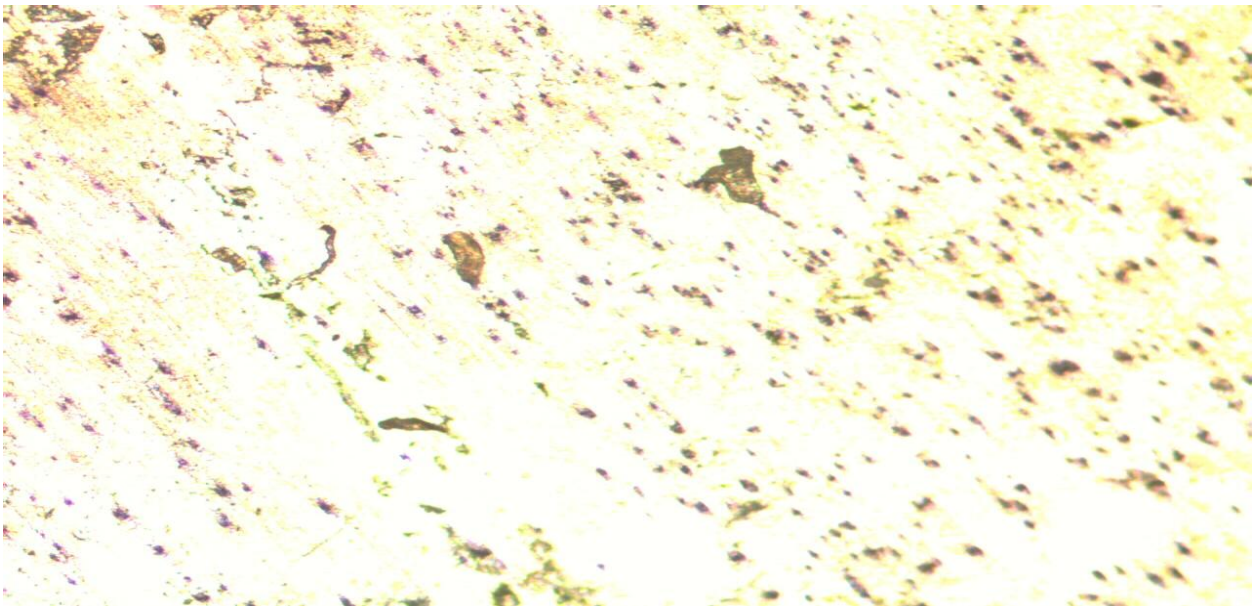

Figure 6.6: Optical micrograph of composite with 5% Al_2O_3 brine solution cooled and 220 stirring speed at 10X

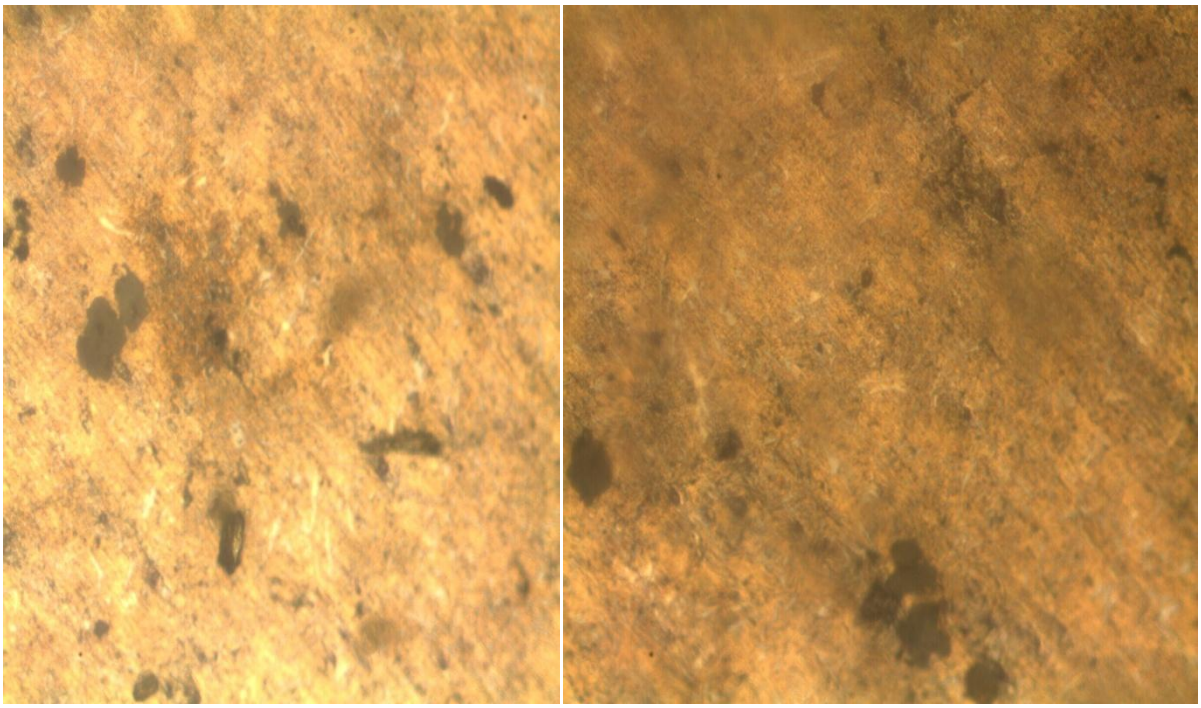

Figure 6.7: Optical micrograph of composite with 5% Al_2O_3 brine solution cooled and 220 stirring speed at 20X

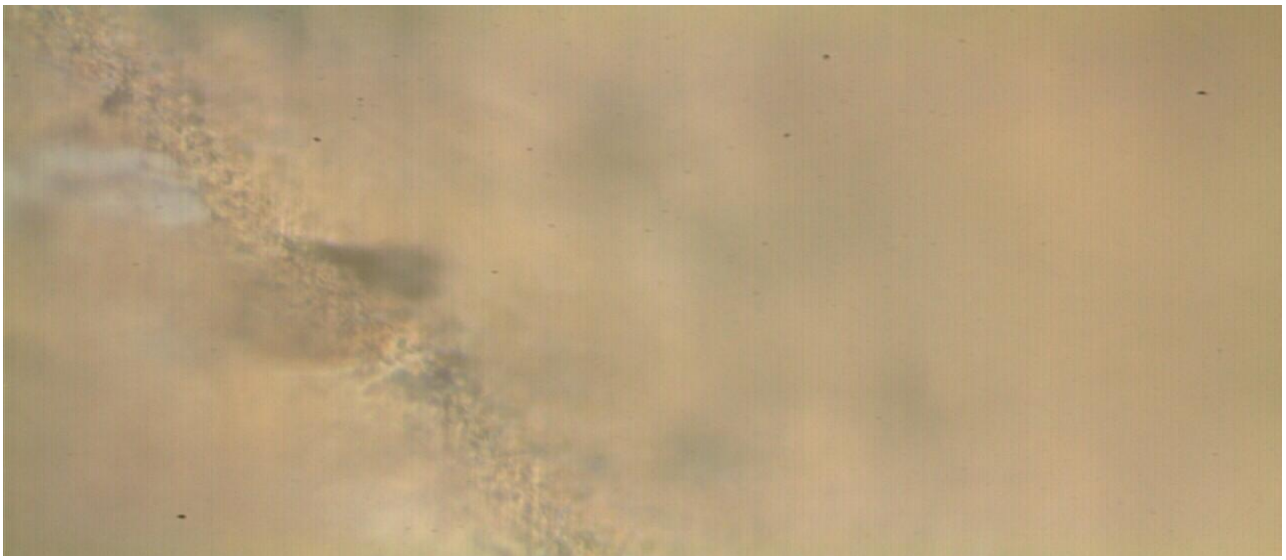

Figure 6.8: Optical micrograph of composite with 5% Al_2O_3 brine solution cooled and 220 stirring speed at 50X

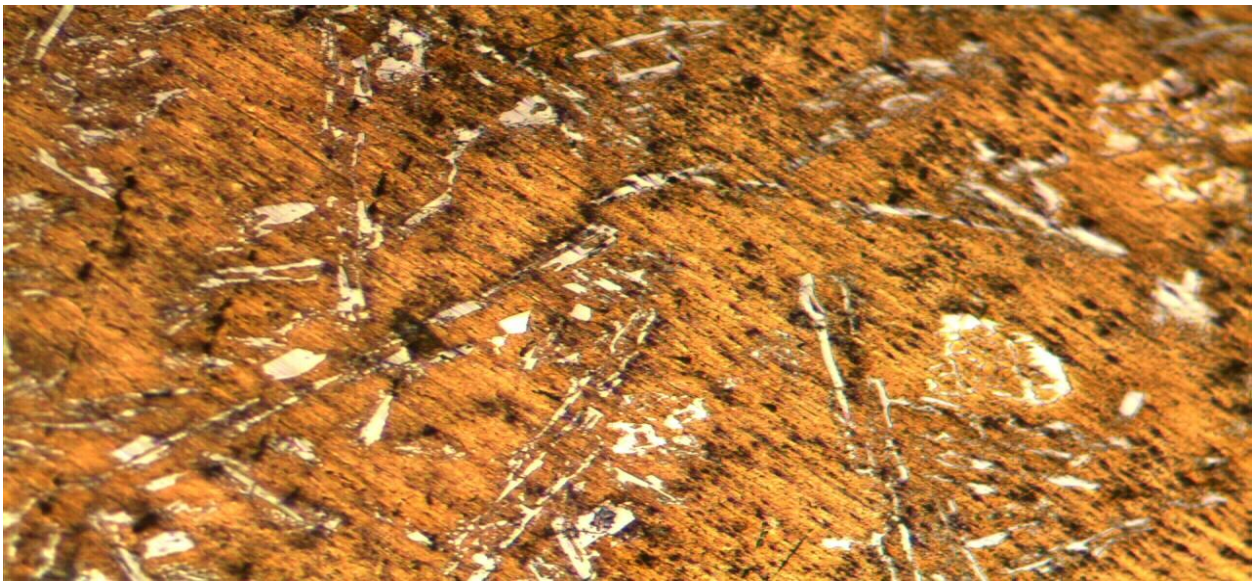

Figure 6.9: Optical micrograph of composite with 5% Al_2O_3 furnace cooled and 440 stirring speed at 10X

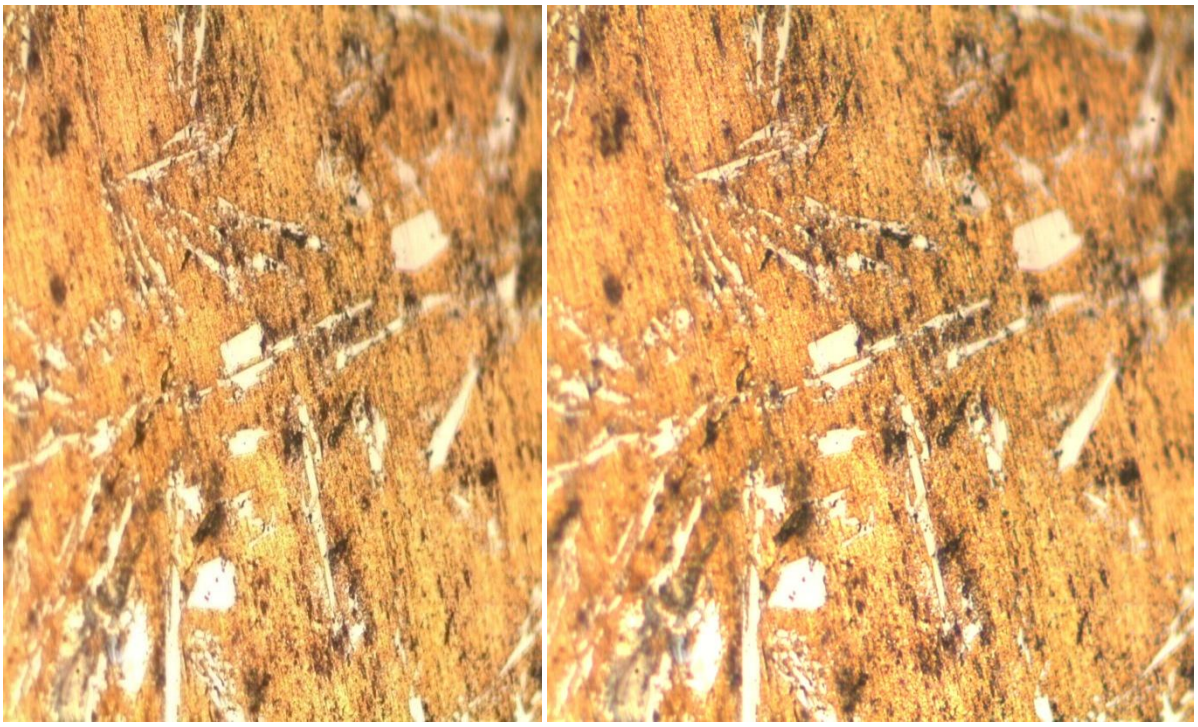

Figure 6.10: Optical micrograph of composite with 5% Al_2O_3 furnace cooled and 440 stirring speed at 20X

Figure 6.11: Optical micrograph of composite with 5% Al_2O_3 furnace cooled and 440 stirring speed at 50X

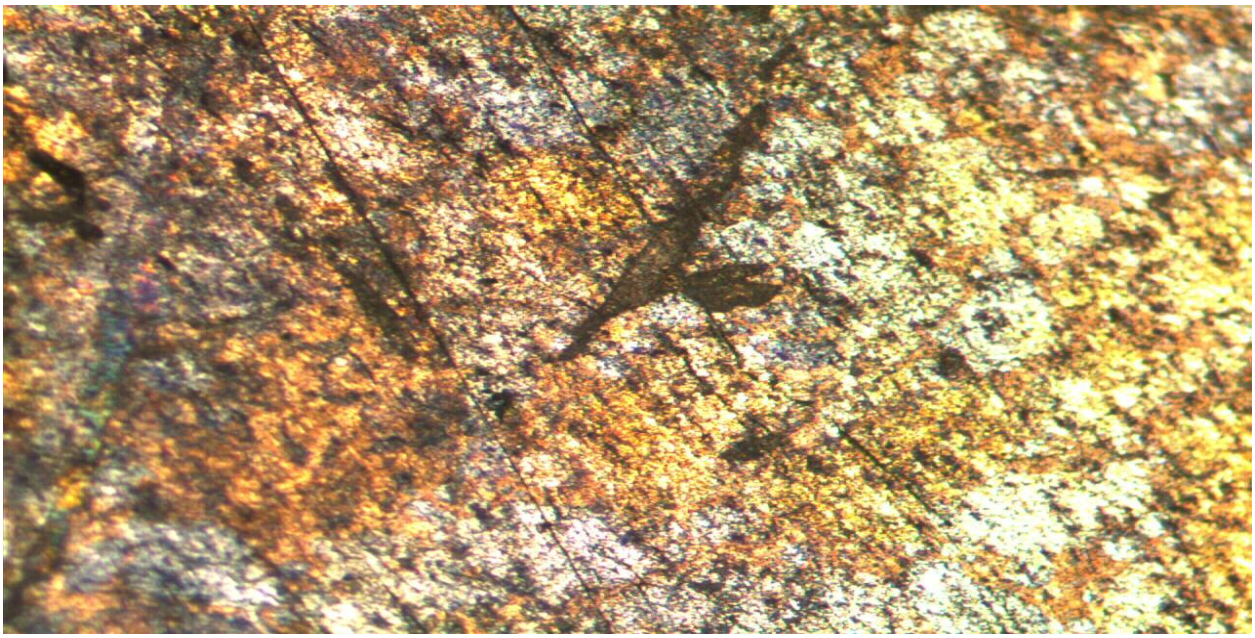

Figure 6.12: Optical micrograph of composite with 7.5% Al_2O_3 air cooled and 580 stirring speed at 10X

Figure 6.13: Optical micrograph of composite with 7.5% Al_2O_3 brine solution cooled and 440 stirring speed at 10X

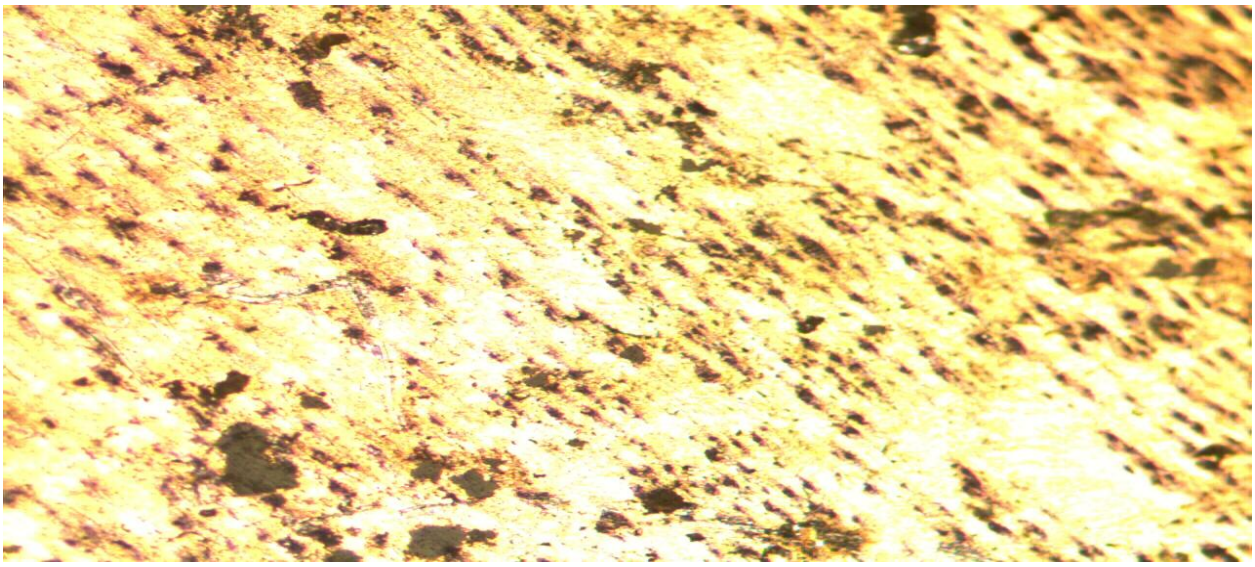

Figure 6.14: Optical micrograph of composite with 7.5% Al_2O_3 furnace cooled and 220 stirring speed at 10X

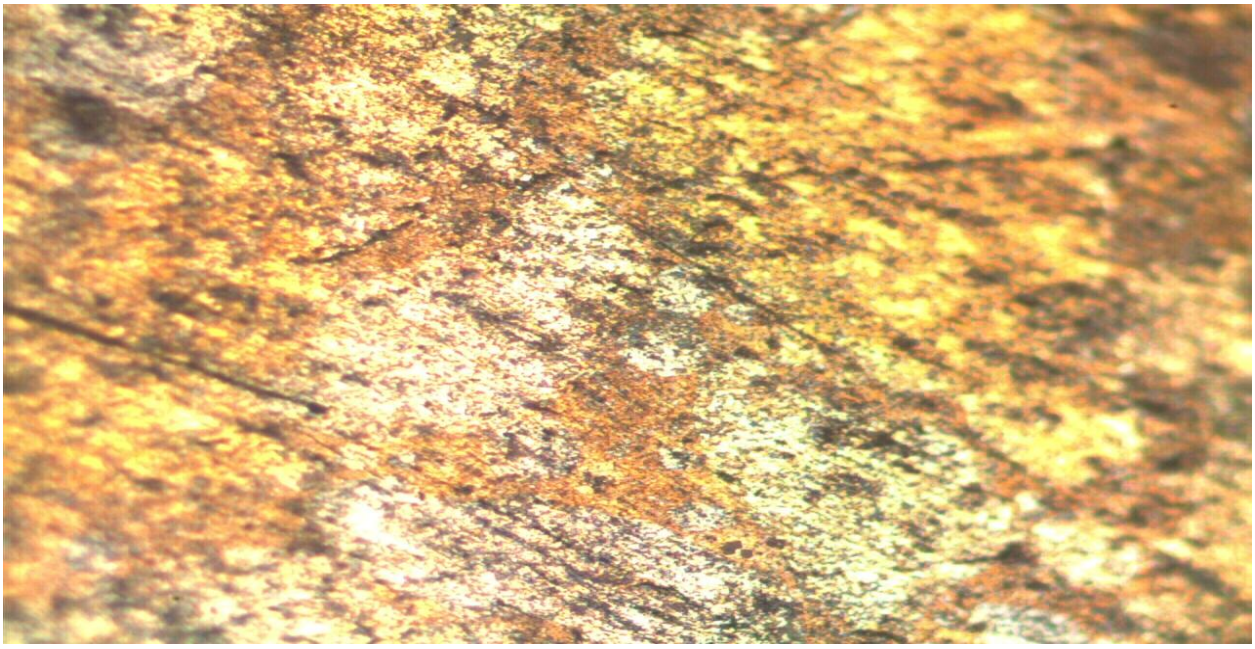

Figure 6.15: Optical micrograph of composite with 7.5% Al_2O_3 furnace cooled and 220 stirring speed at 20X

It is clear from the figure 6.1 to 6.15 that the white particles of the Al_2O_3 are present in the aluminium matrix alloy. From the above figures it was found that the particle size of the alumina is very fine that's why at 10X the particles look very small. From above figures it can

be easily detected that the distribution of the particles is almost uniform. By comparing the above micrographs it was analyzed that by comparison of the distribution of particles on the basis of cooling medium, furnace cooling is better. Furnace cooling is better because the microstructure formed during furnace cooling is denser than that of brine solution and air cooling. So the interfacial bonding is obtained in case of furnace cooling.

It is also found that as the percentage of reinforcement increase the area fraction also increases as shown in the optical micrographs. It is also observed that there is increase in hardness and wear resistance this can be attributed to the increase in interfacial bonding of reinforcement with the aluminium matrix alloy. Good interfacial bonding can be obtained by pre-heating of Al_2O_3 particulates before adding in the matrix.

6.4 SCANNING ELECTRON MICROSCOPY (SEM) ANALYSIS

The cleaned, dried and etched specimens is prepared and subsequently mounted on specially designed aluminium stubsusing (holder). The specimens thus mounted were viewed under jeol, JSM 6510 LV scanning electron microscope at an accelerating voltage of 20 kv. Following figures shows the micrographs of different composites prepared according to the parameters given in Table 6.1.

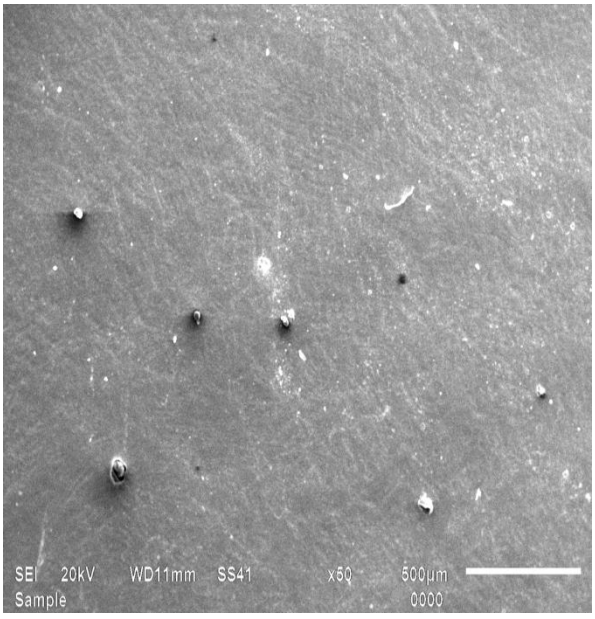

Figure 6.16: SEM micrograph of composite with 7.5% Al_2O_3 air cooled and 580 stirring speed at 50X

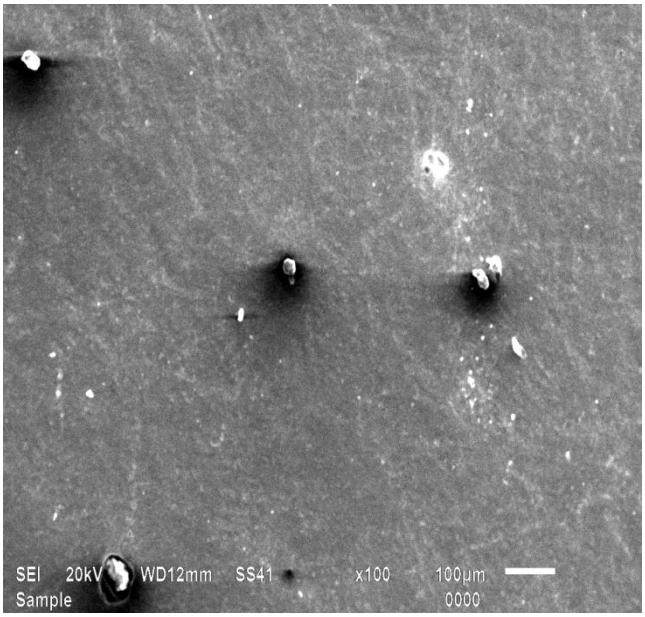

Figure 6.17: SEM micrograph of composite with 7.5% Al_2O_3 air cooled and 580 stirring speed at 100X

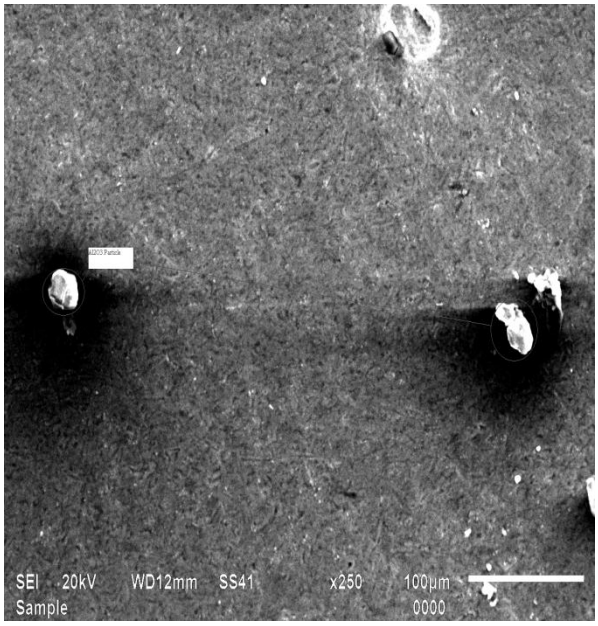

Figure 6.18: SEM micrograph of composite with 7.5% Al_2O_3 air cooled and 580 stirring speed at 250X

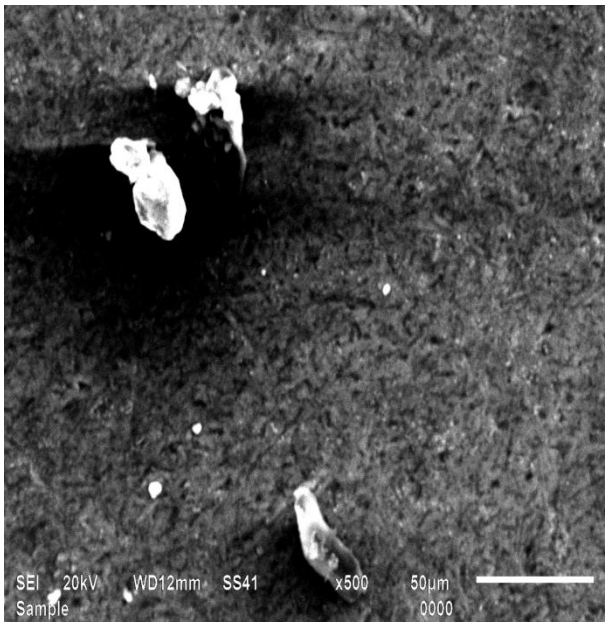

Figure 6.19: SEM micrograph of composite with 7.5% Al_2O_3 air cooled and 580 stirring speed at 500X

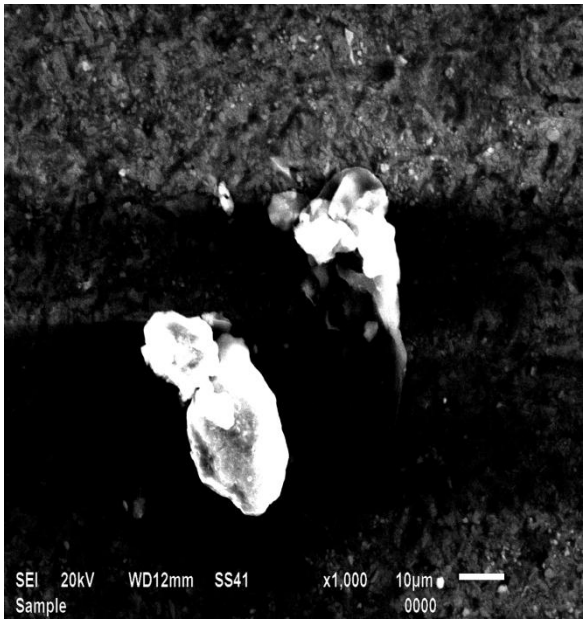

Figure 6.20: SEM micrograph of composite with 7.5% Al_2O_3 air cooled and 580 stirring speed at 1000X

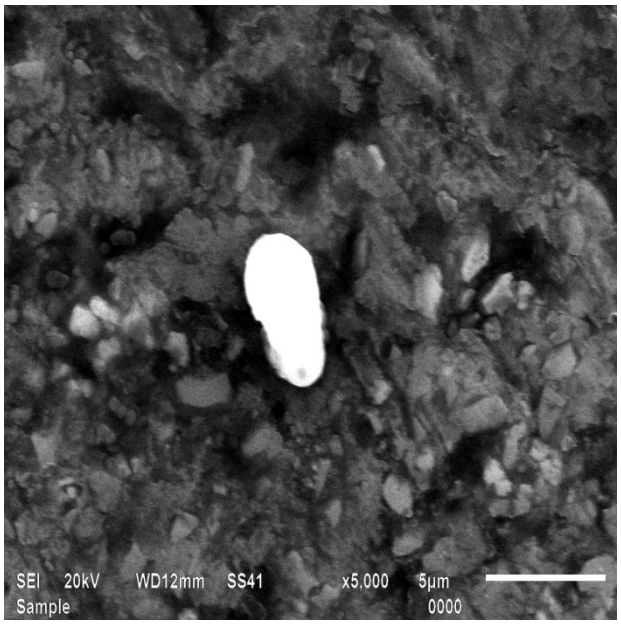

Figure 6.21: SEM micrograph of composite with 7.5% Al_2O_3 air cooled and 580 stirring speed at 5000X

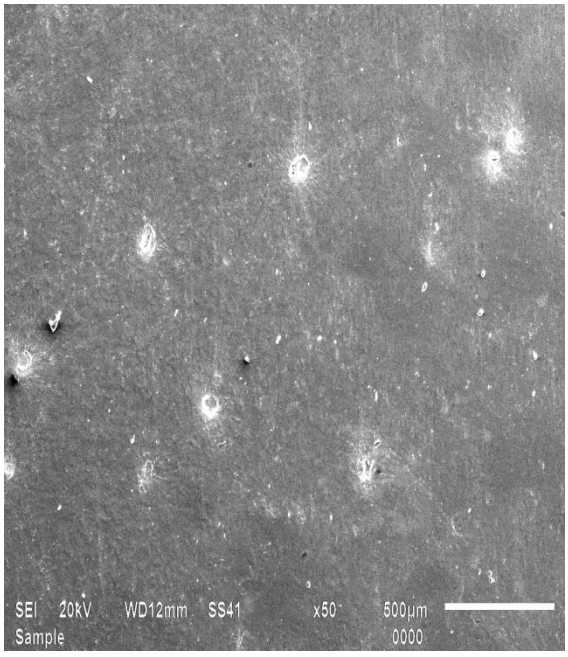

Figure 6.22: SEM micrograph of composite with 7.5% Al_2O_3 brine solution cooled and 440 stirring speed at 50X

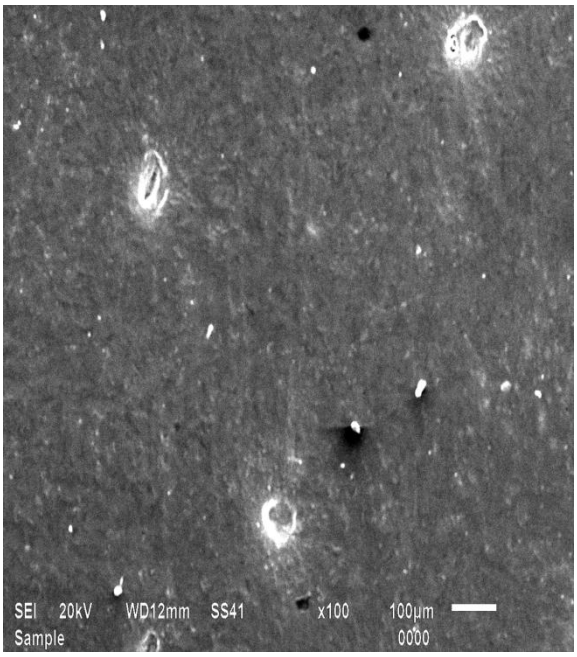

Figure 6.23: SEM micrograph of composite with 7.5% Al_2O_3 brine solution cooled and 440 stirring speed at 100X

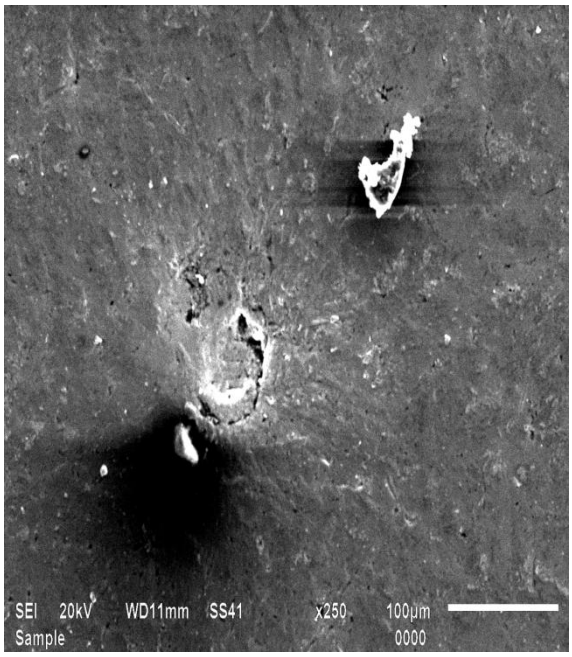

Figure 6.24: SEM micrograph of composite with 7.5% Al_2O_3 brine solution cooled and 440 stirring speed at 250X

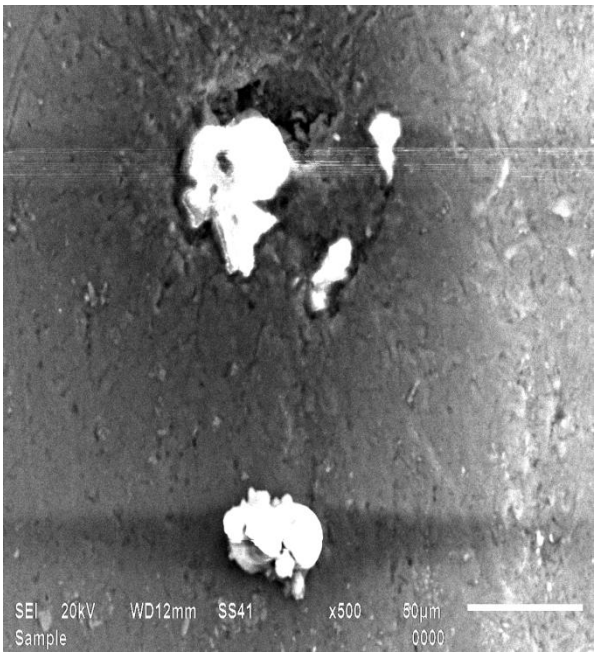

Figure 6.25: SEM micrograph of composite with 7.5% Al_2O_3 brine solution cooled and 440 stirring speed at 500X

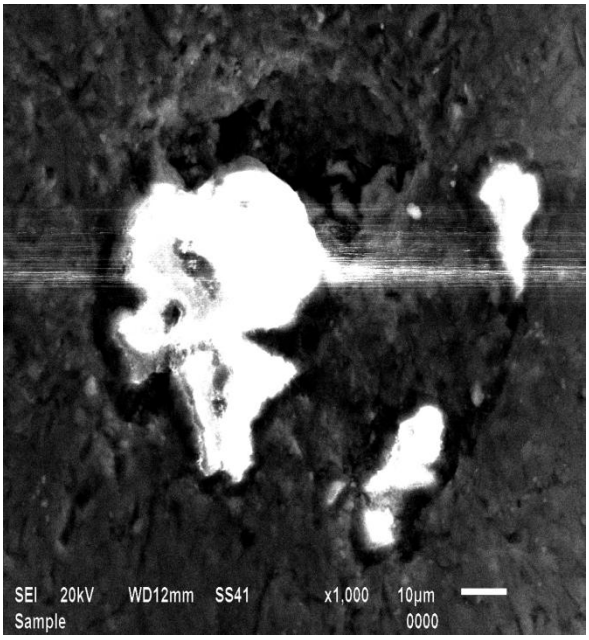

Figure 6.26: SEM micrograph of composite with 7.5% Al_2O_3 brine solution cooled and 440 stirring speed at 1000X

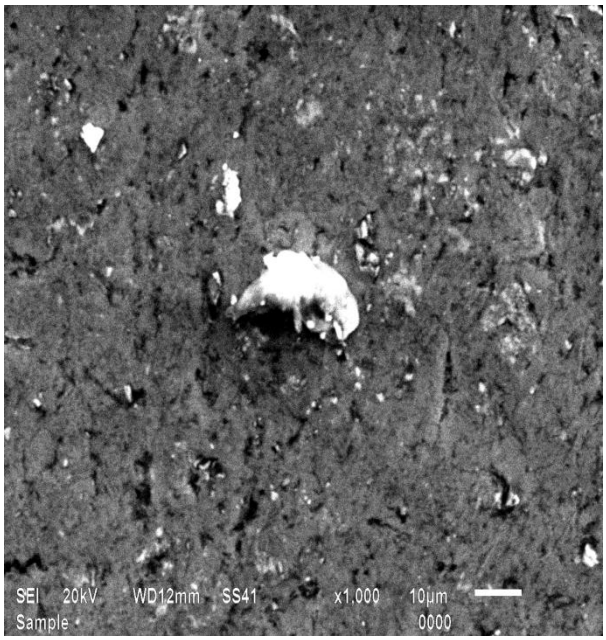

Figure 6.27: SEM micrograph of composite with 7.5% Al_2O_3 brine solution cooled and 440 stirring speed at 2000X

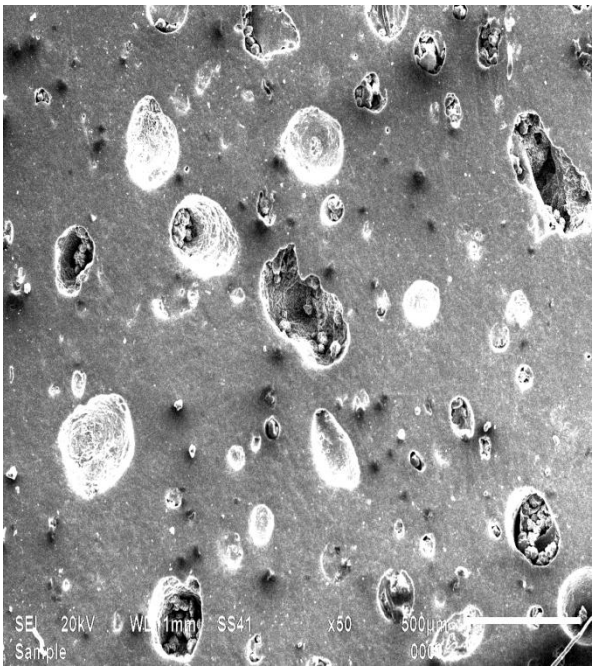

Figure 6.28: SEM micrograph of composite with 7.5% Al_2O_3 furnace cooled and 220 stirring speed at 50X

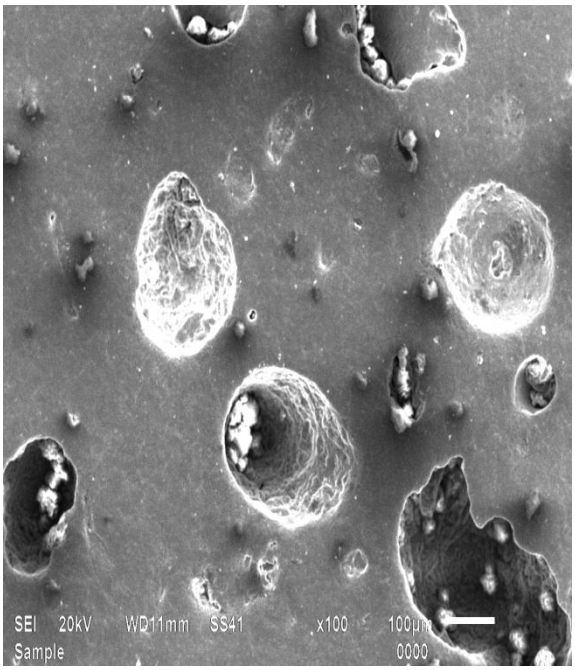

Figure 6.29: SEM micrograph of composite with 7.5% Al_2O_3 furnace cooled and 220 stirring speed at 100X

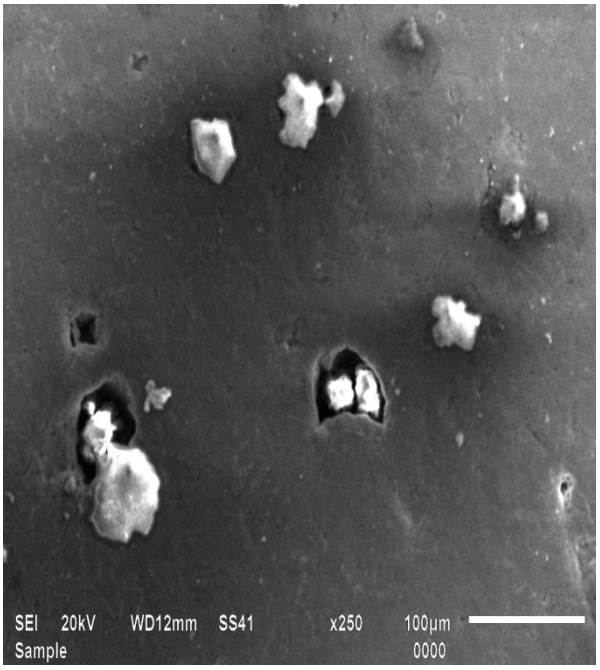

Figure 6.30: SEM micrograph of composite with 7.5% Al_2O_3 furnace cooled and 220 stirring speed at 250X

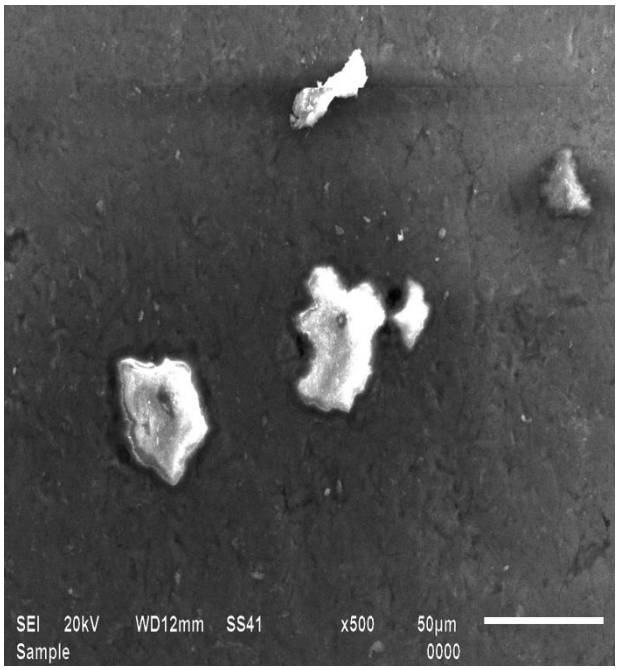

Figure 6.31: SEM micrograph of composite with 7.5% Al_2O_3 furnace cooled and 220 stirring speed at 500X

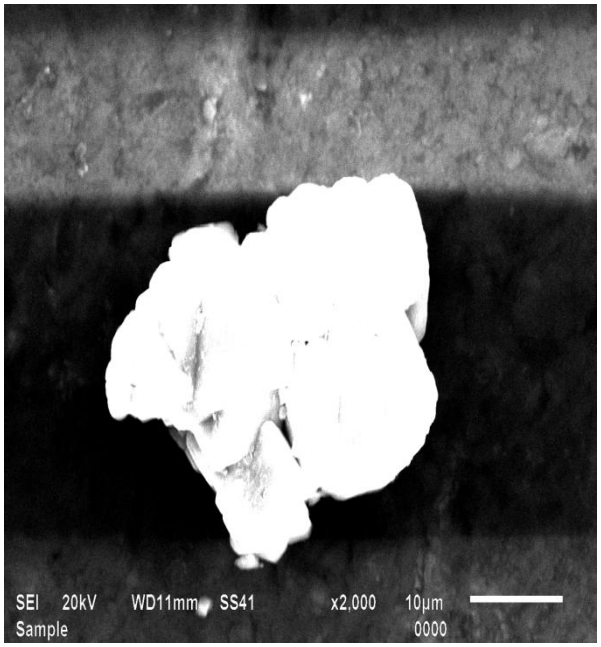

Figure 6.32: SEM micrograph of composite with 7.5% Al_2O_3 furnace cooled and 220 stirring speed at 1000X

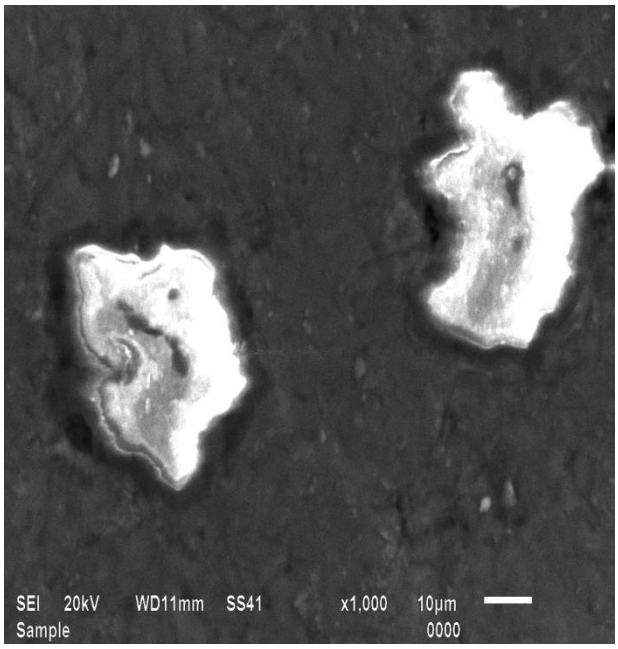

Figure 6.33: SEM micrograph of composite with 7.5% Al_2O_3 furnace cooled and 220 stirring speed at 2000X

Scanning electron micrographs at lower magnification shows that the distribution of Al_2O_3 particulate throughout the MMC's. Scanning electron micrographs at higher magnification shows the particle matrix interfaces.

Fig. 6.16, 17, 22, 23, 28 and 29 shows the homogeneous distribution of Al_2O_3 particles in alloy matrix. Homogeneous distribution of particles is desired for achieving better wear behavior and mechanical properties. Homogeneous distribution of particles in molten alloy is achieved due to the shear rate caused by stirring which also minimize the particle settling.

However, agglomeration of particles in some regions is clearly visible in furnace cooling case; this is due to the presence of porosity associated to it. Presence of entrapped air and moisture in the reinforcement particles results in the voids/ porosity after casting.

Further SEM reveals the excellent bond between the matrix alloy and Al_2O_3 reinforcement particles at higher magnifications.

CHAPTER 7

EDS AND XRD ANALYSIS

7.1 ENERGY DISPERSIVE SPECTROSCOPY (EDS)

The SEM is equipped with a spectrometer capable of detecting X-rays emitted by the specimen during electron beam excitation. The two basic types of X-ray microstructure analysis used in conjunction with SEMs are energy dispersive spectroscopy and wavelength dispersive spectroscopy. In EDS there are two types of analysis 1) Qualitative analysis 2) Quantitative analysis.

A qualitative analysis is conducted to determine the elemental composition of a specimen, whereas a quantitative analysis reveals the relative concentration of the elements detected. In either situation the data must be of high quality to ensure analytical confidence.

7.2 EDS FOR Al_2O_3 PARTICLES

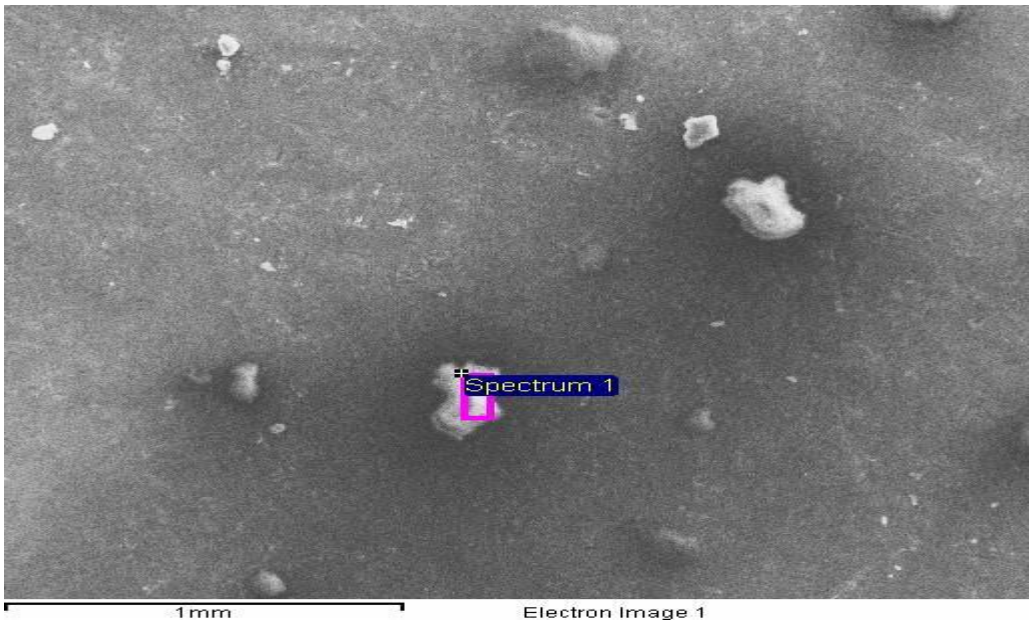

Figure 7.1 EDS image of a Al_2O_3 particle reinforced in LM6

Table 7.1: Elemental composition of Al_2O_3 particle

Element	Weight%	Atomic%
O k	51.01	63.72
Al k	48.99	36.28
Totals	100.00	

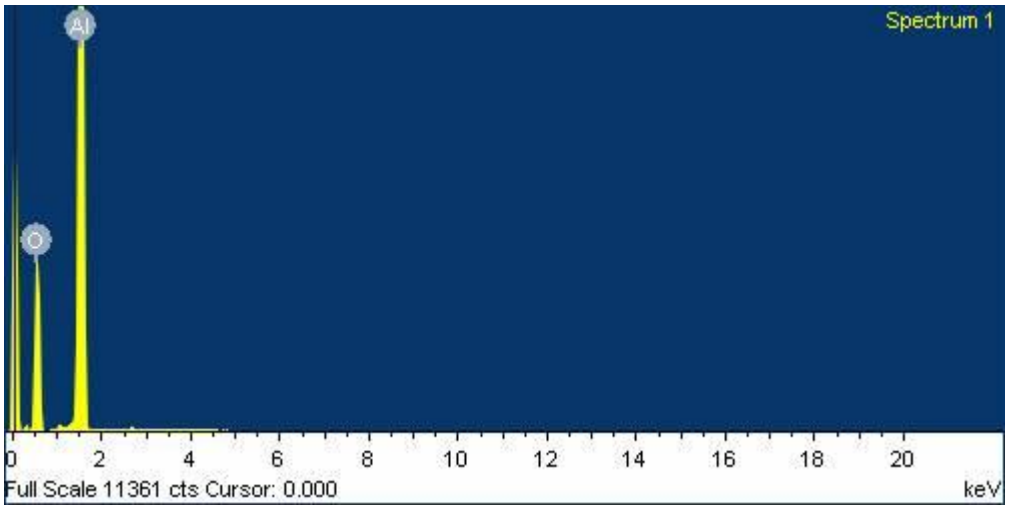

Figure 7.2: Elements present in Al_2O_3 particle

7.3 EDS OF A COMPOSITE

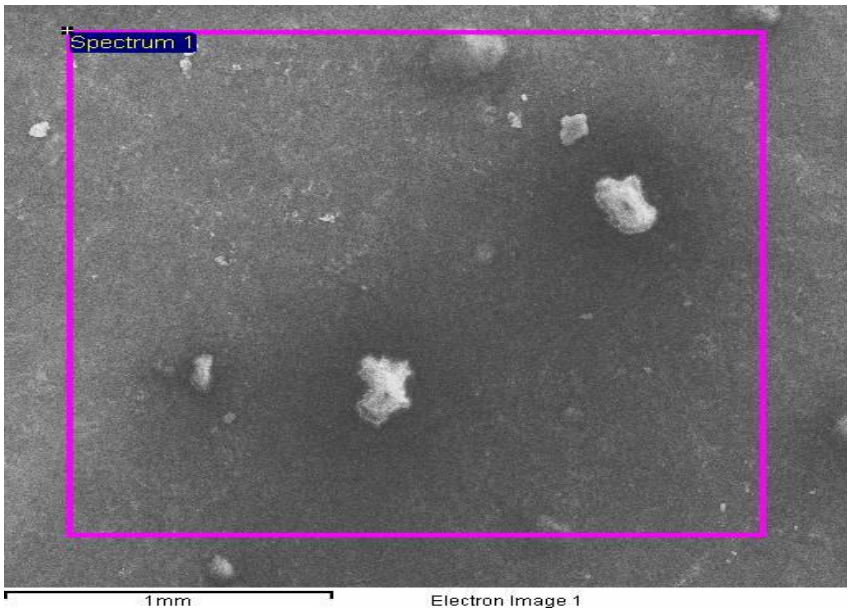

Figure 7.3: EDS image of a full composite reinforced with Al_2O_3

Table 7.2 Elemental composition of composite

Element	Weight%	Atomic%
C K	4.56	9.08
O K	11.76	17.57
Na K	0.19	0.20
Al K	71.89	63.67
Si K	10.68	9.08
Mn K	0.29	0.13
Fe K	0.62	0.27
Totals	100.00	

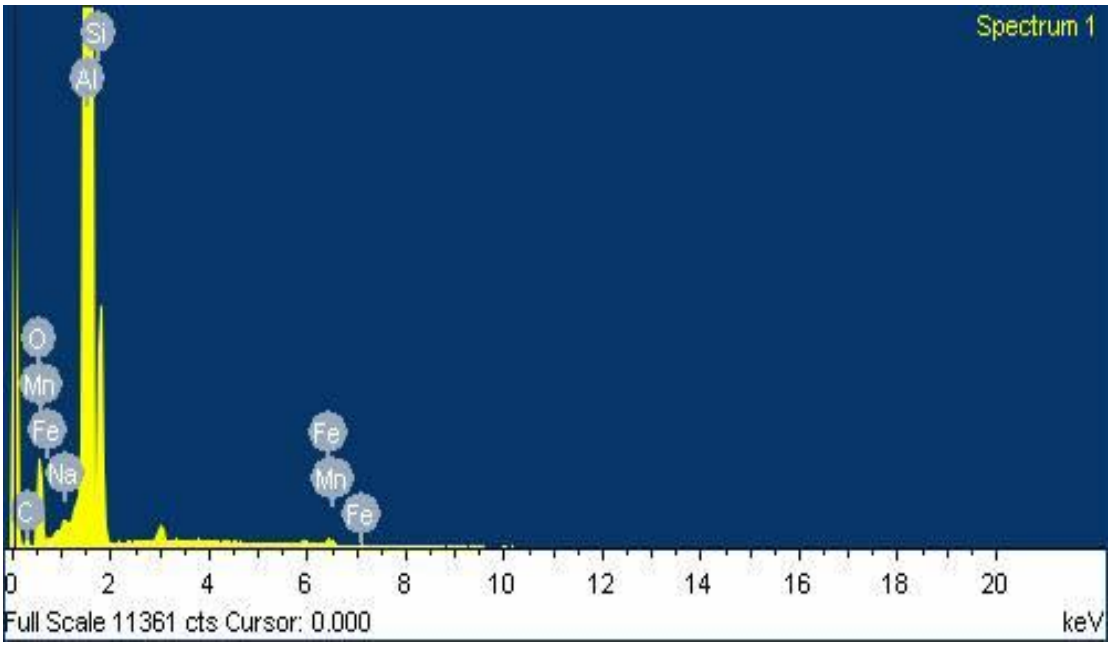

Figure 7.4: Elements presents in composite

7.4 X-RAY DIFFRACTION ANALYSIS

An X-ray diffraction (XRD) pattern of aluminium alloy matrix composites were shown in following figures. X-ray diffraction of different samples was carried out by X'PERT PRO of PAN ANLYTICAL using CuKα radiation. In XRD, the physical content of constituents present in the samples are indicated in the form of a graphs and tables shows the name and percentage of elements/ compounds present in respective samples. Following figure shows the XRD analysis of LM6+Al2O3 composites of different composition.

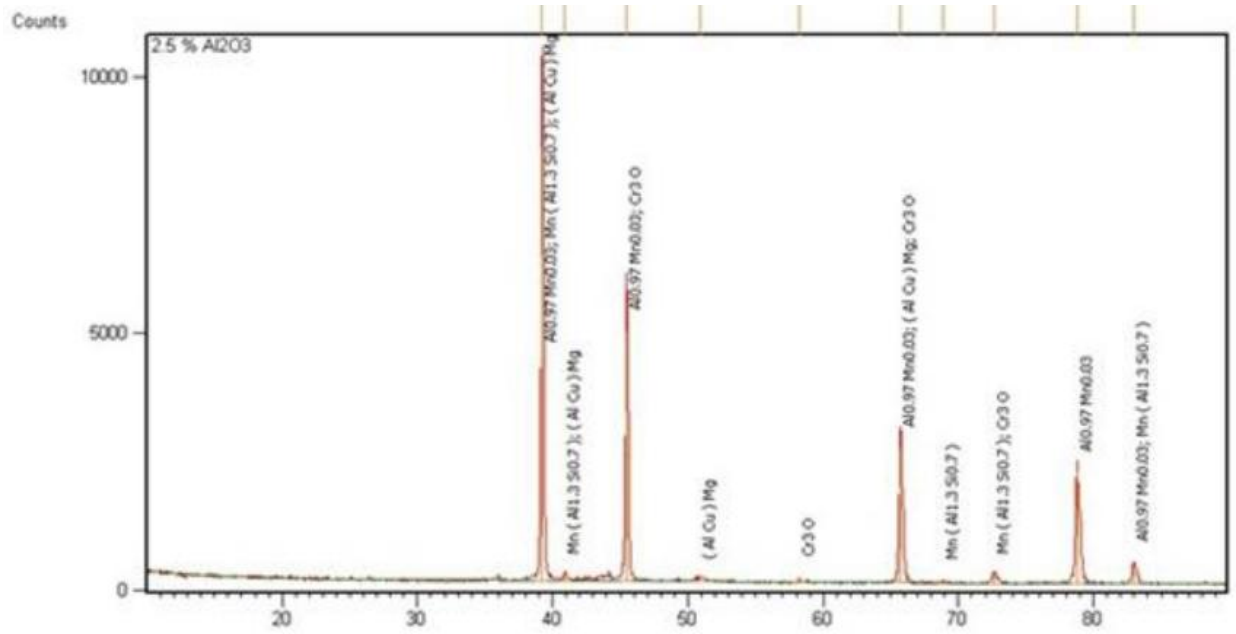

Figure 7.5: X-ray diffraction pattern of alloy having 2.5% Al_2O_3

Table 7.3: XRD analysis for 2.5 % Al_2O_3 composite

Ref. code	Score	Compound name	Scale factor	Weight fraction (%)
01-071-4624	35	Aluminium	0.782	54.5
01-074-6395	12	Silicon	0.171	5
03-065-3163	3	Silicon oxide	0.015	30
01-073-0368	5	Aluminum oxide	0.125	8

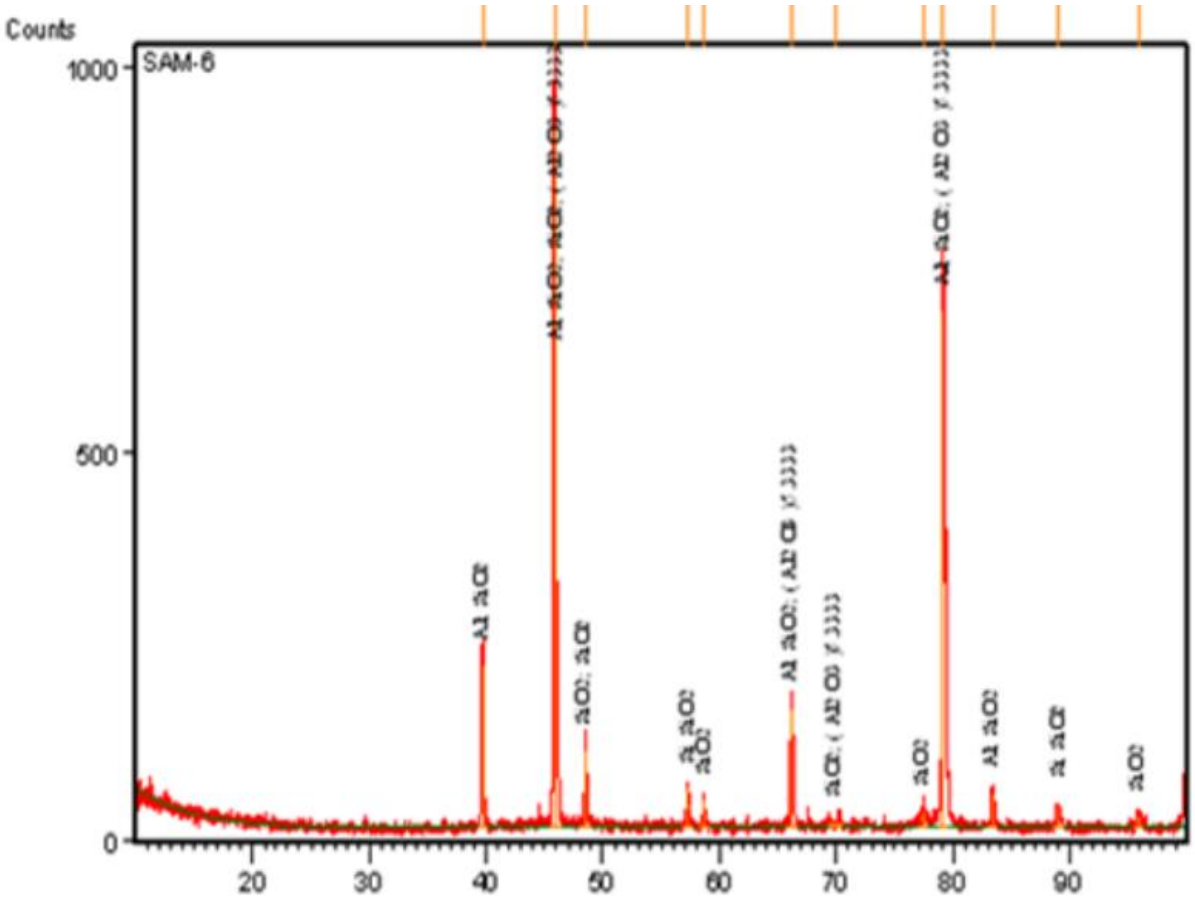

Figure 7.6 X-ray diffraction pattern for aluminium alloy with 5 % wt. Al_2O_3

Table 7.4: X-ray diffraction of alloy with 5% wt. Al_2O_3

Ref. code	Score	Compound name	Scale factor	Weight fraction
01-071-4624	19	Aluminium	0.868	54.5
01-074-6395	7	Silicon	0.171	6
03-065-3163	3	Silicon oxide	0.013	30
01-073-0368	4	Aluminum oxide	0.031	5.1

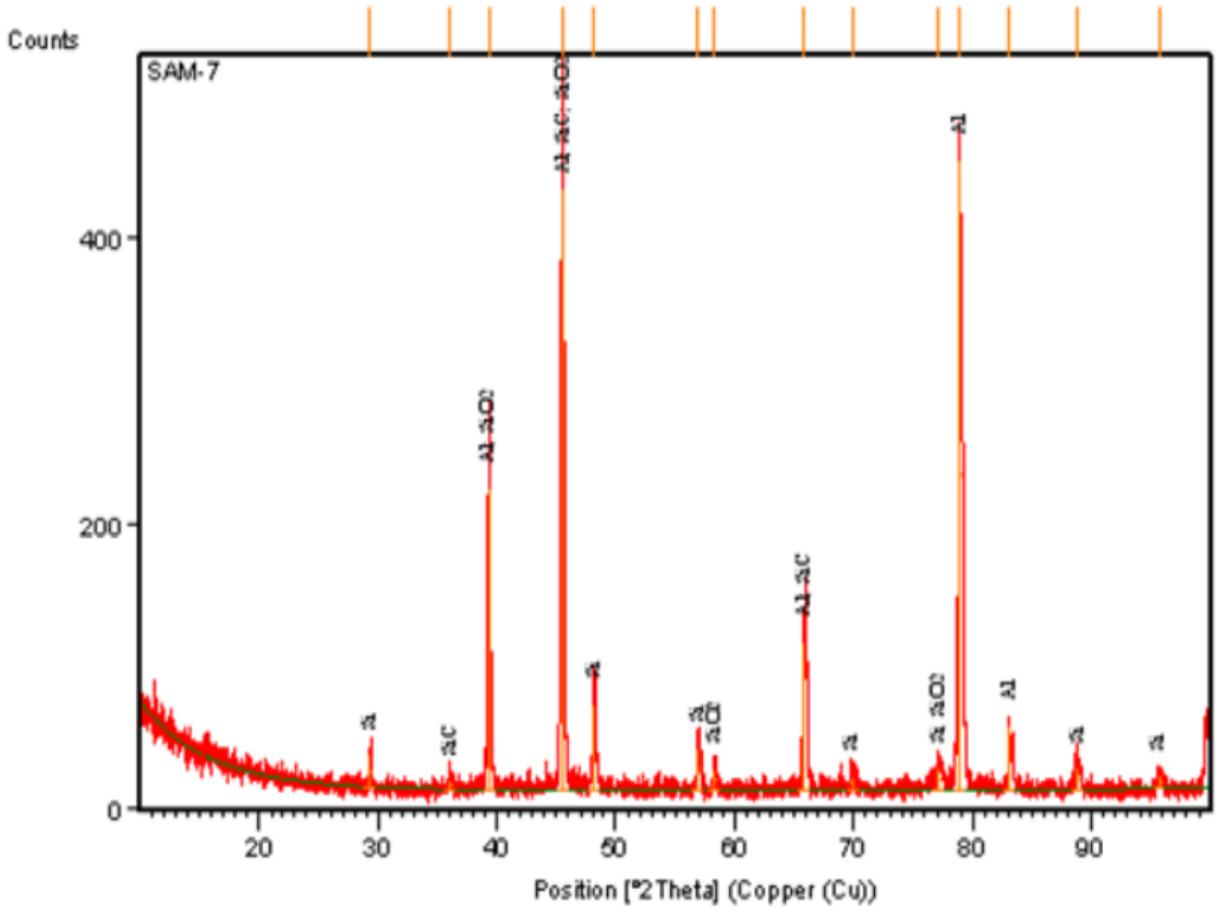

Figure 7.7: X-ray diffraction pattern for aluminium alloy with wt. 7.5% Al_2O_3

Table 7.5 X-ray diffraction pattern with 7.5% Al_2O_3

Ref. code	Score	Compound name	Scale factor	Chemical formula	Weight fraction (%)
01-089-2837	53	Aluminium	0.606	Al	71.2
01-089-2955	24	Silicon	0.171	Si	4
01-075-1541	13	Aluminum oxide	0.013	SiC	21
01-079-1913	2	Silicon oxide	0.031	Si	2.0

CHAPTER 8

RESULTS, CONCLUSIONS AND RECOMMENDATIONS

8.1 RESULTS

The effect of parameters i.e. composition, cooling and stirring speed were evaluated using ANOVA and factorial design analysis. The purpose of the ANOVA was to identify the important parameters in prediction of micro hardness and on wear rate with time, sliding distance and load. Some results consolidated from ANOVA and plots are given below:

8.1.1 MICRO HARDNESS

Composition and cooling was found to be the significant factors in micro hardness. The value of 'p' in case of composition and cooling was less than 0.05. The results were analyzed using ANOVA for identifying the significant factors affecting the performance at 95% confidence interval.

ANOVA Table shows that factors, namely composition (p= 0.001), cooling (p= 0.046) were found to be significant factors. Stirring speed was found insignificant.

Composition has the highest rank, signifying the highest contribution in micro hardness and stirring speed has the lowest rank and was observed to be insignificant in micro hardness of composites. The micro hardness was found to be high when composition is about 7.5% and cooling is furnace cooling.

The estimated mean value of micro hardness when two factors, namely, composition (7.5%), cooling (Furnace cooling). were considered with 95% confidence interval was found to be 69.198±0.625 HVN.

8.1.2 WEAR RATE

Wear rate is observed at different conditions like load , time and sliding distance to analyze the behavior of the composites at different composition level.

Firstly the wear with time was calculated using ANOVA by considering the three factors i.e. composition, cooling and stirring speed. It has been seen that the two factors cooling and composition was significant factors and stirring speed was insignificant.

Also it has been observe that as the time was increasing the wear rate was also increasing.

Secondly the effect of the sliding distance was observed using ANOVA to find out the significant and insignificant factors. It has been observed that composition and cooling were significant factors and the stirring speed was insignificant factor.

From results it has been seen that initially as sliding distance increasing the wear was also increasing but further as the sliding distance increase the wear rate was decreasing.

8.1.3 MICROSTRUCTURE ANALYSIS

Optical microstructure and SEM were analyzed to observe the presence and distribution of Al_2O_3 particles in aluminium alloy. It was observed that particulates are fairly distributed in aluminium alloy. It was also seen that at some places voids present in composites. Various SEM images were taken at different magnifications like 50X, 100X, 250X, 500X, 1000X and 2000X.

Scanning electron micrographs at lower magnification shows that the distribution of Al_2O_3 particulate throughout the MMC's. Scanning electron micrographs at higher magnification shows the particle matrix interfaces

8.1.4 EDS AND XRD ANALYSIS

XRD analysis was carried out to observe the presence of various phases present in the composites at different composition. XRD pattern of 2.5, 5 and 7.5 % composites were analyzed and from the pattern it can be easily analyzed that oxide phase Al_2O_3 in different amount as the composition of Al_2O_3 varied.

8.2 SCOPE FOR FUTURE WORK

This work can be further extended by increasing the percentage of the composition more than 7.5%.

The rate of cooling can be varied by changing the cooling conditions to see the effect on distribution of particles, wear behaviour, micro hardness.

Stirring time can be considered as a new factor for producing the composites. The type of reinforcement and particle size can be varied.

In wear load can also be taken as a variable and the friction disc can be changed by thermal spraying and dry condition can be changed in to wet condition.

REFERENCES

[1] Rohatgi P.K., (1994), "Low-cost, Fly-Ash-Containing Aluminum-Matrix Composites", *JOM - The Member Journal of TMS JOM,* Vol. 46, pp. 55–59.

[2] T.P.D. Rajan, R.M. Pillai, B.C. Pai, K.G. Satyanarayana, P.K. Rohatgi, Proceedings of National Conference on: Recent Advances in Materials Processing (RAMP-2001), India, 2001, pp. 327–334.

[3] Rohatgi P.K., R.Q. Guo, P. Huang, S. Ray, (1997), "Friction and Abrasion. Resistance of Cast Aluminum Alloy-Fly Ash Composites" *Metall. Mater. Trans*. Vol. 28, pp. 245–250.

[4] Akbulut, M. Darman, F. Yilmaz, (1998), "Dry wear and friction properties of -Al_2O_3 short fiber reinforced Al-Si (LM 13) alloy metal matrix composites", Wear, Vol. 215, pp. 170–179.

[5] S. Skolianos, T.Z.Kattamis, (1993), "Cast microstructure and tribological properties of particulate TiC-reinforced Ni-base or stainless steel matrix composites", *Journal of Material Science and Engineering,* Vol. 183, pp. 197-204.

[6] Surapa M.K. and Parsad S.C. and Rohatgi P.K., (1982), "Wear and abrasion of cast Al-Alumina particle composites" *Wear,* Vol. 77, pp.295-312.

[7] R.Q.Guo, P.K.Rohatgi, Fuel and energy Abstracts, (1997) 828.

[8] R.Q.Guo, P.K.Rohatgi, Fuel and energy Abstracts, (1997) 157.

[9] M.J.Koczak, M.K.Prem Kumar, JOM 45 (1993) 44.

[10] P.C.Maity, P.N.Chakraborty, S.C.Panigrahi, Scripta Metall. Mater. 28 (1993)

[11] Jartiz, A.E., Design 1965, pp. 18

[12] Karl Ulrich Kainer, Metal Matrix Composites. Custom-made Materials for Automotive and Aerospace Engineering, Wiley-Vch, 3-527-31360-5

[13] Introduction to composite materials www.substech.com

[14] Anthony Kelly, Karl Zweben, Comprehensive composite materials: design and application, Elsevier, volume 6, ISBN-0-08-043724-9

[15] S.Bandyopadhay, T.Das , and P.R.Munroe ,Metal Matrix Composites -The Light Yet Stronger Metals For Tomorrow, A Treaise On Cast materials, p-17-38.

[16] T.W.Clyne, (2001), Metal Matrix Composites: Matrices and Processing, Encyclopedia of Materials : Science and Technology ,p- 8

[17] Composite Materials: Engineering and Design by F.L.Matthews and R.D.rawlings, Chapman & Hall publication

[18] T. V. Ranjan, C.P. Sharma, Ashok Sharma, Heat Treatment Principles and techniques, Prentice Hall India, ISBN-81-203-0716-X

[19]Rehimian Mehadi, Nader Pravin and Eshani Naser, (2011), "The effect of production parameters on microstructure and wear resistance of powder metallurgy Al-Al_2O_3 composite", *International Journal of Materials and Design,* Vol. 32, pp. 1031-1038.

[20] Rao R.N. and Das S., (2011), " Effect of SiC content and sliding speed on the wear behavior of aluminium matrix composites", *International Journal of Materials and Design,* Vol. 32, pp. 1066-1071

[21] Sajjadi S.A., Ezatpour H.R. and Parizi M.T., (2011), "Comparison of microstructure and mechanical properties of A356 Al-Al_2O_3 composites fabricated by stir and compo-casting process", *International Journal of Materials and Design*, Vol. 34, pp. 106-111.

[22] Swamy N.R., Ramesh C.S. and Chanderasheker T., (2010), "Effect of heat treatment on strength and abrasive wear behavior of Al6061-SiC composites", *Indian Academy of Science,* Vol. 33, pp. 49-54.

[23] Prabu S.B., Kaurnamoorthy L., Kathiresan S. and Mohan B., (2006), "influence of stirring speed and starting time on distribution of particles size in metal matrix composite", *International Journal of Material Processing Technology,* Vol. 171, pp. 268-273.

[24] Wahab M.N., Daud A.R. and Gazali M.J., (2009), "Preparation and characterization of stir cast aluminum-nitride reinforced aluminum matrix composites", *International Journal of Mechanical and Material Engineering,* Vol. 4, pp. 115-117.

[25] Suresh S.M., Mishra D. Srinivasan A., Arunachalam R.M. and Sashikumar R, (2011) "Production and characterization of micro and nano Al_2O_3 particle reinforced LM25 aluminium alloy composites", *ARPN Journal of Engineering and Applied Sciences,* Vol. 6, pp. 94-98.

[26] Wang Hailong, Zhang Rui, Xing Hu, Wang Chang-An and Yong Huang, (2008) *"*Characterization of a powder metallurgy SiC/Cu–Al composite*",* J*ournal of Materials Processing Technology*, Vol. 197, pp. 43–48.

[27] Hassan S.B. and Aigbodion V.S., (2009), "The Effect of thermal ageing on microstructure and mechanical properties of Al–Si–Fe/Mg alloys", *Journal of Alloys and Compounds*, Vol. 23, pp. 126-130.

[28] Demir Halil and Gunduz Suleyman, (2009), "The effects of ageing on machinability of 6061 aluminium alloy*",International Journalof Materials and Design,* Vol. *30* , pp. 1480–1483.

[29] Shivanand H.K. and Benal Mahagundappa M., (2007) , " Effects of reinforcements content and ageing durations on wear characteristics of Al (6061) based hybrid composites*", Journal of Materials Engineering*, Vol. 262, pp. 759-763.

[30] Zhang Liangchi, Zhang Chunliang and Chen Zichen, (2011), "Effect of artificial aging (T6) on microstructure of Al-AC8H/Al_2O_3 MMC produced by Stir Casting Route", *Journal of Advanced Materials Research*, Vol. 328, pp. 1552-1555.

[31] Yilmaz O and Buytoz S, (2001), "Abrasive wear of Al_2O_3-reinforced aluminium-based MMCs", *Journal of Composits Science and Technology*, Vol. 61, pp. 2381-2392.

[32] Christy T.V., Murugan N. and Kumar S., (2010), "A comparative study on microstructure and mechanical properties of Al 6061 alloy and the MMC Al 6061/TiB_2/12p", *Journal of Minerals & Materials Characterization & Engineering*, Vol. 9, pp. 57-65.

[33] Kumar G.B.V., Rao C.S.P., Selvaraj N. and Bhagyashekar M.S., (2010), "Studies on Al 6061-SiC and Al7075-Al_2O_3 Metal Matrix Composites", *Journal of Minerals & Materials Characterization & Engineering*, Vol. 9, pp. 43-55.

[34] Reddy A.C.. and Zitoun E., (2010), "Tensile behavior of 6063/Al_2O_3 particulate metal matrix composites fabricated by investment casting process", *International Journal of Applied Engineering Research*, Vol. 1, pp. 542-552.

[35] Luangaraunt T., Tamrongpoowadon L. and Kondoh K., (2007), "Fabrication of Al/Al_2O_3 composites by powder forging of aluminum powder and manganese oxide powders", *16th International Conference on Composites Materials"*, pp. 1-4.

[36] Chou S.N., Huang J.L., Lii D.F. and Lu H.H., (2007), "The mechanical properties and microstructure of Al_2O_3/Aluminum alloy composites fabricated by squeeze casting", *Journal of Alloys and Compounds*, Vol. 436, pp. 124-130.

[37] Deshmanya I.B. and Purohit G.K., (2011), "Development of models for predicting impact strength of Al7075/Al_2O_3 composites produced by stir casting", *International Journal of Advanced Engineering Sciences and Technologies*, Vol. 11, pp. 238-252.

[38] Nripjit, Tyagi A.K. and Singh N., (2009), "Al-Cu-Si-(Al2O3) composites using A 384.1 Al alloys", *Asian Journal of Chemistry*, Vol. 21, pp. 66-71.

[39] Das S., Das S. and Das K., (2007), "Abrasive wear of zircon sand and alumina reinforced Al-4.5 wt% Cu alloy matrix composites – A comparative study", *Journal of Composites Science and Technology*, Vol. 67, pp. 746-751.

[40] Daouda A. and Reif W., (2002), "Influence of Al_2O_3 particulate on the ageing response of A356 Al-based composites", *Journal of Materials Processing Technology*, Vol. 123, pp. 313–318.

[41] Narayan M., Surappa M. and Pramila B.N.B. , (1995), "Dry sliding wear of Al alloy 2024-Al2O3 particle matrix composites", *Journal of Material Science and Technology*, Vol. 181, pp. 563-570.

[42] Liu Bing, Li Xin M., Sun Y N., Liu X., and Wang C Y., (2011), "Study on erosion-abrasion properties of Al-Mn alloy and its composite reinforced with Al_2O_3 particulates",

Journal of Advanced Material Research, Vol. 287, pp. 599-602.

[43] X M., Liu B., Sun W L., Jin A F. and Liu X., (2011), "Abrasion and erosion-corrosion behaviour of Al-Mn alloy matrix composites reinforced with Al2O3 particulates", *Journal of Key Engineering Material,* Vol. 462, pp. 996-1001.

[44] Pruthviraj R.D., (2011), "Wear Characteristics of chilled zinc-aluminium alloy reinforced with silicon-carbide particulate composites", *Journal of Chemical Sciences,* Vol. 1, pp. 17-24.

[45] Kok M. and Ozdin K., (2007), "Wear resistance of aluminium alloy and its composites reinforced by Al_2O_3 particles", *Journal of Material Processing Technology,* Vol. 183, pp. 301-309.

[46] Curle U.A. and Ivanchev L., (2010), "Wear of semi-solid rehocast SiC/Al metal matrix composites", *Journal of Materials Science and Manufacturing,* Vol. 20, pp. 852-856.

[47] Wang X., Liang S., Yang P. And Fan Z., (2009), "Effect of Al_2O_3 particle size on vacuum breakdown behaviour of Al_2O_3/Cu composites", *Journal of Material Science and Engineering,* Vol. 83, pp. 1475-1480.

[48] Umanath K., Selvamani S.T. and Palanikumar K., (2011), "Friction and wear behaviour of Al6061 alloy (SiC+Al_2O_3) hybrid composites", *International Journal of Engineering Science and Technology,* Vol. 3, pp. 5441-5451.

[49] Lashgari H.R., Zangeneh Sh., Shahmir H., Saghafi M. And Emamy M., (2010), "Heat treatment effect on the microstructure, tensile properties and dry sliding behaviour of Al356-10%B_4C cast composites", *Journal of Material and Design,* Vol. 31, pp. 4414-4422.

[50] Li Y.W., Yang C. And Liao H., (2011), "Effect of vacuum heat treatment on microstructure and microhardness of cold sprayed TiN particles reinforced Al alloy based composites", *Journal of Material and Design,* Vol. 32, pp. 388-394.

[51]Zhu H., Jia C., Li J., Zaho J., Song J., Yao Y. And Xie Z., (2012), "Microstructure and high temperature wear of aluminium matrix composites fabricated by reaction from Al-ZrO2-B elemental powders", *Journal of Powder Technology,* Vol. 217, pp. 401-408.

[52] Roy R.K., (1990), "A primer on the Taguchi method", *Van Nostrand Reinhold,* New York.

[53] Ross Phillip J., (1990), “Taguchi Techniques for Quality Engineering”, McGraw-Hill, ISBN 0-07-053866-2